Aus dem Bereich Med. Biophysik

Theoretische Medizin und Biowissenschaften

der Medizinischen Fakultät

der Universität des Saarlandes, Homburg/Saar

Response of immune killer cells to mechanical cues and living therapeutic materials

Dissertation zur Erlangung des Grades eines Doktors der

Naturwissenschaften

der Medizinischen Fakultät

der UNIVERSITÄT DES SAARLANDES

2023

vorgelegt von: **Archana Kaushik Yanamandra Guruvenkata**

geb.am: **20.06.1986 in Hyderbad, India**

Tag des Promotionskolloquiums:

Dekan:

Vorsitzender:

Berichterstatter:

Dedicated to my beloved father

Contents

Abstract

NK cells are one of the major immune killer cell types exhibiting anti-tumor activity. During immune surveillance NK cells infiltrate into tissues and come in contact with cells and organs with varied stiffness. It has been shown that tumor cells with a lower elasticity modulus than their counterparts to have a higher metastatic potential. Whether the change in tumor cell stiffness affects the functionality of NK cells is not well understood. In this work, to test the effect of substrate stiffness on NK responses, PAAm-co-AA hydrogels of varied stiffness (2 kPa,12 kPa, 50 kPa) functionalized with biotinylated NKp46 activating antibody, prepared by Dr. Jingnan Zhang (research group of Prof. del Campo, INM-Leibniz Institute for New Materials) were used. Stiffness of substrate indeed played a huge role in modulating NK responses with stiffer substrates (12 kPa, 50 kPa) eliciting a stronger response in most donors whereas the soft substrates (2 kPa) failed to do so. To further test the impact of target cell stiffness on NK cytolytic activity, stiffness of target cells was altered using blebbistatin (made cells stiffer) and DMSO (made cells softer). Cytotoxicity of NK cells was boosted against stiffened tumor cells and impaired against softened tumor cells. In addition, the time required for NK cell to detach from the stiffened target cell after apoptosis or necrosis of the latter was significantly shorter, also contributing to a more effective cytotoxicity. To further decipher the role of mechanosensing in killing processes, functions of mechanosensitive ion channels was blocked using unspecific antagonizers (gadolinium and nifedipine), and it was found that blockage of mechanosensing substantially impaired NK mediated cytotoxicity as determined by 2D and 3D killing assays. Regarding the responsible mechanosensor, we have identified from the microarray data of our lab (by Dr. Eva Schwarz) that PIEZO1 are the predominately expressed mechanosensitive ion channels in NK cells. Blockade of PIEZO1 in NK cells by GsMTx4 impaired NK mediated cytotoxicity and activation of PIEZO1, using its specific agonist Yoda-1, potentiated NK mediated killing of the target cells. Blockade of PIEZO1 was shown to decrease the infiltration of NK cells into 3D collagen matrices, and activation of PIEZO1 boosted the infiltration of NK cells into 3D collagen matrix. As the role of PIEZO1 to be a major mechanosensor in NK cells was established, its role in sensing the stiffness of substrates was explored. Perturbation of PIEZO1 channels abrogated NK responses to substrate stiffness. Together, these data emphasize the role of mechanosensing in regulating NK cytotoxicity and the central role of tumor cell stiffness in evading immune surveillance.

To fight cancer and other infective diseases, living therapeutic materials (LTMs) offer possibilities to release therapeutics in a sustainable and tunable manner. LTMs contain genetically engineered biological component encapsulated in a polymeric material such as hydrogels to contain their exposure in the host. LTMs are being extensively researched for their use in treatment of cancer with many

studies reinforcing the beneficial effects of using smart materials. To contain the exposure of living component such as bacteria and to protect it from adverse environmental conditions of the host and to avoid a direct contact with immune cells, they are often encapsulated. However, one major concern for LTMs is that they may trigger an immune response and create a pro-inflammatory milieu in the host which could lead to critical situations if unregulated. So, the second part of my thesis is to characterize the immune response of PBMCs to PluDA hydrogel encapsulated *E.coli* and *ClearColi* bacteria. This work was carried out in collaboration with the group of Dr. Shrikrishnan Sankaran, Bio-programable materials, INM-Leibniz Institute for New Materials, Saarbrücken. The *ClearColi* strain was produced from *E.coli* after genetically deleting LPS. *ClearColi* was encapsulated in Pluronic F127-based hydrogels (PluDA). It has to be noted that the bacteria were not in direct contact with the host so any immune reaction elicited would be due to the release of soluble factors and metabolites. The release of pro-inflammatory cytokines (IL-2, IL-4, IL-6, IL-10, IL-17A, TNFα and IFNγ) and cytotoxic proteins (granzyme A, granzyme B, perforin, granulysin, sFas, and sFasL) by PBMCs in response to bacteria and bacteria encapsulated gels was checked along with its influence on immune killer cells' subtypes. Interestingly, PBMCs from the blood donors could be grouped in to two groups, donors with low spontaneous IL-2 and high spontaneous IL-2 release, based on the IL-2 release when PBMCs were cultured alone. Our results show that co-incubation of PluDA blank gels with PBMCs did not alter their profiles of cytokines and cytotoxic proteins, and had no influence on differentiation of NK cells, $CD4^+$ and $CD8^+$ T cells in donors with low spontaneous release of IL-2. *ClearColi* elicited release of IL-6 and IFNγ from PBMCs. Interestingly, the predominantly released cytokine was IL-6 for low spontaneous IL-2 release donors, but IFNγ for high spontaneous IL-2 release donors. Both the transwell condition and the encapsulated gel condition showed the same tendency. When the bacteria were in direct contact with the PBMCs they triggered the apoptosis of PBMCs on day 3 but encapsulation of the bacteria in PluDA gels completely abolished this effect.

Zusammenfassung

NK-Zellen sind eine der wichtigsten Arten von Killerzellen des Immunsystems im Kampf gegen Krebs. . Während der Immunüberwachung infiltrieren NK-Zellen ins Gewebe und kommen mit Zellen und Organen unterschiedlicher Steifigkeit in Kontakt. Es hat sich gezeigt, dass Tumorzellen mit einem niedrigeren Elastizitätsmodul ein höheres Metastasierungspotenzial haben als solche mit einem höheren Elastizitätsmodul. Ob sich die veränderte Steifigkeit der Tumorzellen auf die Funktionalität der NK-Zellen auswirkt, ist noch nicht ausreichend geklärt. In dieser Arbeit wurden PAAm-co-AA-Hydrogele unterschiedlicher Steifigkeit (2 kPa, 12 kPa, 50 kPa), die mit einem biotinylierten, NKp46 aktivierenden Antikörper funktionalisiert waren, von Dr. Jingnan Zhang (Forschungsgruppe von Prof. del Campo, INM-Leibniz-Institut für Neue Materialien) verwendet, um die Auswirkungen der Substratsteifigkeit auf NK-Zellfunktionen zu untersuchen. Die Steifigkeit des Substrats spielte in der Tat eine große Rolle bei der Modulation der NK-Funktionalität, wobei steifere Substrate (12 kPa, 50 kPa) bei den meisten Spendern eine stärkere Reaktion auslösten, während dies bei den weichen Substraten (2 kPa) nicht der Fall war. Um die Auswirkungen der Steifigkeit der Zielzellen auf die zytotoxische Aktivität der NK-Zellen weiter zu testen, wurde die Steifigkeit der Zielzellen mit Hilfe von Blebbistatin (machte die Zellen steifer) und DMSO (machte die Zellen weicher) verändert. Die Zytotoxizität der NK-Zellen gegen steifere Tumorzellen war stärker als gegen weichere Tumorzellen. Darüber hinaus war die Zeit, die die NK-Zellen benötigten, um sich nach der Apoptose oder Nekrose einer steiferen Krebszelle von dieser zu lösen, deutlich kürzer als bei einer weicheren Krebszelle, was ebenfalls zu einer effektiveren Zytotoxizität beitrug. Um die Rolle der Mechanosensorik im Tötungsprozess weiter zu entschlüsseln, wurden die Funktionen mechanosensitiver Ionenkanäle mit Hilfe unspezifischer Antagonisten (Gadolinium und Nifedipin) blockiert. Es zeigte sich, dass die Blockierung der Mechanosensorik die durch NK-Zellen vermittelte Zytotoxizität erheblich beeinträchtigte, wie durch 2D- und 3D-Zytotoxizitätsassays ermittelt wurde. Was den verantwortlichen Mechanosensor betrifft, so haben wir anhand bereits vorhandener Microarray-Daten (von Dr. Eva Schwarz) unseres Labors festgestellt, dass PIEZO1 Kanäle die vorwiegend exprimierten mechanosensitiven Ionenkanäle in NK-Zellen sind. Die Blockade von PIEZO1 in NK-Zellen durch GsMTx4 beeinträchtigte die NK-vermittelte Zytotoxizität, und die Aktivierung von PIEZO1 durch seinen spezifischen Agonisten Yoda-1 verstärkte die NK-vermittelte Abtötung der Zielzellen. Die Blockade von PIEZO1 verringerte die Infiltration von NK-Zellen in 3D-Kollagenmatrizen, während die Aktivierung von PIEZO1 die Infiltration von NK-Zellen in die 3D-Kollagenmatrix verstärkte. Da die Rolle von PIEZO1 als wichtiger Mechanosensor in NK-Zellen somit

nachgewiesen wurde, wurde seine Rolle bezüglich der Steifigkeit von Substraten untersucht. Eine Inhibierung der PIEZO1-Kanäle verminderte die Reaktionen der NK auf die Steifigkeit des Substrats. Zusammengenommen unterstreichen diese Daten die Rolle der Mechanosensorik bei der Regulierung der NK-Zytotoxizität und die zentrale Rolle der Steifigkeit von Tumorzellen bei der Umgehung der Immunüberwachung.

Zur Bekämpfung von Krebs und anderen Infektionskrankheiten bieten lebende therapeutische Materialien (LTM) die Möglichkeit, Therapeutika auf nachhaltige und abstimmbare Weise freizusetzen. LTMs enthalten gentechnisch veränderte biologische Komponenten, die in einem Polymermaterial wie Hydrogelen eingekapselt sind, um ihre Exposition im Wirt zu begrenzen. LTMs werden derzeit intensiv für ihren Einsatz in der Krebsbehandlung erforscht, wobei viele Studien die positiven Auswirkungen der Verwendung intelligenter Materialien unterstreichen. Um die Exposition von lebenden Komponenten wie Bakterien einzudämmen, sie vor ungünstigen Milieubedingungen im Wirt zu schützen und einen direkten Kontakt mit Immunzellen zu vermeiden, werden sie häufig eingekapselt. Eine große Sorge bei LTMs ist jedoch, dass sie eine Immunreaktion auslösen und ein entzündungsförderndes Milieu im Wirt schaffen können, das zu kritischen Situationen führen könnte, wenn es nicht reguliert wird. Der zweite Teil meiner Dissertation besteht darin, die Immunantwort von PBMCs auf in PluDA-Hydrogel eingekapselte *E.coli* und *ClearColi* Bakterien zu charakterisieren. Diese Arbeit wurde in Zusammenarbeit mit der Gruppe von Dr. Shrikrishnan Sankaran (Bio-programmierbare Materialien, INM-Leibniz-Institut für Neue Materialien, Saarbrücken) durchgeführt. Der *ClearColi*-Stamm wurde aus *E.coli* nach genetischer Deletion von LPS hergestellt. *ClearColi* wurde in Hydrogelen auf der Basis von Pluronic F127 (PluDA) eingekapselt. Somit war gewährleistet, dass die Bakterien nicht in direktem Kontakt mit dem Wirt standen, so dass jede ausgelöste Immunreaktion auf die Freisetzung von löslichen Faktoren und Metaboliten zurückzuführen ist. Die Freisetzung von pro-inflammatorischen Zytokinen (IL-2, IL-4, IL-6, IL-10, IL-17A, TNFα und IFNγ) und zytotoxischen Proteinen (Granzym A, Granzym B, Perforin, Granulysin, sFas und sFasL) durch PBMCs als Reaktion auf Bakterien und bakterienverkapselte Gele wurde zusammen mit ihrem Einfluss auf die Subtypen der Immunkillerzellen untersucht. Unerwarteterweise konnten die PBMCs der Blutspender in zwei Gruppen eingeteilt werden: Spender mit geringer spontaner IL-2-Freisetzung und Spender mit hoher spontaner IL-2-Freisetzung, basierend auf der IL-2-Freisetzung von PBMCs ohne Stimulus. Unsere Ergebnisse zeigen, dass die Co-Inkubation von PluDA-Gelen mit PBMCs deren Profile von Zytokinen und zytotoxischen Proteinen nicht veränderte und keinen Einfluss auf die Differenzierung von NK-Zellen, $CD4^+$ und $CD8^+$ T-Zellen bei Spendern mit geringer spontaner IL-2-Freisetzung hatte. *ClearColi* löste die Freisetzung von IL-6 und IFNγ aus

PBMCs aus. Interessanterweise war das vorwiegend freigesetzte Zytokin IL-6 bei Spendern mit geringer spontaner IL-2-Freisetzung, aber IFNγ bei Spendern mit hoher spontaner IL-2-Freisetzung. Sowohl bei der Transwell-Bedingung als auch bei der verkapselten Gel-Bedingung zeigte sich die gleiche Tendenz. Wenn die Bakterien in direktem Kontakt mit den PBMCs waren, lösten sie am dritten Tag die Apoptose der PBMCs aus, die Verkapselung der Bakterien in PluDA-Gelen hob diesen Effekt jedoch vollständig auf.

1. Introduction

1.1 The immune system – a fortress

Humans are exposed to various pathogenic and non-pathogenic microbes, allergen and toxins in day to day lives [1]. The word immunity has its origin from the Latin word *Immunis* which itself means shielding against infections or diseases. The immune system is the host's defense mechanism against pathogens and foreign materials [2]. It consists of a plethora of immune cells, lymphoid organs, cytokines and humoral factors. Immune surveillance is carried throughout the body where immune cells constantly looking for pathogens, infectious materials or toxins [3]. Colonizing and reproducing in the host are the major aim of the invading pathogen along with evading the host immune system. The immune system has also evolved to come up with better defense mechanisms for pathogen elimination. For the pathogen to infect the host it has to first breach the epithelial barrier. Innate immune system, the first line of defense plays a major role in eliminating microbes here [4]. Innate immune cells patrol the human body at all times and can be activated by pathogen associated molecular patterns (PAMPs) or non-self-molecules [5]. The major hallmark of innate immunity is that it elicits a quick and robust response against the pathogen and recruits other immune cells to site of infection via secretion of certain cytokines and chemokines. It is antigen-independent and has no memory should the same pathogen infect the host again[6]. Macrophages, neutrophils, natural killer cells (NK cells), dendritic cells, mast cells etc. belong to the innate immune system[7]. Adaptive immunity is antigen specific and generates effector and memory cells which can rapidly eliminate the pathogen should the infection recur. Major cells of adaptive immune system are T and B cells [8], [9].

1.2 Natural Killer cells (NK cells) – sentinels of immune system

NK cells belonging to innate immune system were accidently discovered when experiments were being conducted on T cell mediated cytotoxicity. As the name itself suggests these cells have an intrinsic cytotoxic capability to destroy pathogen infected or aberrant cells without any prior antigenic exposure [10]. NK cells make up to 5 to 20 % of lymphocytes which are circulating in the humans[11]. NK cells express surface receptors which can be either activated or inhibited depending on the expression or downregulation of certain molecules by target cells. A fine balance is maintained between these two which determines the fate of target cells. Expression of MHC class I by healthy cells engages the inhibitory receptors which turns the NK cells "off". To evade immune response many tumor cells and pathogenic cells downregulate MHC class I or upregulate a few ligands for activating receptors of NK cells which engages the activating receptors ultimately lysing the target

[12]. Depending on the expression of surface molecules these cells can be further grouped into $CD56^{bright}$ $CD16^{-}$, $CD56^{dim}$ $CD16^{bright}$, $CD56^{dim}$ $CD16^{-}$; $CD56^{dim}$ $CD16^{+}$; $CD56^{-}$ $CD16^{+}$. $CD56^{bright}$ cells are potent secretors of pro inflammatory cytokines such as IFN-γ, TNF-α, IL-13, IL-10 which can activate other immune cells [13]. The $CD56^{dim}$ NK subpopulation has a higher cytotoxicity owing to its immense perforin and granzyme A content and higher stable conjugates formation ability when compared to $CD56^{bright}$ NK cells [14]. There are two different modes that NK cells can employ to exert their cytolytic activity. Granule mediated cytotoxicity pathway is the major route employed by the killer cells to eliminate their target. Upon recognition of the target cell, a contact is established between the target cell and NK cell via integrins, and an immunological synapse (IS) is established. Lytic granules, which are secretory lysosomes containing cytotoxic proteins are then polarized along with microtubule organizing center (MTOC) towards the synapse. Contents of the lytic granules are then released in the synaptic cleft. This process is known as degranulation. Degranulation is characterized by exposure of lysosomal-associated membrane protein-1 (LAMP-1 or CD107a) and 2 (LAMP-2 or CD107b) for a brief amount of time on NK cell surface. This is widely used as a marker for NK cell activation and cytotoxicity. Another mode of killing employed by NK cells is mediated via the death receptors where FasL, TNF and TRAIL bind to corresponding receptors [15][9][11], [16], [17].

1.3 T cells- impeccably trained special soldiers

T cells have a T cell receptor (TCR) which is activated by antigens that are presented by antigen presenting cells (APCs) on MHC class I or II molecules. TCR is non covalently couple to CD3 molecule which transduces the activation signal to intracellular signaling molecules. T cells require a co-stimulatory CD28 signal along with CD3 receptor engagement for naïve T cell activation[18]. Naïve T cells are the ones which circulate by shuttling between blood stream and lymphoid organs where they encounter antigen presenting cells. These cells are positive for CD45RA, CCR7, CD62L, CD127, CD132 and negative for CD25, CD44, CD69, CD45RO[18], [19]. There are two kinds of T cells – $CD4^{+}$ or T helper cells and $CD8^{+}$ or Cytotoxic T Lymphocytes (CTLs). Upon activation of Pattern recognition receptors (PRRs) on antigen presenting cells by Pathogen associated molecular patterns (PAMPs) they migrate to secondary lymphoid organs and present the antigenic peptide either on MHC I which primes naïve $CD8^{+}$ cells [20] [21]or MHC II leading to activation of $CD4^{+}$ cells and subsequent generation of effector $CD8^{+}$ or $CD4^{+}$ cells. $CD4^{+}$ cells are the major cytokine producing T cell subpopulation which can mount an immune response by activating other immune cells or recruiting more immune cells to the infected area [22]. $CD8^{+}$ cells on the other hand have cytolytic function on pathogen laden host cell where the major killing machinery is exocytosis of cytotoxic granules such as perforin, granzymes at the IS [23]. Once the effector functions of these cells are

carried out a small pool of T cell population with "memory" to the eliminated pathogen remains in the host. These memory cells display a higher proliferative capability and more susceptible to antigenic stimulation than the naïve cells. Memory T cells can be further divided into central memory T cells (T_{CM}) and effector memory T cells (T_{EM}) which differ in the expression of surface molecules and also functionality. T_{CM} are characterized by a high expression of CCR7, CD62L, CD44 whereas T_{EM} have a low CD62L, CD127 and $CCR7^-$ and have an immediate effector function [24][25].

1.4 Cytotoxic Proteins – major ammunition

Exocytosis of the contents of lytic granules in the synaptic cleft efficiently eliminates the pathogen or aberrant cell. The contents of lytic granules are cytotoxic proteins which are perforin and serine proteases [26].

Perforin, a glycoprotein has been identified as a pore-forming protein. Inside lytic granules perforin is in an inactive globular form which is chaperoned by calreticulin to protect it from degradation and activation. Activity of perforin is calcium dependent. Perforin polymerizes and forms pores on target cells by binding to phospholipids of cell membrane. Disruption of cell membrane, induction of pro-apoptotic pathways ultimately leads to target cell lysis. Major cell types which produce perforin are NK cells, $CD8^+$ cells [27], [28].

Granzymes are serine proteases and five types have been discovered in humans so far (A, B, H, M and tryptase-2). Granzymes are produced by many immune cells such as NK cells, $CD8^+$ cells, mast cell etc. Granzymes are secreted as zymogens and cleavage of amino-terminal dipeptide activates them. Granzymes exhibit a cytolytic activity on the target cells but in a perforin dependent manner. Among all the granzymes, granzyme B (Gzm B) has a potent cytotoxic activity in the target cells. It has been shown that granzyme mediated pathways to be not activated in perforin deficient mice showing perforin dependency for granzyme activity[29]. Granzyme B enters the cytosol of target cell, converts pro-apoptotic Bid to truncated Bid which ultimately leads to mitochondrial cytochrome c release and formation of apoptosome which leads to caspase induced apoptosis or disruption of mitochondria which can cause apoptosis independent of caspases [30], [31].

Granulysis, a pro-inflammatory molecule is also present in the cytotoxic granules. It exhibits anti-microbial activity. It is cleaved from a 15kDa peptide to form an active 9kDa peptide. Granulysin disrupts the integrity of cell membrane, causes mitochondrial damage, obstructs oxidative phosphorylation ultimately leading to target lysis[32]. Many studies have shown presence of perforin to boost the activity of granulysin upon pathogenic insult[33].

1.5 Immune response- a double edged sword

Upon antigenic encounter activated innate immune cells secrete a plethora of pro-inflammatory cytokines which help in mounting a robust attack on the invading pathogens. These cytokines also activate and recruit other immune cells to the site of infection which in turn orchestrate a full-fledged immune response. However, an overwhelming and uncontrolled inflammation can potentially damage tissues and organs [34], [35]. Hence, the immune system also releases anti-inflammatory molecules to suppress the inflammatory milieu. Most significant cytokine producers among lymphocytes are $CD4^+$ T cells [21]. Major inflammation related cytokines that are released upon bacterial encounter are IL-6, IL-8, IL-10, tumor necrosis factor α (TNFα), interferon-gamma (IFNγ), IL-17A and cytotoxic proteins such as. perforin, granzyme A, granzyme B, granulysin, soluble Fas and soluble Fas. [36]–[45]. IL-6 is a cytokine which has both protective functions and at the same time plays a huge role in inflammatory reactions to the extent that it is being used as a marker for autoimmune diseases and cancer. It induces production of acute phase proteins, promotes differentiation of $CD4^+$ and $CD8^+$ cells into effector phenotype and B cells into antibody producing plasma cells. Apart from PRR, danger associated molecular patterns (DAMPs) from dying cells also activates IL-6 production. In a cytokine storm predominant production of IL-6 has been observed [34], [46]. TNFα was identified for being cytotoxic to tumor cells and has been implicated in developing chronic inflammation. It is released in response to bacterial infections especially in response to bacterial lipopolysaccharides (LPS). Apart from $CD4^+$ cells, $CD8^+$ cells and NK cells, macrophages are also major contributors to its production. It is involved in activation of NFκB pathway, a main coordinator for production of pro-inflammatory cytokines such as IL-6, recruitment and activation of other immune cell types [47]. On one hand TNFα can enhance activation and proliferation of T cells which is essential to mount an immune response but at the same time it can also influence the activation of regulatory T cells. A hallmark of activated immune cells especially NK cells, $CD4^+$ and $CD8^+$ cells is the production of interferon-γ (IFNγ). It regulates both innate and adaptive immune responses [48]. IFNγ activates NFκB pathway, induces production of other pro-inflammatory cytokines such as IL-12, IL-15, TNFα and has been linked with autoimmune diseases and hyper-inflammation [49]. IL-2 is a pro-inflammatory cytokine with $CD4^+$ cells being the major source of it. IL-2 plays a central role in activation and proliferation of immune killer cells [50]. It promotes production of IFNγ, TNF-α, and lymphotoxin α in killer cells [51]. High levels of IL-2 enhance $CD8^+$ effector functions whereas low levels polarize them to a memory phenotype. IL-2 has a dual role where it also plays a pivotal role in boosting the development of regulatory T cells [52]. IL-17A is secreted by cells in response to pathogenic insult especially bacterial and fungal [53]. It is one of the major players in driving

inflammation by recruiting neutrophils to the infection site [54]. Both IL-4 and IL-10 have been known to have anti-inflammatory effect [55].

1.6 Impact of substrate stiffness on NK cells

Immune surveillance is carried out by a variety of cells which are trafficked through various organs and tissues of the body to carry out their effector functions. During this process they are exposed to a highly dynamic environment where they experience high shear flow especially in blood capillaries and lymph nodes[56]. They also have to infiltrate through tissues, come into contact with cells and organs with varied stiffness thus, constantly exposing the cells to a myriad mechanical cues [57]. Stiffness or elasticity is a physical cue, which often differs between healthy and diseased conditions. Stiffness of tumor tissue is more than its normally healthy counterpart owing to proliferating cells, restructuring of microvasculature but tumor cells (0.05-3.0 kPa) are softer than normal cells (0.75-90 kPa) [58]. When the stiffness of a malignant liver tumor (10.1 kPa) and benign tumor (2.7 kPa) was compared the former was stiffer. The parenchyma of a normal liver (2.3 kPa) was softer than that of a fibrotic one (5.9 kPa) [59]. The stiffness of breast cancer tissue (33 kPa) was shown to have quadrupled than the normal fibroglandular tissue (7.5 kPa) [60], prostate cancer tissue (10.84 ± 4.65 kPa) has double the stiffness than normal tissue (5.44 ± 4.40 kPa) [61]. There are also some tumors which are softer than the normal cells such as ovarian tumors which equips them with a higher metastatic potential [62]. The role of stiffness in modulating the function of NK cells has been of interest in the recent years. It was shown recently that stiff substrates(142 kPa) elicited a release of granzymes A, B and FasL and stiff beads (254 kPa) mimicking the target cells induced higher degranulation and an impaired MTOC polarization was observed against soft beads in NK cells [63]. NK cells were shown to follow a bell-shaped curve when activated on stiff substrates where a maximum activation was achieved on a 150kPa substrate but the increase of stiffness to Mpa range (3Mpa) brought down NK mediated response [64]. These studies show that substrate stiffness can actually regulate NK function. The stiff substrates used in these studies are at least 3 times more than that of a cancerous tissue (1.08–68 kPa) [65]. The effect of target stiffness in physiologically relevant range on the NK cell function and its cytotoxicity still remains elusive.

1.7 Mechanosensing- when cells are under the gun

Adaptation to surrounding environment is one of the essential skills for survival in all living forms. Cells interrogate the stiffness of surrounding cells through mechanosensing. It is the ability of a cell to sense or perceive mechanical cues in its environment [66]. It plays an important role in embryonic

development [67], would healing [68] and tissue reorganization [69]. Translating the perceived mechanical input to a biochemical signal is known as mechanotransduction [70]. A vast amount of evidence shows immune cells to be mechanosensitive [71]–[73], enabling them to adapt their functions to the changing environment. Mechanotransduction occurs at the plasma membrane which consists of various mechanosensors for different mechanical cues. Integrins directly sense the mechanical cues with their extracellular domain and the signal is transmitted to actin via the cytoplasmic tail. Focal adhesion kinase is recruited to the integrins and a number of docking and scaffolding proteins such as talin, vinculin, paxillin assist in transferring the mechanical stimulus to actin which leads to cytoskeletal rearrangement. These signals are also transmitted to the nucleus via linkers for cytoskeleton and nucleoskeleton complex consisting of SUN and nesprin proteins which ultimately leads to gene expression. A few shuttling proteins such as YAP and TAZ are also shuttled between cytoplasm and nucleoplasm in response to mechanical stimulus [74].

1.7.1. Mechanosensitive channels

Mechanosensitive channels (MSCs) were first identified in embryonic chick muscles [75]. Since then, they have been extensively investigated. MSCs respond to mechanical stimuli and are permeable to ions. They can be anionic selective, cationic selective or non-selective channels. To study the impact of MSCs, inhibitors such as gadolinium, nifedipine etc., are widely employed.

1.7.2. Non-specific inhibitors of mechanosensitive channels

Gadolinium is a trivalent cationic lanthanide which has been widely used to inhibit stretch activated channels (SACs). These channels respond to mechanical stimulus upon which they allow entry of ions. As the name indicates SACs are prevalent in vascular endothelium, sensory neuron, cardiac muscle etc., where they have proven to be mechanosensitive. There is no specific inhibitor for these channels but Gadolinium, a broad range inhibitor is used to antagonize these channels [76]–[79]. Voltage-gated calcium channels (VGCCs) allow the entry of calcium ions in response to external mechanical stimulus. Among VGCCs, long lasting or L-type channels are expressed in many cell types such as smooth and skeletal muscle, dendritic cells etc. These channels translate the perceived electrical stimulus to a biochemical function in the cells [80]. NK cells have been shown to express these channels [81]. Nifedipine, FDA approved drug to treat hypertension belongs to the class of 1,4-dihydropyridines selectively inhibits L-type calcium channels [80]. There is no data till now on the influence of these channels on NK functionality.

1.7.3. PIEZO1- professional mechanotransducer

PIEZO family of proteins consisting of PIEZO1 and PIEZO2 have been shown to be mechanosensitive. PIEZO2 is expressed in sensory tissues [82]. Microarray data from our lab has shown a very high expression of PIEZO1 but not PIEZO2 in primary human NK cells. PIEZO1 expression is seen in blood vessels, lungs, bones, urinary bladder, skin etc., where cells are under a lot of mechanical stress [83]. PIEZO1 has been shown to be a key player in conducting mechanical stimuli in immune cells. In macrophages, activation of PIEZO1 polarizes macrophages into a pro-inflammatory M1 subtype and also plays an important role in perceiving the stiffness [84]. T cells whose PIEZO1 was knocked down in experimental autoimmune encephalomyelitis mouse model showed reduced disease burden and influenced regulatory T cell proliferation via transforming growth factor- β pathway [85]. Activation of T cells under fluid shear stress was dependent on PIEZO1 [86]. PIEZO1 was shown to be indispensable in activation of T cell receptor and downstream signaling cascades [87], knockdown of PIEZO1 in $CD4^+$ T cells led to an inefficient antigen priming by APCs [88]. PIEZO1 signalling via calcium ions was shown to be very important for T cell activation [87]. Expression of PIEZO1 was enhanced in dendritic cells cultured on stiff substrates compared to the softer ones [89]. Nevertheless, functional role of PIEZO1 in NK cells was not investigated till now. GsMtx4, a toxin isolated from the venom of tarantula can specifically block the PIEZO1 channel [90]It was used in this project to inhibit the PIEZO1 channel.

1.8 Living therapeutic materials (LTMs)

LTMs consist of biological and synthetic components, such as living cells in scaffolding synthetic materials [91], [92]. The living component of LTMs is often microorganisms such as bacteria as they are pliable to genetic engineering, adapt to severe conditions and are hassle-free to process but apart from bacteria other cells have also been used. Genetic engineering of living component and fabricating it with a material can be exploited to improve therapeutic efficacy. LTMs have been used in the field of biomedicine where Escherichia coli (*E. coli*) was engineered to secrete CsgA-C5 protein which would bind to H1N1 virus and disarm it, anti-tumor effect of NK cells could be maintained with sustained release of cytotoxic proteins when the cells were encapsulated in microspheres, microspheric encapsulation of probiotics packaged separately could ameliorate the effects of metabolic syndrome [93],a genetically engineered self-regenerating *E.coli*-encapsulated in hydrogel used as a patch in gut could help with delivering anti tumor effect and treatment of gastrointestinal diseases [94], hydrogel encapsulated *Bacillus subtilis* engineered to produce antifungal was used to combat fungal infections, *Lactobacillus* encapsulated in hydrogels aided wound healing,

thermoresponsive hydrogel with *Lactococcus* as the cargo was efficient in aiding diabetic wound healing, *Spirulina platensis,* a photosynthetic bacteria embedded in hydrogels produced oxygen in hypoxic tissues [95]. These studies reinforce the beneficial effects of using smart materials in the field of biomedicine. One major challenge/concern for living therapeutic materials is the immune responses, which could lead to critical situations if out of control. LPS on the outer membrane of *E.coli* can activate NLRP3 inflammasome via Toll-like receptor 4 (TLR4) and induce an endotoxic response by releasing pro-inflammatory factors leading to cytokine associated toxicity[96]. Macromolecular compound and proteins synthesized by *E.coli* also contain LPS. To circumvent this issue, LPS are genetically deleted in *E.coli*-derived strain *ClearColi*, which can serve as an optimal cellular biofactory to produce drug inducible molecules for living therapeutic materials. For potential therapeutical application, bacteria producing desired biologically functional substances are often encapsulated in hydrogels. Hydrogels are proven to be stable and their physiochemical and mechanical properties can be easily tuned. Often the scaffolds used are made of agarose, alginate, Pluronic F127 (PluDa) or chitosan [97]–[99]. Encapsulation of bacteria protects them from clearance and inactivation by the host and at the same time allows the diffusion of nutrients and metabolites. In this work, bacteria were encapsulated in the central core of Plu/PluDA hydrogel, and the outer shell had a heavy crosslinking of PluDA to prevent any leakage of bacteria. But one major limiting factor here could be the immunogenicity associated with the LTM. It has to be noted that the bacteria are not in direct contact with the host so any immune reaction elicited would be due to the release of soluble factors and metabolites.

1.9 Goals

External cues in the microenvironment can have a profound impact on immune responses. In the context of solid tumor, the malignant tumor cells are softer than their non-malignant counterparts. Softening of tumor cells is also linked to stemness and metastasis. How the changes in tumor cell stiffness influences immune surveillance is not well understood. The first part of my thesis is aimed to understand how functionality of NK cells is regulated by tumor cell stiffness and the underlying mechanisms. LTMs have emerged as a promising approach in treating tumors and other diseases. Yet, one important point remains to be determined is whether the encapsulation provides sufficient isolation to separate the bacterial components from the host immune system to avoid undesired side effects. In the second part of my thesis, the goal was to comprehensively characterize the immune responses triggered by LTMs composed of Pluronic F127 and *ClearColi*.

Regarding the first part, to explore the role of mechanosensing in regulation NK mediated cytotoxicity, I used primary human NK cells, functionalized hydrogels with three different stiffness and softened or stiffened tumor cells. These materials and functional assays have enabled me to tackle the following questions:

1. How does physiologically relevant stiffness influence NK mediated responses?
   In order to address this question, the response of NK cells to hydrogel substrates of varied stiffness functionalized with NKp46 was investigated. Tumor cells were either softened or stiffened and NK cytotoxicity against these cells was tested.
2. Which molecule is responsible for mechanosensing in NK cells?
   To answer this question, the effect of widely used non-specific mechanosensitive channel inhibitors (gadolinium and nifedipine) on NK cells was first determined. Later PIEZO1, a predominantly expressed mechanosensitive ion channel in NK cells was investigated for its effect on regulating functionality of NK cells.

Regarding the second part of my thesis, to characterize immune responses to LTMs, I used pluronic F127 encapsulated with *ClearColi*. This combination has been shown to have great potential for clinical application. To investigate the immunogenicity of the bacteria-encapsulated hydrogels and its two components, the goals were:

1. Characterizing immune responses of *ClearColi* in direct contact with PBMCs or separated by a nanoporous membrane.
2. Assessing the immunogenicity of black PluDA hydrogels
3. Immune response elicited by *ClearColi*-encapsulated in Pluronic F127-based hydrogels

2. Materials and Methods

2.1 Antibodies and reagents

The following antibodies were purchased from Biolegend- PerCP anti-human CD3, BV421 anti-human CD3, APC anti-human CD56, BV421 anti-human CD107a (LAMP1), Biotin anti-human NKp46 (CD335), Biotin Mouse IgG1 k Isotype Ctrl, BV421 anti-human Perforin, PE anti-human Perforin, BV521 anti-human Granzyme B, PE anti-human Granzyme B. The following inhibitors were used GsMTx4(Smartox Biotechnology), Gadolinium(III) chloride Hexahydrate(Sigma Aldrich), Nifedipine(Sigma Aldrich), Blebbistatin, Latrunculin A, Nocodazole, Jasplakinolide (Cayman Chemical) and the agonist Yoda-1 was purchased from Tocris. Fibricol Collagen solution 10mg/ mL Bovine and Cytosoft discovery kit was bought from Advanced Biomatrix. The following reagents were used for experiments – DMSO (Sigma Aldrich), FCS (PanBiotech), HEPES (Sigma Aldrich), PBS (Thermo Fisher Scientific), Penicillin/Streptomycin (Sigma Aldrich), Calcein-AM (Thermo Fisher Scientific), AIMV (Thermo Fisher Scientific)

2.2 Cells

2.2.1. Isolation of PBMCs

Human Peripheral blood mononuclear cells (PBMCs) were isolated from Leucocyte reduction chamber (LRC) of healthy donors. LRCs were obtained from Blutspendedienst der Universitätskliniken des Saarlandes der Abteilung für klinische Hämostaseololgie und Transfusionsmedizin. The following protocol was followed to isolate PBMCs:

- In a 50 mL Leucosep tube (227290, Greiner) 17 mL of lymphocyte separation buffer was added and centrifuged at 1000 x g and RT for 30 seconds.
- The LRS chamber is cut, and the blood is added to the tubes. Make up the volume to 50 mL in the tubes using HBSS (Hanks BSS, PAA Laboratories).
- Centrifuge the tube at 450 x g for 30 minutes at RT with brake-0 and acceleration-1 as the centrifuge settings.
- A white leucocyte ring is noticed between blood plasma and the separation medium.

- Aspirate this ring carefully using a pipette, transfer it to a 50 mL falcon tube and make up the volume to 50 mL using HBSS.

- Centrifuge the falcon tube at 250 x g for 15 minutes at RT.

- Aspirate the supernatant and add 1-3 mL of lysis buffer (155 mM NH4Cl, 10 mM KHCO3, 13 mM EDTA, pH 7.3) to the pellet depending on the size of the pellet.

- After keeping the cell pellet in lysis buffer for a minute and fill up to 50 mL of HBSS.

- Centrifuge the tube at 130 × g for 10 min at room temperature.

- The supernatant was aspirated, and the cell pellet was resuspended in 1 mL of PBS/0.5% BSA.

- The cells were then strained using MACS SmartStrainer. The obtained cell suspension was stored at 4°C until further use.

2.2.2. Isolation of NK cells

NK cells were negatively isolated from the PBMC pool using autoMACS ProSeparator. The following protocol was followed.

- Based on the number of NK cells required PBMCs were collected in 15 mL falcon tubes (normally NK yield is estimated to be 5% for 100 x 10^6 PBMCs).

- PBMCs were centrifuged at 300g for 10 minutes at 4°C.

- The supernatant was aspirated. Appropriate volume of pre-chilled PBS+0.5% was added to the cell pellet (40 µL of PBS/0.5% BSA for 10 x 10^6 PBMCs).

- Cell suspension was placed in chill racks.

- Two empty falcons were also placed in the chill rack to collect NK cells and bead bound positive cells. The following order was followed in placing the falcon tubes in chill racks- position A = sample, position B = negative fraction or NK cells, position C = positive fraction or bead bound cells.

- autoMACS Pro Separator was switched on. Using read reagent option the bar codes on antibody cocktail and microbead cocktail were scanned and then placed on the appropriate rack.

- Chill racks were placed on the instrument. From the menu separation option was selected and Depletes protocol was chosen for negative isolation. The volume of the sample was then entered, and the protocol was run by selecting the run option.

- After the isolation was completed, the obtained negative cell suspension was centrifuged at 200g for 5 minutes. The supernatant was aspirated and appropriate amount of AIMV medium supplemented with 10% FCS was added to the cell pellet.

- Cells were counted and then cultured at a desired density.

2.3 Cell culture

- NK cells were maintained at 2 x 10^6 / ml density in AIMV medium supplemented with 10% FCS and 100 U / ml of recombinant human IL-2 for 3 days.

- K562-pCasper cells were maintained at a density of 0.4 x 10^6 / ml in RPMI 1640 medium supplemented with 10% FCS, 1 % Penicillin / Streptomycin, 125µg / ml of G418 selective antibiotic.

- Treating K562-pCasper cells with cytoskeleton destabilizers

    - K562-pCasper, with a density of 0.4 x 10^6 / ml were treated with 1 ml of RPMI 1640 medium supplemented with 10% FCS, 1 % Penicillin / Streptomycin, 125µg / ml of G418 selective antibiotic plus Blebbistatin (50 µM and 25 µM) or Nocodazole (50 µM, 25 µM and 12.5 µM) or Latrunculin-A (5 µM and 10 µM) or Jasplakinolide (0.009 µM, 0.187 µM, 0.375 µM, 0.75 µM, 1.5 µM) for 12 hours in a 48 well plate at 37 °C, 5% CO2. The corresponding DMSO controls were also treated the same way.

2.4 Real time killing assay

Real time killing assay is a 2D killing assay carried out in a plate reader as described elsewhere [100].

- K562 were used as target cell line.
- 50 µM of Calcein-AM solution was prepared in AIMV medium supplemented with 1 % HEPES.
- K562 was initially centrifuged at 200 x g for 5 minutes. To the cell pellet Calcein staining solution was added. Cells were allowed to stain in dark for 20 minutes at room temperature.
- The cells were then washed twice with AIMV medium by centrifuging at 200 x g for 5 minutes.
- A 96 full well plate was then taken. K562 cells stained with Calcein-AM were resuspended in AIMV medium so that each well of 96 well plate would have 200 µL. Each condition had duplicate wells.
- The cells were allowed settle for at least 20 minutes.
- In addition, the following controls were also used-
    - Medium control: 250 µL AIMV
    - Lysed medium control: 250 µL AIMV + 20 µL Triton X-100
    - Live control: 200 µL of target cell suspension + 50 µL AIMV
    - Lysed control: 200 µL of target cell suspension + 50 µL AIMV +20 µL Triton X-100
- If there were any inhibitors used, then an inhibitor containing medium was also used as one of the controls. The volume of each well was made up to 250 µL by addition of AIMV medium.
- Primary human NK cells were collected depending on the E:T ratio to be used. They were centrifuged at 200 x g for 5 minutes, resuspended in AIMV medium.
- NK cells (50 µL per well) were then loaded on the target cells very gently.
- Fluorescence intensity is measured using the bottom mode of the plate reader which reflects the number of cells with calcein in them.
- This assay was performed for 4 hours with a 10-minute interval.

2.5 Determination of duration required for killing and detachment

Live cell imaging was performed using high content imaging system, ImageXpress (Molecular Devices). The protocol followed for this assay is as follows.

- Target cells used for this assay were K562-pCasper which has a stably transfected FRET based apoptosis reporter.
- K562-pCasper were counted using Z2 cell counter.

- The required number of target cells were calculated based on the Effector to Target (E: T) and resuspended in AIMV medium without FCS.
- 96 well half area plate was used for this assay. Each well had 12,500 target cells resuspended in 100 µL of AIMV medium supplemented with 1% HEPES without FCS.
- The cells were allowed to settle for at least 20 minutes at room temperature.
- Primary human NK cells were collected based on the desired E : T ratios to be used and resuspended in AIMV medium with 1% HEPES buffer. 25 µL of killer cell suspension will be added to each well. There will be a live control well with only target cells and no killer cells.
- The focus for the well to be measured was checked using ImageXpress. Just before starting the measurement killer cells were gently added to the target cells without disturbing them. Killing was visualized for 4 hours with 1 minute interval in Translight, FRET and GFP channels. The obtained imaging data was quantified using ImageJ software.
- Durations required for killing are defined as the time from the establishment of the contact until death of target cells, either apoptosis or necrosis. Durations required for NK detachment are defined as the time from the death of target cells until the departure of NK cells.
- The NK cells, which killed at least one target cells, were chosen for analysis. ImageJ was used to merge the all the channels and make movies. NK cells were tracked manually.

The 3D killing assay was performed as described elsewhere[101]. The following protocol was followed:

- Target cells used for this assay were K562-pCasper which have a transfected FRET based apoptosis reporter.
- 10 mg/ml of bovine Type I collagen was diluted to 8 mg/ mL by adding 100 µL of 10X PBS to 800 µL of 10 mg/ mL of bovine Type I collagen. This was neutralized with 0.1M NaOH.
- Neutralized 8 mg/ml was further diluted with equal volume of AIMV medium supplemented with 10 % FCS and 1 % HEPES buffer which now gives a density of 4 mg/ml.
- This was mixed with equal volume of target cell suspension to obtain a 2 mg/ml collagen gel containing K562-pCasper cells.
- The cell suspension mixed with collagen was pipetted out into 96 well plate. All the steps detailed till here were carried out on ice.

- 96 well plate was centrifuged at 200 x g for 5 minutes at 4°C and then the plate was turned and centrifuged for another 3 minutes before it was allowed to polymerize at 37°C for 45 minutes.
- After that AIMV medium or inhibitor containing medium was added to the wells containing the collagen matrix.
- Primary NK cells either incubated with the inhibitors or vehicle control were then loaded on top of the target cells polymerized in collagen matrix and a time-lapse based imaging was done on screening microscope for 48 hours with an interval of 20 minutes.
- The data was quantified using ImageJ software.

2.6 NK degranulation assay

A degranulation assay was performed where the membrane expression of CD107a which was used as a marker for NK cell activation and cytotoxic activity was evaluated using flow cytometry. When K562 cells were used to trigger degranulation, the following steps were conducted:

- The E: T ratio of 1:1 used for killing assays was used for this assay too.
- K562-pCasper were the target cells used for this assay.
- Target cells were counted, collected and resuspended in AIMV medium supplemented with 10 % FCS and 1 % HEPES buffer. 50 µL of cell suspension was loaded on to each well of a V-bottomed 96 well plate.
- To each well 2 µL of CD107a antibody conjugated with BV421 fluorophore and 0.5 µL of Golgi stop which is a protein transport inhibitor, containing monensin were added to each well.
- The target cells were allowed to settle for at least 20 minutes at room temperature, in dark.
- Primary human NK cells were collected, resuspended in AIMV medium supplemented with 10 % FCS and 1 % HEPES buffer. 50 µL of killer cells were gently added to the target cells.
- 96 well plate was incubated for 4 hours at 37 °C, 5 % CO_2
- NK cell alone without any target cells was used as a control to check for any spontaneous degranulation.
- After 4 hours, cells were harvested and washed twice with PBS + 0.5 % BSA by centrifuging at 200 x g for 5 minutes.
- For NK cell surface staining, APC anti-human CD56 antibody was diluted in the ratio of 1:50 with PBS + 0.5 % BSA. 50 µL of antibody mix was added to the cells and incubated for 30 minutes at 4 °C.

- The data were acquired using a flow cytometer and analysed using FlowJo v10 (FLOWOJO, LLC).

2.7 Biofunctionalization of hydrogels with NKp46 antibody

Functionalization of hydrogels with anti-NKp46 or IgG was done by Dr. Jingnan Zhang (Group of Prof. del Campo, INM-Leibniz Institute for New Materials, Saarbrucken). It was carried out as described elsewhere [102]. A brief description of the protocol is as follows:

- The product of mixing of Acrylamide monomer with N,N'-methylenebis-acrylamide monomer was Poly (PAAm-co-AA) hydrogels.
- Crosslinking of the monomers in different ratios by maintaining a constant ratio of acrylic acid gave rise to PAAm-co-AA hydrogels of varied stiffness.
- Two coverslips were used where one was coated with 3-acryloxypropyltrimethoxysilane and the other with sigmacote which makes the coverslip hydrophobic. These two coverslips were used to prepare the hydrogel discs.
- The next step was to functionalize the hydrogel with biotin-PEG_8-NH_2
- 100 µL of EDC/NHS (39 mg/12 mg in 0.1 M, pH 4.5 MES buffer) was used to cover the hydrogel for 15 minutes.
- The hydrogel was then washed with PBS.
- Hydrogel was then incubated with 100 µL biotin-PEG_8-NH_2 (1 mg/mL) for 2 hours at RT.
- The hydrogels were washed and stored at 4°C.
- The fluorescence intensity of streptavidin was imaged after hydrogels were incubated with it for different time points.
- For 2 kPa it was 1–1.5 h and 2.5–3 h for 12 and 50 kPa.
- The hydrogels which are now streptavidin functionalized were incubated with biotinylated anti-NKp46 (100 µg /ml, 30 µL) or IgG isotype (100 µg /ml, 30 µL) overnight at 4°C.

When functionalized hydrogels were used to trigger degranulation, the following steps were conducted:

Hydrogel substrates of various quantified stiffness (2 kPA, 12 kPA and 50 kPA) were produced in the group of Prof. del Campo, INM-Leibniz Institute for New Materials, Saarbrucken. These substrates were functionalized with NKp46 antibody which can activate NK cell activating receptor NKp46. The activation of this receptor leads to NK cell degranulation.

- 0.3 x 10^6 NK cells were collected for each condition, resuspended in 80 µL of AIMV medium supplemented with 10 % FCS and 1 % HEPES. 3.2 µL of BV421 anti-human CD107a and 0.8 µL of Golgi stop was added to the cells which was then gently pipetted on each hydrogel substrate.
- For the condition where the Piezo 1 channel of NK cells was inhibited, 0.3 x 10^6 NK cells were collected, resuspended in 80 µL of AIMV medium supplemented with 10 % FCS and 1 % HEPES containing 50 µM of GsMTx4 (Stock 1mM). 3.2 µL of BV421 anti-human CD107a and 0.8 µL of Golgi stop was added to the cells which was then gently pipetted on each hydrogel substrate.
- The substrates were then incubated for 4 hours at 37 °C, 5% CO_2
- NK cells were collected from each substrate. The substrates were washed once with PBS/0.5% BSA to collect any remaining NK cells.
- The cells were washed twice with PBS + 0.5 % BSA.
- For NK cell surface staining, APC anti-human CD56 antibody was diluted in the ratio of 1:50 with PBS + 0.5 % BSA. 50 µL of antibody mix was added to the cells and incubated for 30 minutes at 4 °C.
- The data were acquired using a flow cytometer and analysed using FlowJo.

2.8 Cytotoxic protein expression

Perforin and Granzymes are the major cytotoxic proteins of the lytic granules which cause target cell apoptosis. Hence, the expression of perforin and granzyme B in NK cells was determined as follows:

- Primary human NK cells (at least 0.5 x 10^6 NK cells) incubated in the inhibitor or agonist containing medium and the corresponding controls were collected, washed twice with PBS + 0.5 % BSA by centrifuging at 200 x g for 5 minutes.
- The cells were then fixed in 1 ml of pre-chilled 4 % PFA for 20 minutes at room temperature.
- The fixed cells were then permeabilized with 50 µL of 0.1% saponin in PBS/0.5% BSA and 5% FCS for 10 minutes at room temperature.
- 2 µL of either BV421 / PE anti-human Perforin or PE anti-human Granzyme B was added to 50 µL of 0.1% saponin in PBS/0.5% BSA and 5% FCS. perforin or granzyme B containing antibody mix was then added to the fixed cells which are being permeabilized.
- Intracellular staining was carried out for 40 minutes at room temperature in dark.
- FACSVerse (BD Biosciences) was used for data acquisition and FlowJo v10 (FLOWOJO, LLC) for data analysis.

Release of lytic granules is the major ammunition of NK cells. Perforin drills holes on the target cells and granzymes initiate apoptotic pathway. To test whether softened tumor cells were resistant to cytotoxic proteins, the levels of perforin and granzyme B were determined as follows:

- Primary human NK cells (at least 0.5 x 10^6 NK cells) were co-incubated with either stiffened or softened K562-pCasper cells in E:T ratio of 1:1 for 4 hours. Later they were collected, washed twice with PBS + 0.5 % BSA by centrifuging at 200 x g for 5 minutes.
- The cells were then fixed in 1 ml of pre-chilled 4 % PFA for 20 minutes at room temperature.
- The fixed cells were then permeabilized with 50 µL of 0.1% saponin in PBS/0.5% BSA and 5% FCS for 10 minutes at room temperature.
- 2 µL of either BV421 anti-human Perforin or PE anti-human Granzyme B was added to 50 µL of 0.1% saponin in PBS/0.5% BSA and 5% FCS. Perforin or granzyme B containing antibody mix was then added to the fixed cells which are being permeabilized.
- Intracellular staining was carried out for 40 minutes at room temperature in dark.
- FACSVerse (BD Biosciences) was used for data acquisition where K562-pCasper cells were gated to assess the perforin and granzyme B content in target cells. FlowJo v10 (FLOWOJO, LLC) for data analysis.

2.9 Determination of NK-Target conjugation

- K562 cells were used as target cells.
- E:T ratio of 1:1 was used to replicate the conditions used for 3D killing assay.
- K562 cells were stained with 50µM Calcein AM in AIMV supplemented with 1 % HEPES for 20 minutes in dark at room temperature.
- K562 cells were then washed with AIMV medium twice at 200 x g for 5 minutes.
- Primary human NK cells were collected and washed twice with PBS/0.5% BSA at 200 x g for 5 minutes.
- APC anti-human CD56 antibody was diluted 1 to 50 with PBS/0.5% BSA and added to NK cells. Surface staining was performed for 30 minutes at 4 °C.
- NK cells were again washed twice with pre-warmed AIMV medium.
- K562 cells were resuspended in 100 µL of AIMV medium and NK cells were also resuspended in 100 µL of AIMV medium.
- 100 µL of target cells were aliquoted into a 2 mL Eppendorf tube and 100 µL of labelled NK cells to it were added to it.
- The tube was centrifuged at 20 x g for 1 minute.

- The cells were then incubated at 37 °C for 10 minutes after which they were vortexed at 0 speed to break apart any NK-target conjugation which was superficial or not strong enough.
- The cells were immediately fixed by adding 300 mL of ice-cold 0.5 % paraformaldehyde.
- Using the gates set with different controls data was acquired on BD FACSVerse.
- Data were analysed using FLOWJO and percentage of NK cells conjugated with the target was calculated.

2.10 Infiltration of NK cells into a 3D collagen matrix

- Primary human NK cells were stained with CFSE according to the manufacturer's instructions and allowed to recover overnight in AIMV medium supplemented with 10 % FCS and 100 U/ mL of recombinant human IL-2.
- 10 mg/ml of bovine Type I collagen was diluted to 8 mg/ mL by adding 100 µL of 10X PBS to 800 µL of 10 mg/ mL of bovine Type I collagen. This was neutralized with 0.1M NaOH.
- Neutralized 8 mg/ml was further diluted with equal volume of AIMV medium supplemented with 10 % FCS and 1 % HEPES buffer to have a density of 4 mg/ml.
- This was mixed with equal volume of AIMV medium supplemented with 10 % FCS and 1 % HEPES buffer to obtain a 2 mg/ml collagen gel.
- 20 µL of 2 mg/ml collagen gel was pipetted out into 96 well half area plate or 40 µL to a 96 full well plate. All the steps detailed till here were carried out on ice.
- CFSE stained NK were added on top of the collagen matrix and the infiltration of NK cells into the collagen matrix was acquired using ImageXpress for 48 hours with a 20-minute interval. Data from the GFP channel was quantified using ImageJ.

2.11 Real-time deformability cytometry (RT-DC)

This equipment was used at the lab of Dr. O Otto, University of Greifswald and Prof. F. Lautenschläger, University of Saarland for measuring the stiffness of K562-pCasper cells treated with blebbistatin, nocodazole and Latrunculin A. The cells were centrifuged for 5 minutes at 200g and resuspended in cell carrier B solution. The cells were loaded on a PDMS microfluidic chip using a syringe pump where the cells are exposed to shear stress. At least 3000 events of cell deformation were recorded live. The data obtained were analysed using ShapeOut [103].

2.12 siRNA knockdown of PIEZO1

The following protocol was followed for siRNA interference in knocking down PIEZO1.

- P3 solution for primary cells should be brought to room temperature.
- Add 1.5 mL of pre-warmed AIMV medium to a 24 well plate and put it in an incubator.
- Take 4 x 10^6 NK cells and wash once with PBS/0.5% BSA. Switch on Lonza instrument. Select cuvette 1, 2, enter suspension solution as P3, volume 100 µL and choose CN-114 for NK cells.
- Resuspend NK cell pellet in 210 µL of P3 solution, transfer 100 µL to siRNA containing tube (150nM) and directly transfer to the cuvette. Do the same for the negative control.
- Start transfection. Once done add 500 µL of pre-warmed AIMV medium quickly. Transfer the cell suspension to 24 well plate. After for 6 hours add 50 U / ml of IL-2.
- Check for PIEZO1 expression at regular time points. Take at least 0.5 x 10^6 cells. Fix the cells with 4 % PFA for 10 minutes. Permeabilize the cells with 1:1 of acetone:methanol for 20 minutes at -20°C. Incubate with anti-PIEZO1 primary antibody (1:25) for 1 hour. Wash twice with PBS/0.5% BSA. Incubate for 30 minutes at room temperature with Alexa 647 anti-rabbit secondary antibody. Wash twice with PBS/0.5% BSA. Measure the sample on flow cytometer.

2.13 Cell culture of PBMCs with bacteria-encapsulated thin-film hydrogel constructs

To test the immune response of PBMCs to bacteria-encapsulated PluDA hydrogel constructs the PBMCs were cultured in different conditions. The protocol followed is detailed here:

- Freshly isolated PBMCs were first counted. Desired number of PBMCs were taken (3 x 10^6 / ml per condition) and resuspended in RPMI-1640 medium (Thermo Fisher Scientific) supplemented 10% FCS (Thermo Fisher Scientific) and 1 % ampicillin. A very important point has to be noted here to not use medium containing penicillin/streptomycin as the bacteria are sensitive these antibiotics.

- Control: PBMCs alone without any bacteria or hydrogels were cultured in a 24 well plate at a density of 3 x 10^6 / ml.

- Blank gel: In a 24 well plate 3 x 10^6 / ml PBMCs were added to blank gels (PluDA gels without any bacteria).

- *E.coli*-encapsulated gels: To the *E.coli*-encapsulated gel (provided in a 24 well plate) 3 x 10^6 / ml PBMCs were added.

- *ClearColi*-encapsulated gels: To the *ClearColi*-encapsulated gel (provided in a 24 well plate) 3 x 10^6 / ml PBMCs were added.

- *E.coli* in direct contact with PBMCs: Add 3 x 10^6 / ml PBMCs to a 24 well plate. *E.coli* strains with OD 0.5 were provided which were stored at 4°C for a couple of hours till they were used. Centrifuge the bacterial strain at 1000 x g for 5 minutes. To the cell pellet add 2 mL of RPMI-1640 medium (Thermo Fisher Scientific) supplemented 10% FCS (Thermo Fisher Scientific) and 1 % ampicillin medium. To the PBMCs suspension add 0.2 µL of bacterial culture.

- *ClearColi* in direct contact with PBMCs: Add 3 x 10^6 / ml PBMCs to a 24 well plate. *ClearColi* strains with OD 0.5 were provided which were stored at 4°C for a couple of hours till they were used. Centrifuge the bacterial strain at 1000 x g for 5 minutes. To the cell pellet add 2 mL of RPMI-1640 medium (Thermo Fisher Scientific) supplemented 10% FCS (Thermo Fisher Scientific) and 1 % ampicillin medium. To the PBMCs suspension add 0.2 µL of bacterial culture.

- *E.coli* separated from PBMCs by a nanoporous membrane: Add 3 x 10^6 / ml PBMCs to a 24 well plate. *ClearColi* strains with OD 0.5 were provided which were stored at 4°C for a couple of hours till they were used. Centrifuge the bacterial strain at 1000 x g for 5 minutes. To the cell pellet add 2 mL of RPMI-1640 medium (Thermo Fisher Scientific) supplemented 10% FCS (Thermo Fisher Scientific) and 1 % ampicillin medium. Take a 400nm transwell insert and add 0.2 µL of bacterial culture to it. Gently place the insert in the PBMCs containing well of the 24 well plate.

- *ClearColi* separated from PBMCs by a nanoporous membrane: Add 3 x 10^6 / ml PBMCs to a 24 well plate. *ClearColi* strains with OD 0.5 were provided which were stored at 4°C for a couple of hours till they were used. Centrifuge the bacterial strain at 1000 x g for 5 minutes. To the cell pellet add 2 mL of RPMI-1640 medium (Thermo Fisher Scientific) supplemented 10% FCS (Thermo Fisher Scientific) and 1 % ampicillin medium. Take a 400nm transwell

insert and add 0.2 µL of bacterial culture to it. Gently place the insert in the PBMCs containing well of the 24 well plate.

2.14 Collection of cell culture medium

- PBMCs were cultured in different conditions. After 24, 48 and 72 hours 100 µL of cell culture supernatant was collected in Eppendorf tubes from all eight different conditions.
- 100 µL of fresh RPMI-1640 medium (Thermo Fisher Scientific) supplemented 10% FCS (Thermo Fisher Scientific) and 1 % ampicillin medium was added to all the conditions.
- The collected cell culture media was centrifuged at 1000 x g for 10 minutes.
- Duplicates for each sample were made where 80 µL of supernatant was transferred to 0.5 mL Eppendorf tube with each tube containing 40 µL.
- The tubes were then labelled and stored at -80°C until further use.

2.15 Identification of subpopulations of immune cells

The following protocol was followed for identification of subpopulations of immune cells:

- PBMCs which were co-incubated in different conditions were collected on day 3.
- They were centrifuged at 200 x g for 5 minutes.
- The supernatant was aspirated, and the cells were washed twice with PBS/0.5% BSA.
- The obtained cell pellet was resuspended in 110 µL of PBS/0.5% BSA. Two Eppendorf tubes were taken and to each 50 µL of cell suspension was added. One of these two tubes was used for identifying the subtypes of NK cells and the other for T cells.
- To identify the subtypes of NK cells 1 µL of the following antibodies to stain the surface markers of the cells was added to the cell suspension containing Eppendorf tube- BV421 anti-human CD3, APC anti-human CD56, PerCP anti-human CD16.
- PBMCs 8 colour panel settings were loaded as tube setting.
- The following panel was used to identify subtypes of T cells – BV421 anti-human CD3, PerCP anti-human CD8, PE anti-human CD45RO, Alexa 647 anti-human CCR7. 1 µL of each antibody was used to stain the surface markers of PBMCs. For 50 µL of PBS/0.5% BSA 1 µL of antibody was used.
- Cell suspension with antibodies was incubated at 4°C for 30 minutes.
- Centrifuge at 250 x g for 5 minutes
- Wash the cell pellet twice with PBS/0.5% BSA.

- Resuspend the pellet in 100 µL of PBS/0.5% BSA.
- The gating strategy followed for NK panel was as follows: from the lymphocyte population $CD3^-$ cells were gated, from this population $CD56^+$ $CD16^+$ cells were gated to obtain NK subpopulations.
- The gating strategy followed for $CD8^+$ cells was as follows: $CD3^+$ cells were gated from lymphocytes, from this population $CD3^+$ and $CD8^+$ cells were gated, from $CD8^+$ population different subtypes were identified using CD45RO and CCR7 ($CCR7^+$ $CD45RO^-$, $CCR7^+$ $CD45RO^+$, $CCR7^-$ $CD45RO^+$, $CCR7^-$ $CD45RO^-$).
- The gating strategy followed for $CD4^+$ cells was as follows: $CD3^+$ cells were gated from lymphocytes, from this population $CD3^+$ and $CD4^+$ cells were gated, from $CD4^+$ population different subtypes were identified using CD45RO and CCR7 ($CCR7^+$ $CD45RO^-$, $CCR7^+$ $CD45RO^+$, $CCR7^-$ $CD45RO^+$, $CCR7^-$ $CD45RO^-$).
- FACSVerse flow cytometer (BD Biosciences) was used to acquire data and FlowJo v10 (FLOWOJO, LLC) for data analysis.

2.16 Multiplex cytokine assay

This assay was used to determine the release of cytokines and cytotoxic proteins by PBMCs which were co-cultured with *E.coli* or *ClearColi* strains in direct contact or separated by a transwell insert, co-incubated with blank-gels, *E.coli* or *ClearColi-encapsulated* gels and PBMCs alone without any bacteria as the control. Cell culture media which was collected from different PBMC co-incubation conditions and stored at -80°C was used in this assay. Add 150 µL of wash buffer to each well NK/CD8 panel was used in this assay where 13 cytokines can be analysed at the same time from one analyte.

- All the reagents used for assay (provided by the manufacturer in the kit) should be brought to room temperature.
- Reconstitute lyophilized human CD8/NK panel standard cocktail with 250 µL of assay buffer.
- Mix it (vortex vigorously) and allow it to sit at room temperature for 10 minutes.
- Aliquot 70 µL of C7 standard into an Eppendorf tube. Aliquot another 70 µL of C7 standard into an Eppendorf tube and store at -80°C.
- Add 45 µL of assay buffer to Eppendorf tubes labelled C6,C5 and so on till C0.
- A serial dilution was done where 15 µL of C7 was added to C6 mixed well and 15 µL of C6 was added to C5 and so on. C0 has only assay buffer.
- Triplicates of C7 and C0 are required and duplicates for rest of the standards.

- Medium control with RPMI RPMI-1640 medium (Thermo Fisher Scientific) supplemented 10% FCS (Thermo Fisher Scientific) and 1 % ampicillin medium will also be measured.
- A master mix for the samples/analytes was prepared as follows:
    - For each sample – 13 µL of assay buffer + 13 µL of mixed beads + 13 µL of detection antibody.
- Another master mix was prepared for the standards:
    - For each standard – 13 µL of culture medium + 13 µL of mixed beads + 13 µL of detection antibody.
- Take a V-bottomed 96 well plate. To each well aliquot 13 µL of sample/analyte and 13 µL of standards from C7 to C0. Make sure to label the standards on the plate in the same order.
- Now seal the plate with the plastic sticker and press hard. Cover the plate with aluminium foil.
- Put the plate on the shaker at 1000 rpm for 2 hours at room temperature.
- Centrifuge the plate at 250 g for 5 min.
- Aspirate the supernatant carefully without disturbing the beads.
- After 2 hours, carefully pull off the seal and add 13 µL of SA-PE to each well.
- Make sure to not expose anything to light for too long.
- Seal the plate again, cover the plate with aluminium foil and shake at 1000 rpm for 30 minutes at room temperature on a shaker.
- Centrifuge the plate at 250 x g for 5 min.
- Aspirate the supernatant carefully.
- Dilute 10X wash buffer to 1X.
- Add 150 µL of wash buffer to each well. Shake for a minute on the shaker.
- Centrifuge the plate at 250 x g for 5 min.
- Aspirate the supernatant carefully.
- Add 120 µL of wash buffer to each well.
- Measure the samples on flow cytometer.
- Obtained data were quantified using BioLegend's LEGENDplex™ data analysis software.

2.17 Statistical analysis

GraphPad Prism 8.3S Software (San Diego, CA, USA) was used for all the statistical analysis carried out in this work. The following statistical tests were used- for cell stiffness measurements using RT-DC linear mixed models were used, experiments done with hydrogels of varied stiffness a normality test was done using D'Agostino and Pearson test, a paired t-test was used for data following normal

distribution. The statistics used for analysing the differentiation of immune cells into different subtypes was a ratio paired t-test. Wilcoxon matched pairs signed rank was used for non-normal distribution. All the data are presented as mean ± SEM.

3. Results

3.1 Part 1: Role of mechanosensing in regulating NK mediated cytotoxicity

To pinpoint and eliminate their target cells, NK cells have to navigate through a mechanically highly dynamic environment where apart from exposure to mechanical forces such as high fluid shear stress, they also come across cells, tissues and organs of varied stiffness. Tumor microenvironment (TME) is a highly dynamic one where the stiffness of the microenvironment is modulated by the composition of ECM [104]. Tumors have been shown to be stiffer than the surrounding tissue [105], fibrotic tissue is stiffer than normal tissue [105], tumor cells exhibit a heterogeneous stiffness where ovarian cancer cells which were highly metastatic were shown to be softer than their normal counterparts and a lot of data links the stiffness of tumor cells to its metastatic potential. Recent data has also shown the stiffer substrates to enhance NK activation [106] . This shows the indispensable role of mechanosensing in regulating NK response which has not been investigated till now.

3.1.1. Substrate stiffness modulates NK cell response

There is a little data available on investigating the role of substrate stiffness on NK responsiveness, but the major drawback of these studies was that the range of stiffness was not physiologically relevant. Hence, understanding the stiffness dependent cytotoxicity of NK cells in physiologically relevant range is crucial. Hence, we postulated that NK cells can interrogate the stiffness of target cells which in addition modulates their cytotoxicity.

The field of biomaterials has advanced drastically with novel materials being designed to mimic the complex *in vivo* scenario. Such materials provide the biochemical or mechanical cues for the cells which can be employed for *in vitro* studies. The tunability of mechanical properties of these materials makes it more appealing. To examine how the stiffness of target cells can modulate NK cytotoxicity, poly (acrylamide-co-acrylic acid) (PAAm-co-AA) hydrogels with tunable mechanical properties were employed. PAAm-co-AA hydrogels with Young's Modulus of 2, 12, and 50 kPa, which reflects the range of stiffness that NK cells would encounter physiologically were functionalized with NK activating antibody, NKp46. PAAm-co-AA hydrogels were used as surrogate target cells which mimic target cells with varied quantified stiffness. Before functionalizing the hydrogels both NKG2D and NKp46 antibodies were tested for induction of NK degranulation on a 48-well plate. NKp46 could

successfully activate NK cells leading to release of lytic granules which was also shown by others [107], [108](Figure 1).

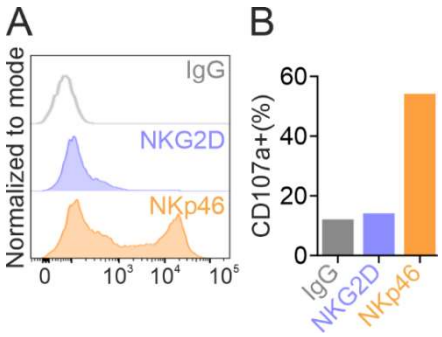

Figure 1: NKp46 antibody induced NK degranulation. *Primary human NK cells were stimulated with 100 U/ mL of IL-2 for three days. CD107a was used as marker for NK degranulation against anti-NKp46 which was coated on a well plate. The flow cytometry data (A) and corresponding quantification from one donor (B) is shown here (n=1).*

PAAm-co-AA hydrogels were functionalized with biotinylated NKp46 antibody or IgG isotype as shown in the schematic (Figure 2A). To examine the response of NK cells to PAAm-co-AA substrates a degranulation assay was performed using primary human NK cells isolated from healthy donors stimulated with 100 U/ mL of IL-2 for 3 days. NK cells were settled on top of each substrate, corresponding IgG control and incubated at 37°C for 4 hours. CD107a, whose surface expression is induced upon degranulation was used as a marker for NK reactivity to substrates. CD107a expression was quantified using a flow cytometer. A total of 17 donors were employed for this study but due to the poor quality (substrates were cracked at the edges) of 2kPa substrates results from 12 donors were taken into consideration. The IgG isotype controls did not trigger NK degranulation. NK cell response to stiffness can be categorized into four- six donors with a peak response to 50kPa (Figure 2B), two donors with a peak response to 2kPa (Figure 2C), two donors who responded to all the substrates (Figure 2D) and two who responded to none (Figure 2E). There was an enhanced degranulation of NK cells with stiffer substrates and on the contrary, for 2kPa which is the softest of the three substrates activation of NK cells was diminished. These results indicate stiffness of the substrate to be a crucial factor in controlling NK cytolytic activity with stiffer substrates eliciting a greater response in most of the donors.

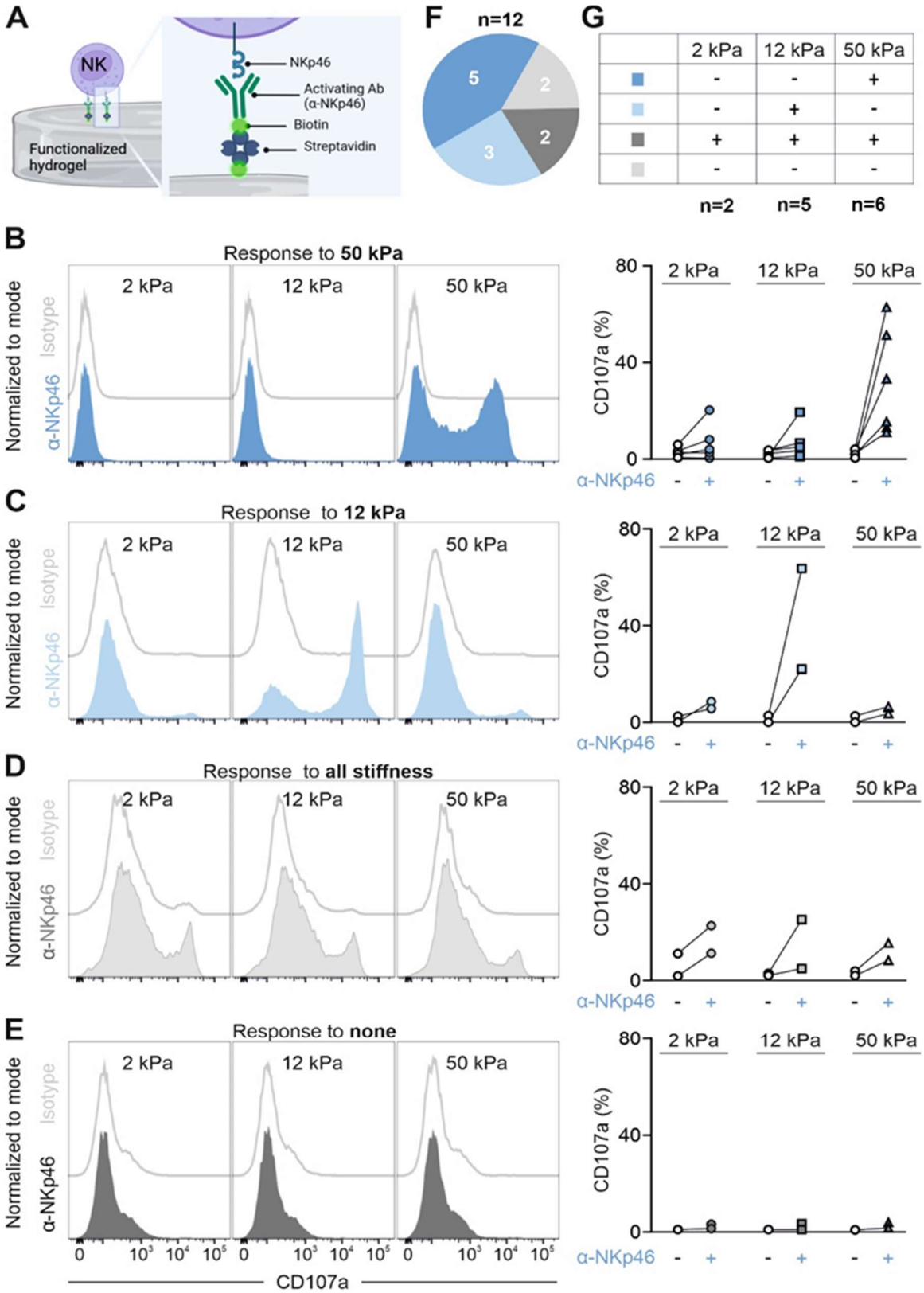
A
NK
NKp46
Activating Ab
(α-NKp46)
Biotin
Streptavidin
Functionalized
hydrogel
F
n=12
5
2
3
2
G
2 kPa
12 kPa
50 kPa
n=2
n=5
n=6
B
Response to 50 kPa
C
Response to 12 kPa
D
Response to all stiffness
E
Response to none
Normalized to mode
Isotype
α-NKp46
CD107a
CD107a (%)

Figure 2: NK response to substrates of varied quantified stiffness. *Primary human NK cells were stimulated with IL-2 for three days. (A) A cartoon depicting the design of hydrogels. PAAm-co-AA hydrogels incubated with streptavidin were later functionalized with biotinylated anti-NKp46 antibodies. (B-E) Substrate stiffness modulates NK response. CD107a was used as a marker for degranulation. The NK cells along with anti-CD107a antibody and Golgi Stop were incubated on functionalized hydrogel substrates at 37°C with 5% CO2 for 4 hours. Later the degranulation data were acquired using flow cytometry. Response of NK cells could be grouped into the following- responded to 50 kPa (B), 12 kPa (C), all substrates (D), or none (E). One representative donor for the flow cytometry data and the quantification is shown here. (F-G) NK response from different donors to substrate stiffness is shown here. The figure has been adapted from* [109].

3.1.2. Impact of target cell stiffness on NK cytolytic activity

We could clearly show that soft substrates do not activate NK cells. Based on this finding we hypothesized that altering the stiffness of tumor cells could also regulate killing functionality of NK cells. To test our hypothesis, pharmaceutical approaches to manipulate stiffness of tumor cells were sought.

Manipulation of tumor cell stiffness

As cytoskeleton is determinant factor for cell stiffness, to manipulate tumor cells stiffness, inhibitors targeting cytoskeletal components including microtubules, actin and myosin IIA were used. Nocodazole which disrupts microtubules, is commonly used in cancer treatment [110]. It binds to β-tubulin and induces microtubule polymerization [111]. To alter the stiffness of target cell, target cells were incubated with different concentrations of nocodazole for 12 hours. The stiffness of cells was then measured using RT-DC as described in section 2.11. 12.5 µM, 25 µM and 50 µM nocodazole was used to treat the target cells. Stiffness of cells for at least 3000 events was measured on RT-DC. There was no significant difference between nocodazole treated and vehicle control (Figure 3A-D). Treatment with 12.5 µM nocodazole significantly increased the stiffness of target which was evaluated using Young's modulus (Figure 3E, F). Target cells treated with nocodazole or vehicle control were co-polymerized in neutralized bovine collagen and killer cells were settled on top of the matrix for a 3D killing assay. It was observed that nocodazole was toxic to the target cells which affected their proliferation in 3D matrix when compared to the vehicle control (Figure 3G). Hence, nocodazole was not used for further experiments.

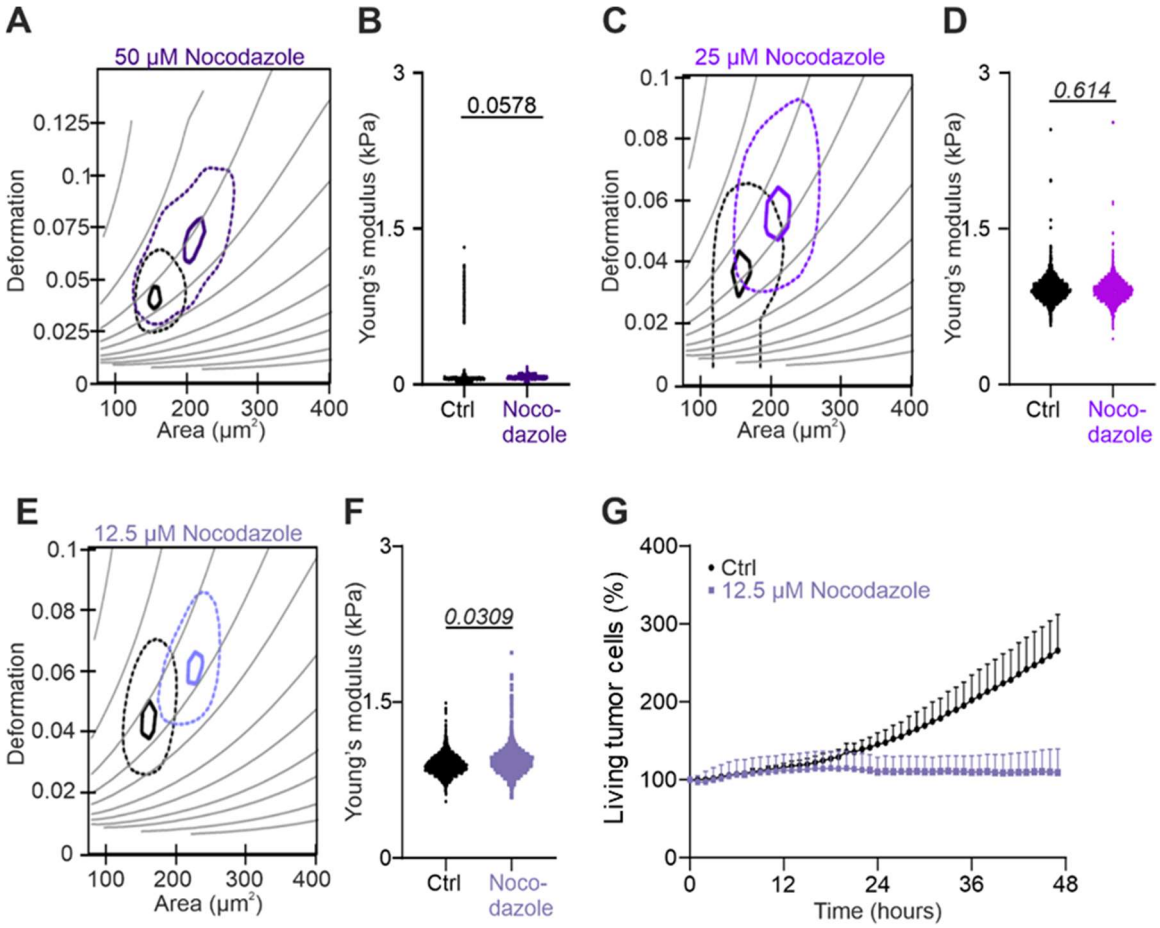

Figure 3: Treatment with nocodazole alters tumor cell stiffness but also affects target cell proliferation. *(A-G) K562-pCasper cells were treated with different concentrations of nocodazole for 12 hours. RT-DC was used to determine the stiffness of the cells. Treatment with 50 and 25 µM of nocodazole did not significantly alter the stiffness. The area vs deformation plots of RT-DC (A, C) and the corresponding quantification (B, D) is shown here (n=3). Treatment with 12.5 µM nocodazole stiffened the target cells (E-F). 12.5 µM nocodazole treated K562 were embedded in 2 mg/ mL collagen to perform a 3D killing assay. The quantification viability of target cells is shown in G (n=2). RT-DC data shown here is from three independent experiments. For statistical analysis, linear mixed models were used.*

Latrunculin A is a reversible inhibitor of actin assembly which binds to actin monomers and prevents their repolymerization [112]. 5 µM and 10 µM of latrunculin A was used to treat target cells. The stiffness of the cells was measured using RT-DC. No significant difference was observed in the stiffness of cells treated with latrunculin A and vehicle control (Figure 4A-D).

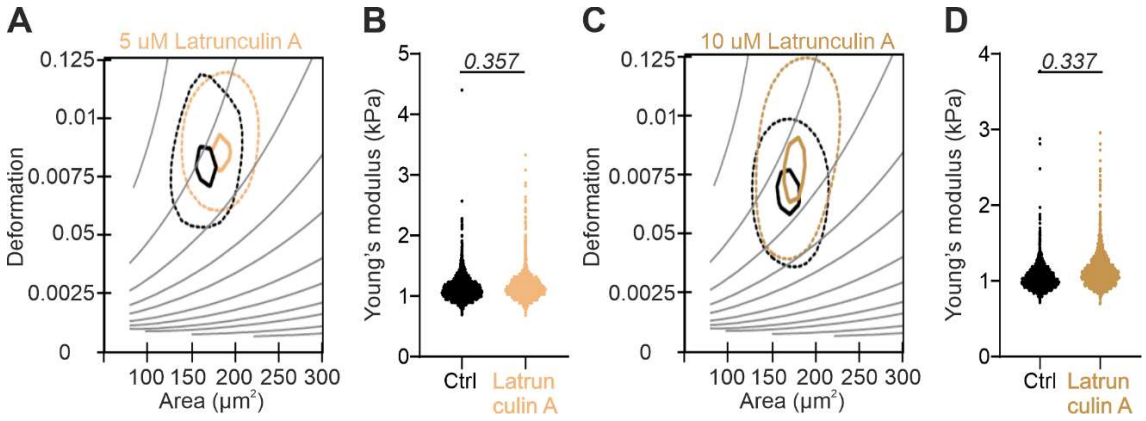

Figure 4: Treatment with Latrunculin A does not alter target cell stiffness. *(A-D) K562-pCasper cells were treated with 5 µM and 10 µM of latrunculin A for 12 hours. RT-DC was used to determine the stiffness of the cells. Treatment with 50 and 25 µM of nocodazole did not significantly alter the stiffness. The area vs deformation plots of RT-DC (A, C) and the corresponding quantification (B, D) is shown here. The data shown here is from three independent experiments. For statistical analysis, linear mixed models were used.*

Jasplakinolide is a cyclo-depsipeptide which polymerizes and stabilizes actin filaments [113]. Different concentrations of jasplakinolide were used to treat target cells. Even very low concentration of the drug was cytotoxic. (Figure 5).

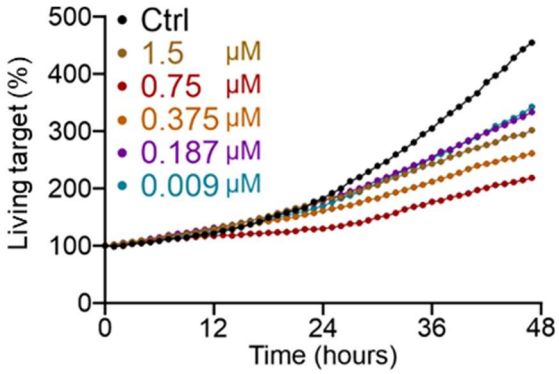

Figure 5: Treatment with Jasplakinolide affects target cell proliferation. *K562-pCasper cells were treated with different concentrations of jasplakinolide for 12 hours. Jasplakinolide treated K562 were embedded in 2 mg/ mL collagen to perform a 3D killing assay for 48 hours with a 20-minute time interval. The quantification viability of target cells is shown here (n=1).*

Target cells were treated with blebbistatin, an inhibitor of class II myosins [114]. The stiffness of the cells was measured by RT-DC. Blebbistatin treated target cells were stiffer than the vehicle control (Figure 6A, B)

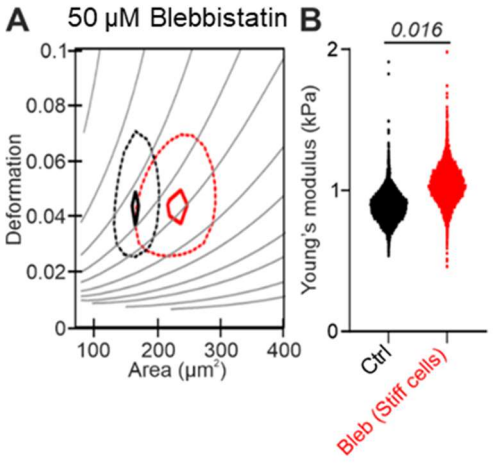

Figure 6: Treatment with Blebbistatin stiffens the target cells. *K562-pCasper cells were treated with 50 µM of blebbistatin for 12 hours. RT-DC was used to determine the stiffness of the cells. Treatment with blebbistatin stiffened the target cells. The area vs deformation plots of RT-DC (A) and the corresponding quantification (B) is shown here. The data shown here is from three independent experiments. For statistical analysis, linear mixed models were used.*

The vehicle control for blebbistatin treated cells was DMSO treatment. Interestingly, treatment with DMSO affected the stiffness of cells. Upon measuring the stiffness of the cells, DMSO treated tumor cells were softer than the untreated cells (Figure 7A, B).

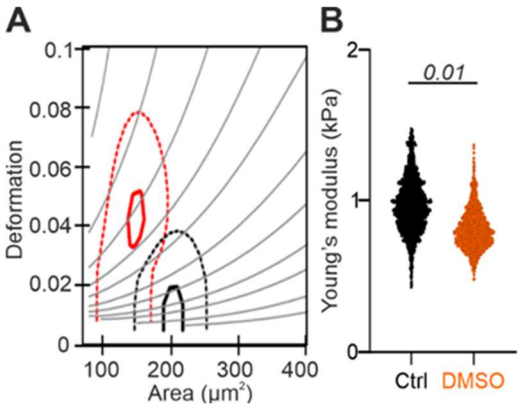

Figure 7: Treatment with DMSO softens the target cells. *K562-pCasper cells were treated with 1:2000 DMSO for 12 hours. RT-DC was used to determine the stiffness of the cells. Treatment with DMSO softened the target cells. The area vs deformation plots of RT-DC (A) and the corresponding quantification (B) is shown here. The data shown here is from three independent experiments. For statistical analysis, linear mixed models were used.*

NK cytotoxicity against soft tumor cells is impaired

To understand the role of tumor cell stiffness in modulating NK cytotoxicity, a 3D killing assay was performed, where the target cells were co-polymerized in bovine collagen matrix and after polymerization of collagen, killer cells were added on top. Target cells express an apoptosis reporter (pCasper-pMax) to differentiate live cells (orange) from apoptotic (green) and necrotic (non-fluorescent) target cells. Target cells were treated with DMSO for 12 hours to soften them. DMSO treated soft tumor cells and the control were co-polymerized in 2 mg / mL of neutralized bovine collagen matrix and NK cells were settled on top. A killing assay was performed on Imagexpress for 48 hours. Tumor cell viability remained unaltered upon DMSO treatment (Figure 8A). A diminished target lysis was observed for soft tumor cells where many cells were still alive even after 48 hours whereas for the control if not all at least most of the tumor cells were killed (Figure 8B,C). These findings clearly show that NK cells mount a very weak attack on soft tumors.

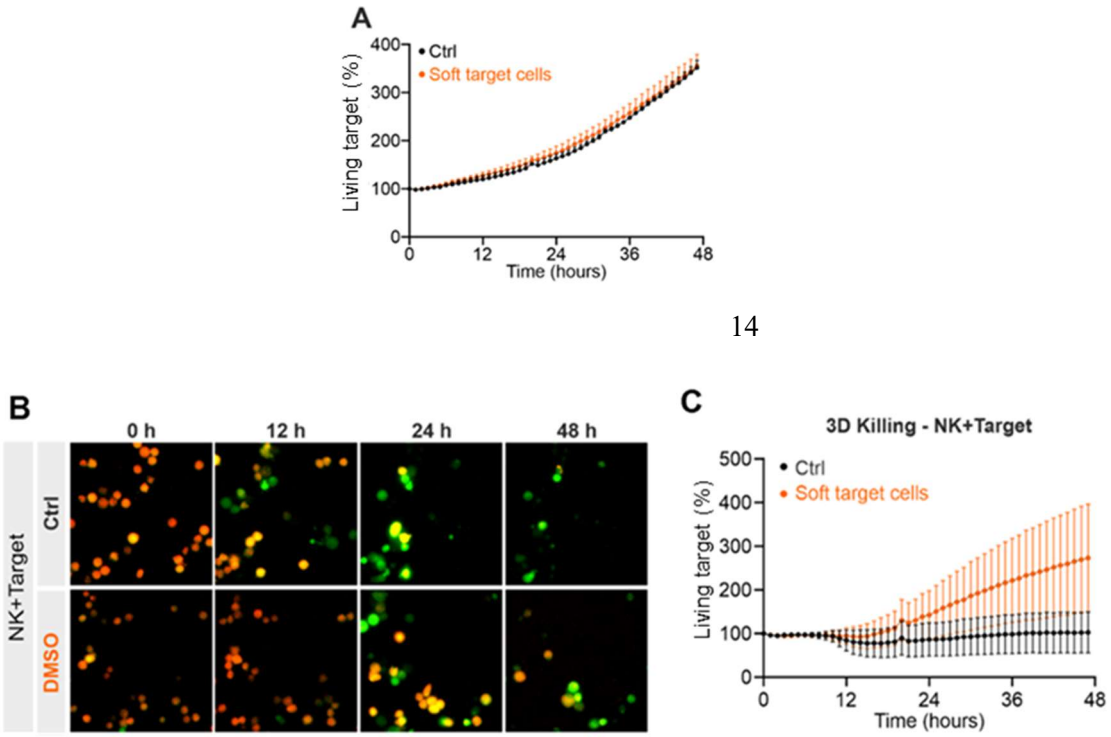

14

Figure 8: Soft tumor cells are not efficiently lysed by NK cells. *Primary human NK cells from healthy donors were stimulated with 100 U/ mL of IL-2. K562 pCasper target cells treated with DMSO (soft target cells) were co-polymerized in collagen matrix and NK cells were settled on top. K562-pCasper cells in orange-yellow were live cells and in green were apoptotic. A) Target cell viability is not affected by DMSO. K562-pCasper were treated for 12 hours with DMSO. The growth and proliferation of these cells in collagen matrix was quantified. (B-C) NK killing efficiency is impaired against soft tumor cells. 3D killing assay was performed with DMSO treated cells (softened target cells) for 48 hours with a 20-minute interval with E:T ratio of 1:1. Time lapse imaging (A) and corresponding quantification from three donors (B) is shown. Scale bars are 40 µm. Data from three independent experiments is shown here. The figure has been adapted from* [109].

NK cytotoxicity is enhanced against stiff tumor cells

Blebbistatin treated tumor cells were shown to be stiffer. Stiff or soft tumor cells were co-polymerized in neutralized bovine collagen matrix and NK cells were settled on top. A killing assay was performed on Imagexpress for 48 hours. Blebbistatin did not affect the viability of tumor cells (Figure 9A,B). Stiff tumor cells were killed faster than the soft cells (Figure 9C, D). This clearly shows that NK cytotoxicity is enhanced against stiff tumor cells.

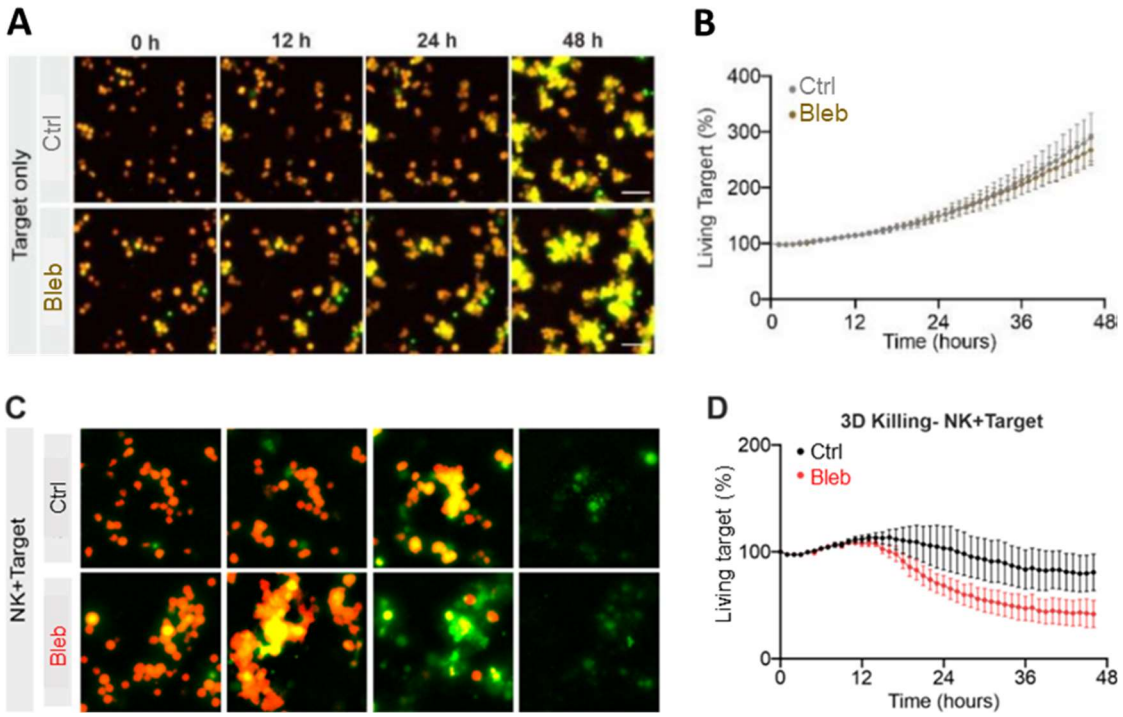

***Figure 9**: **NK cytotoxicity is increased against stiffened tumor cells.** Primary human NK cells from healthy donors were stimulated with 100 U/ mL of IL-2. K562-pCasper target cells treated with 50 µM blebbistatin (stiff target cells) were co-polymerized in collagen matrix and NK cells were added on top. K562-pCasper cells in orange-yellow were live cells and in green were apoptotic. (A-B) Target cell viability is not affected by blebbistatin treatment. C-D) NK killing efficiency is increased against stiffened cells. 3D killing assay was performed with DMSO treated cells (softened target cells) for 48 hours with a 20-minute interval with E:T ratio of 1:1. Time lapse imaging (C) and corresponding quantification from three donors (D) is shown. Scale bars are 40 µm. The figure has been adapted from* [109].

These finding taken together clearly show the cytotoxicity of NK cells to be enhanced against stiffened tumor cells and impaired against softened tumor cells.

To further decipher the mechanism underlying enhanced and impaired activity of NK cells against stiffened and softened tumor cells NK cells were put together with either stiffened or softened tumor cells and live cell images were acquired on Imagexpress. From the imaging data the time taken for NK cells to efficiently lyse the target cell (contact till apoptosis) and then detaching from the cell once killed (apoptosis till detachment) was quantified. The contact till apoptosis and apoptosis till detachment time was significantly shorter for stiffened cells when compared to the softened cells

(Figure 10A, B). Due to this shortened time NK cells were able to detach from apoptotic cells and search for new targets faster in stiffened tumor cells whereas a lack of this led to a failed killing even though the cells were capable of killing in softened tumor cells. These results suggest that stiffening or softening of the cell to have a huge influence on NK cells in exerting their cytotoxicity. Thus, cell softness could be the Achilles heel of NK cytotoxicity.

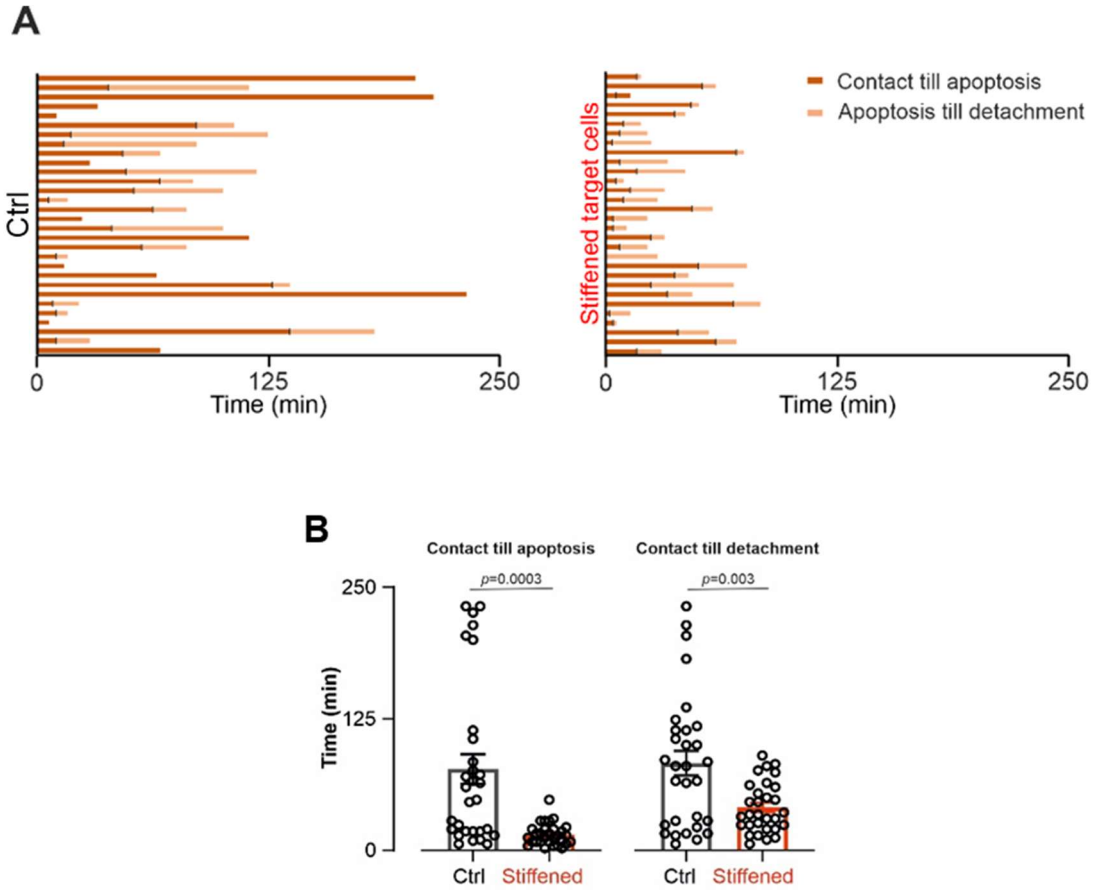

Figure 10: Time taken for NK cells to disengage from target cell after the killing event is shorter for stiffened cells. *K562-pCasper target cells treated with DMSO (Ctrl) or Blebbistatin (Stiffened) were co-incubated with NK cells for 4 hours. Live cell imaging was performed where the time taken for NK cell to initiate a contact with target cell, lead to its apoptosis/necrosis (contact till apoptosis) and finally detach from it (death till detachment) were tracked manually. The analysis is shown in A and quantification of time in B. Data is shown from three independent experiments. For statistical analysis, Mann-Whitney-U-test was used. The figure has been adapted from* [109].

Once NK cells form a stable conjugate polarization of MTOC towards the IS and the release of contents of lytic granules occurs. The cytotoxic proteins of lytic granules lead to target apoptosis. To decipher the underlying cause of accelerated killing kinetics observed in case of stiff target cells, a degranulation assay was performed. NK cells were put together with stiffened cells or softened cells and degranulation assay was performed as explained in section 2.6. CD107a was used as a marker for NK degranulation which was measured on flow cytometer. Stiff tumor cells did not elicit a higher degranulation. The release of lytic granules was comparable between stiff and soft cells (Figure 11A, B).

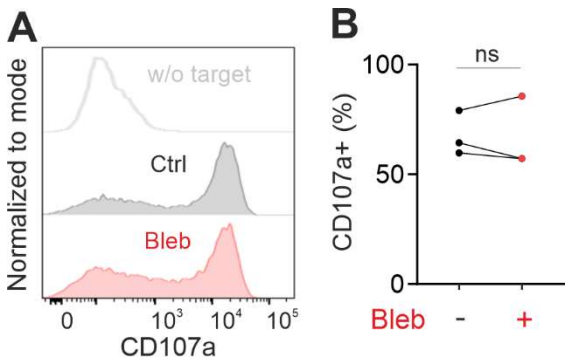

Figure 11: Target cell stiffness does not affect release of lytic granules. *Primary human NK cells were stimulated with 100 U/ mL of IL-2 for three days. CD107a was used as marker for NK degranulation against softened or stiffened tumor cells. The flow cytometry data (A) and corresponding quantification from three donors (B) is shown here. For statistical analysis, Wilcoxon matched pairs signed rank test was used.*

The first step of cytotoxicity is formation of pores by perforin which later would lead to cell death via necrosis or apoptosis through granzyme B uptake. If tumor cells evade this first step by modulating their cell stiffness, then they can escape NK surveillance. Hence, it was examined if impaired killing of soft cells and enhanced killing of stiff cells by NK cells was associated with the ability of NK cells to form pores on target cells. Soft or stiff target cells were incubated with NK cells for 1 hour after which the cells were fixed, permeabilized and perforin and granzyme content in target cells was measured on flow cytometer. No significant difference was observed in perforin and granzyme B content between soft and stiff tumor cells. This experiment further needs to be optimized further by varying the co-incubation time and E: T ratio.

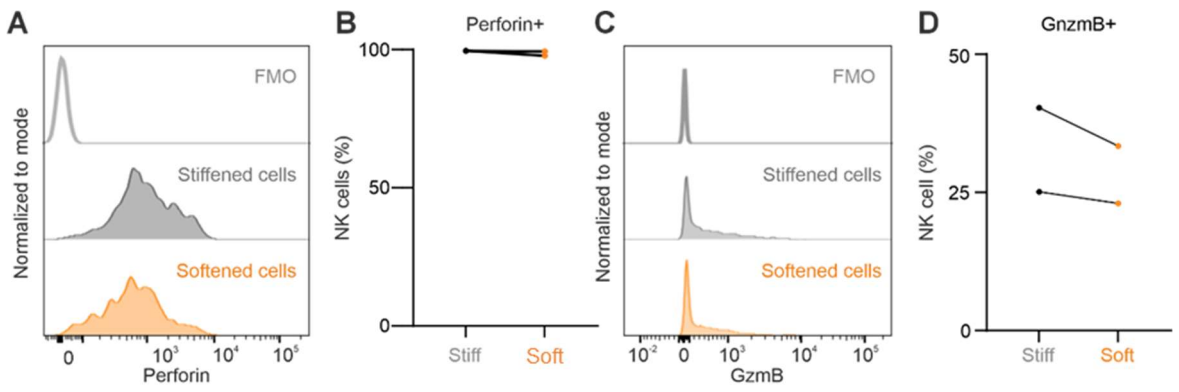

Figure 12: Uptake of perforin and granzyme B by target cells. *Primary human NK cells stimulated with 100 U/ mL of IL-2 were co-incubated with either stiffened or softened target cells for 1 hour. Flow cytometry data for one representative donor perforin and GzmB content in target cells (A, C) and corresponding quantification are shown (B,D). Only two independent experiments were done.*

All these findings taken together indicate that cytotoxicity of NK cells is enhanced against stiffened tumor cells and impaired against softened cells. The shortened contact time between stiffened target cell and NK cell was shown to be a major factor in accelerated killing kinetics of stiffened tumor cells and vice versa for softened tumor cells. Degranulation of NK cells when in contact with stiffened or softened tumor cells remained unaltered. It can be speculated that the pore forming ability of NK cells to be unaltered against softened tumor cells, but more experiments are needed in this direction to further confirm this effect.

3.1.3. Mechanosensing modulates NK mediated cytotoxicity

There is extensive research which shows immune cells to be mechanosensitive [88], [115]–[118], enabling them to adapt their function to the changing environment. Apart from sensing pressure and shear stress interrogating the stiffness of surrounding environment, cells and tissues also constitutes mechanosensing. The results till now clearly indicate mechanosensing to play a decisive role in NK cell mediated cytotoxicity. Hence, investigating the role played by mechanosensitive channels in modulating NK cytotoxicity was of paramount value. In this work widely used unspecific or broad range mechanosensitive channel blockers (gadolinium, nifedipine) and specific mechanosensitive channel inhibitor for PIEZO1 were studied for their effect on NK cells.

3.1.4. Blocking mechanosensing greatly impairs NK mediated cytotoxicity

To analyse whether mechanosensing has an impact on NK mediated target cell lysis, widely used mechanosensing channel inhibitor gadolinium which antagonizes SACs was used. Different concentrations of gadolinium (12.5, 25, 50 and 100 µM) were used to examine the effect of the inhibitor on NK cells. A real time killing assay was performed with different concentrations of gadolinium (Figure 13A). In this assay, target cells stained with calcein-AM were settled in a 96 well plate. Primary human NK cells were loaded on top of the target cells gently. Using the bottom mode of the plate reader, fluorescence intensity was recorded which corresponds to the number of calcein stained cells. This assay was carried out for 4 hours with a 10-minute interval. 100 µM was chosen for further experiments due to its maximum effect on NK cell mediated target lysis. Gadolinium treated NK cells exhibited an impaired target cell lysis, with close to no killing of target cells when compared to control in a real time killing assay (Figure 13B).

To further understand the effect of gadolinium on NK cells, their killing efficiency was examined in a 3D matrix, a more physiologically relevant scenario compared to 2D conditions. The results show that target cell lysis mediated by NK cells was impaired after treatment with gadolinium and the time taken for target cell lysis was considerably longer for gadolinium treated NK cells (Figure 13E, F). As the presence of gadolinium alone did not alter target cell growth (Figure 13C, 1D), we conclude gadolinium to play an essential role in NK killing functions.

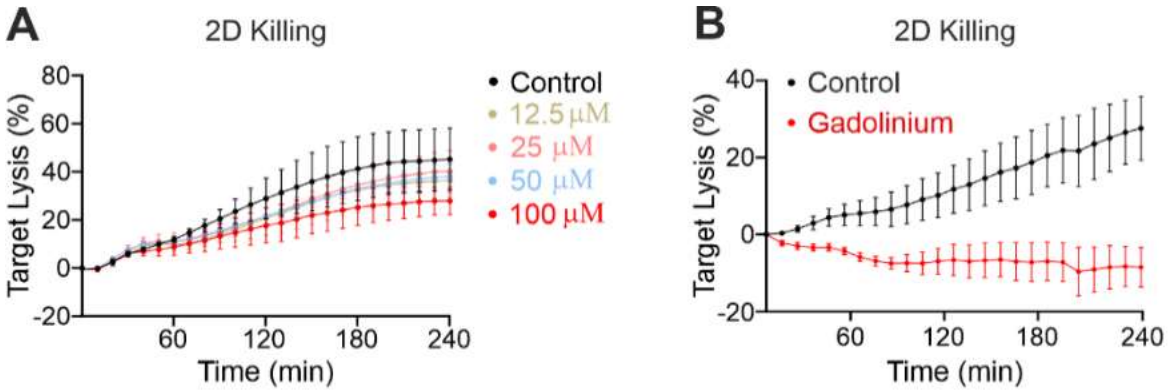

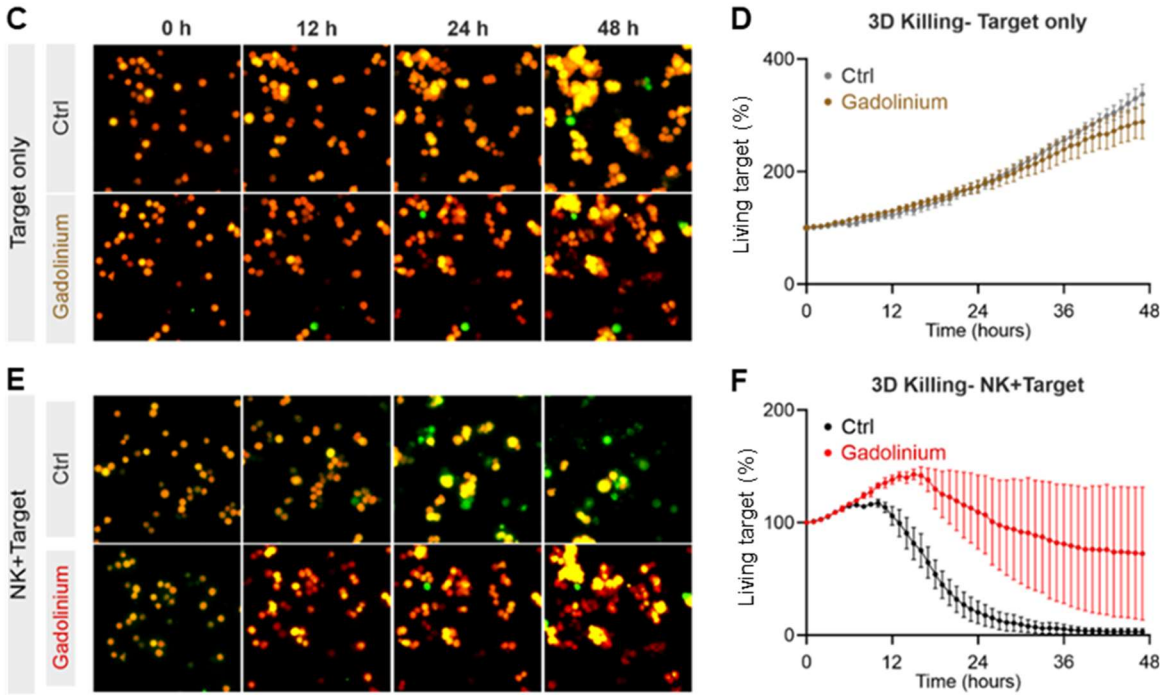

Figure 13: Treatment of NK cells with gadolinium impaired target cell lysis. *Primary human NK cells from healthy donors were stimulated with IL-2 for three days. (A-B) Inhibition of SACs impairs NK cytotoxicity in a 2D real-time killing assay. K562 target cells were stained with Calcein-AM. E:T ratio of 2.5:1 (A) and 1:1 (B) was used. Different concentrations of gadolinium were used to optimize the experimental conditions (A). A real-time killing assay was performed for 4 hours with a 10-minute interval. E:T ratio of 1:1 was used and a concentration of 100 µM was used (B). (C-F) 2mg / mL collagen matrix was prepared with K562pCasper target cells co-polymerized in it. NK cells were settled on top. K562-pCasper cells in orange-yellow were live cells and in green were apoptotic. Treatment with gadolinium does not affect target viability where target cells were in gadolinium containing medium for 48 hours. Time lapse imaging (C) and corresponding quantification (D) are shown. NK cells treated with gadolinium showed a diminished killing. E:T ratio of 2.5:1 was used with the killing being imaged for 48 hours with a 20-minute interval. Time lapse images (E) and corresponding quantification is shown here (F). Scale bars are 40 µm. Data from three independent experiments is shown here.*

Nifedipine is a specific inhibitor for L-type channels. Interestingly, Nifedipine is an antihypertensive drug approved by FDA. To understand the impact of L-type channels on NK effector functions different concentrations of nifedipine (25, 50 and 100 µM) were used. A real time killing assay was

performed with different concentrations of nifedipine in the killing medium (Figure 14A). 100 µM was chosen for further experiments due to its maximum effect on NK cell mediated target lysis. Nifedipine treated NK cells exhibited an impaired target cell lysis when compared to control in a real time killing assay (Figure 14B). A 3D killing assay was performed to analyse the killing kinetics of NK cells treated with nifedipine. The presence of nifedipine affected the target cell viability where a spontaneous apoptosis of the target cells and an impaired cell growth was observed which was not the case in control group (Figure 14C,D). Diminished target cell lysis was observed when NK cells were treated with nifedipine. It should be noted that even though the target cell proliferation was optimal in untreated NK cells the time taken for target cell lysis was considerably shorter where most of the target cells were efficiently killed by 24 hours. (Figure 14F,G).

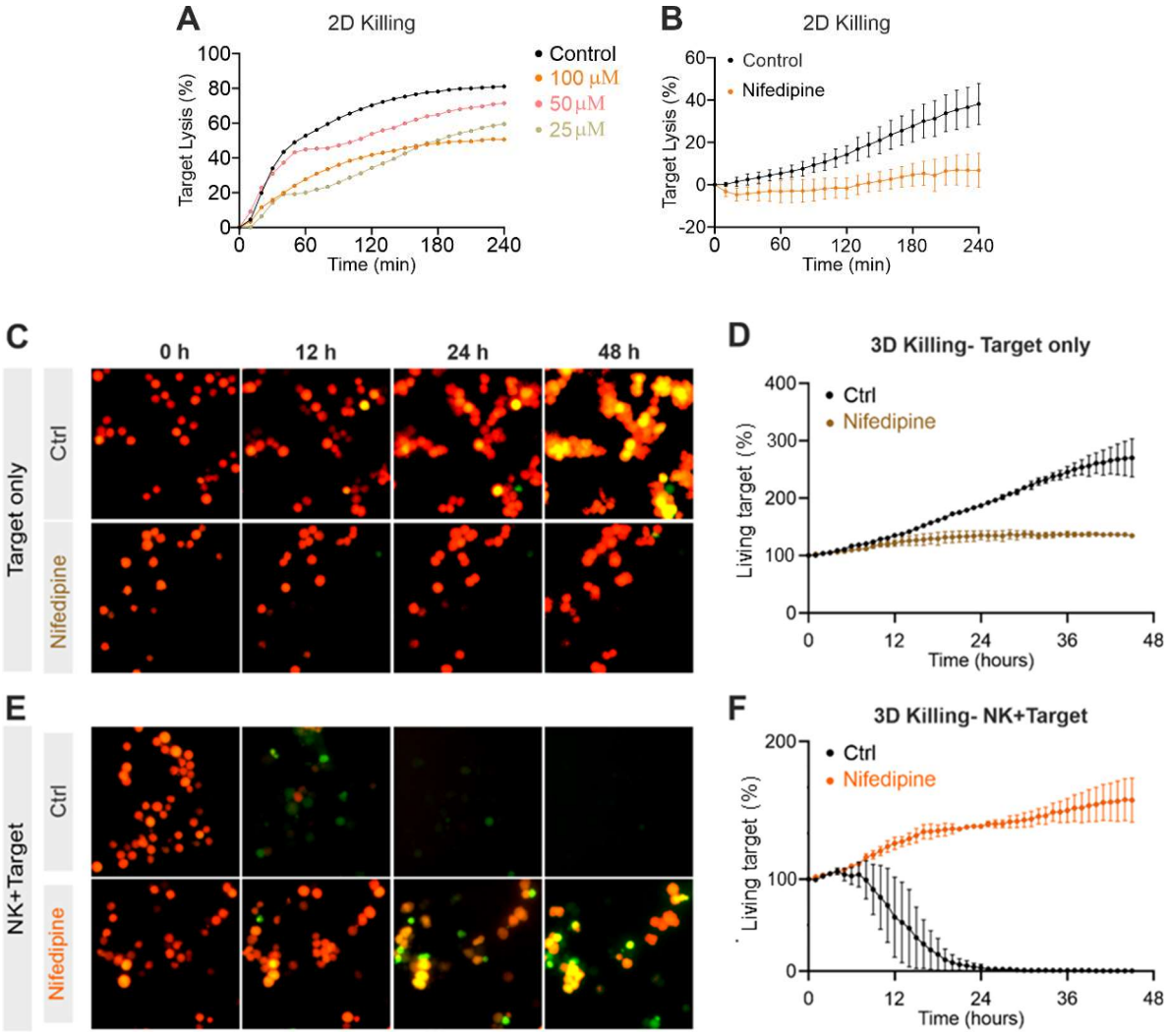

Figure 14: Treatment of NK cells with nifedipine leads to inefficient target cell lysis. *Primary human NK cells from healthy donors were stimulated with IL-2 for three days. A,B) Usage of nifedipine impairs target cell lysis in a real-time killing assay. K562 target cells were stained with calcein-AM. Different concentrations of nifedipine were used to optimize the concentration to be used for further experiments (A). A real-time killing assay was performed for 4 hours with a 10-minute interval with a 100 µM concentration of nifedipine. E:T ratios of 2.5:1 (A) and 1:1 (B) were used .C-F)2mg / mL collagen matrix was prepared with K562 pCasper target cells co-polymerized in it. NK cells were settled on top. K562-pCasper cells in orange-yellow were live cells and in green were apoptotic. (C-D) Treatment with nifedipine (100 µM) affects target viability where target cells were in nifedipine containing medium for 48 hours. Time lapse imaging (C) and corresponding quantification (D) are shown. (E-F) NK cells treated with nifedipine showed a diminished killing. E:T ratio of 2.5:1 was used with the killing being imaged for 48 hours with a 20-minute interval. Time lapse images (E) and corresponding quantification is shown here (n=2) (F). Scale bars are 40 µm. Data from three independent experiments is shown here.*

These results suggest that treatment of NK cells with gadolinium and nifedipine to impair their killing efficiency both in 2D and 3D killing scenarios.

Next, we investigated underlying mechanisms leading to inefficient target cell lysis by NK cells treated with either gadolinium or nifedipine. One of the major ammunitions of NK cells is release of cytotoxic granules which can be estimated by CD107a, a marker for degranulation in NK cells. It was found that the release of lytic granules induced by the target cells was unaltered when gadolinium (Figure 15A,B) and nifedipine were used (Figure 15G, H). The major component of lytic granules is perforin and granzyme B. The expression levels of perforin and granzyme B were examined using a flow cytometer. The expression of perforin and granzyme B was unaltered when NK cells were treated with gadolinium (Figure 15C-F) or nifedipine (Figure 15I-L). These results clearly indicate that the lytic granule pathway remained unaffected in mechanosensing in NK cells treated with gadolinium or nifedipine.

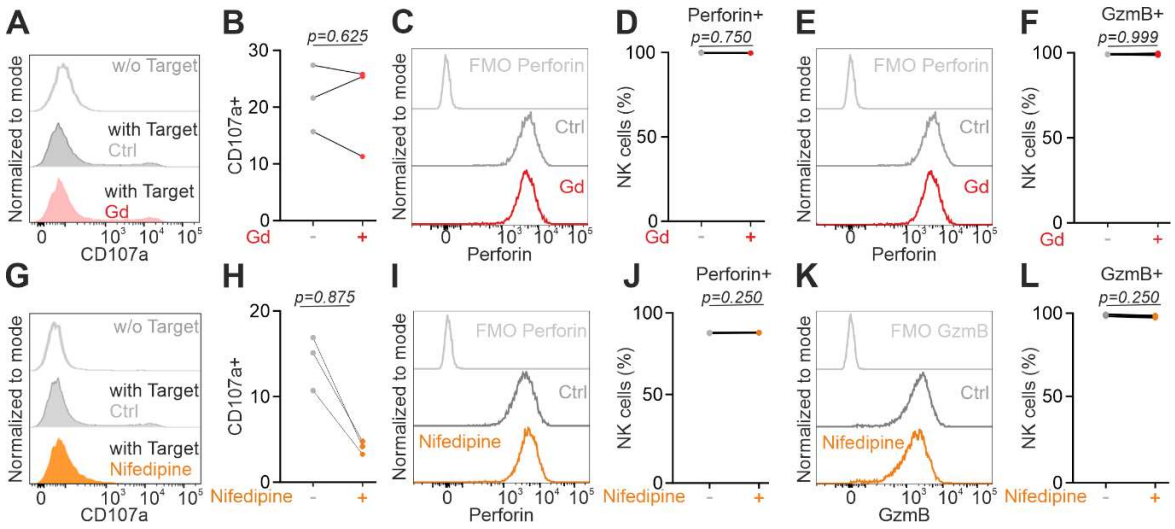

Figure 15: Lytic granule pathway is not affected by mechanosensing. *Primary human NK cells from healthy donors were stimulated with 100 U/ mL of IL-2. Degranulation assay was performed for 4 hours with CD107a as a marker for lytic granule release in presence of gadolinium or nifedipine medium. Treatment with gadolinium did not affect secretion of lytic granules. (A-B) Flow cytometry data from one representative donor (A) and corresponding quantification from three donors (B) is shown here. (G-H) Similarly, treatment of NK cells with nifedipine did not affect secretion of lytic granules. Flow cytometry data from one representative donor (G) and corresponding quantification from three donors (H) is shown here. (C-F; I-L) Expression of Perforin and GzmB is unaltered in NK cells treated with either gadolinium or nifedipine. NK cells were fixed for performing cytotoxic protein expression of perforin and GzmB where they were incubated in the inhibitor containing medium overnight. Flow cytometry data from one representative donor for gadolinium treated (C) or nifedipine treated (I) NK cells and corresponding quantification for three donors (D,J) for perforin is shown here. Flow cytometry data from one representative donor for gadolinium treated (E) or nifedipine treated (K) NK cells and corresponding quantification for three donors (F,L) for GzmB is shown here. For statistical analysis, Wilcoxon matched pairs signed rank test was used. . Data from three independent experiments is shown here.*

All these results taken together show that gadolinium or nifedipine treated NK cells to exhibit diminished target cell lysis even though they possessed an unaltered lytic granule pathway. It also has to be however noted that these two inhibitors even though widely used are non-specific antagonizers of mechanosensitive channels.

In addition, I also tested whether cytotoxicity of NK cells could be influenced when culturing on different stiffness. To mimic *in vivo* scenarios, freshly isolated PBMCs were cultured on substrates with different stiffness without IL-2 for 4 days. Commercially available cell culture plates with substrates of physiologically relevant stiffness of 0.2, 0.5, 2, 8, 16, 32 and 64 kPa were coated with fibronectin. On day 4, a killing assay was performed in 3D scenario where K562, target cell line for NKs was used to assess the cytolytic activity of NK cells. PBMCs cultured on a normal cell culture plate was used as control. PBMCs from 5 donors were used and each donor had a variable response. An enhanced killing of the target was noticed for PBMCs cultured on 64 kPa substrate (donor #1, #3), 8 kPa (donor #2), no significant killing of target (donor #4) and 32 kPa (donor #5). PBMCs cultured on softer substrates showed a poor target killing – 2 kPa (donor #1, #3, #4, #5) and 0.2 kPa (donor #2) (Figure 16A-E). These results corroborate earlier results presented that stiff substrates activate NK cells and softer substrates fail to do so which is also evident from the killing kinetics presented here.

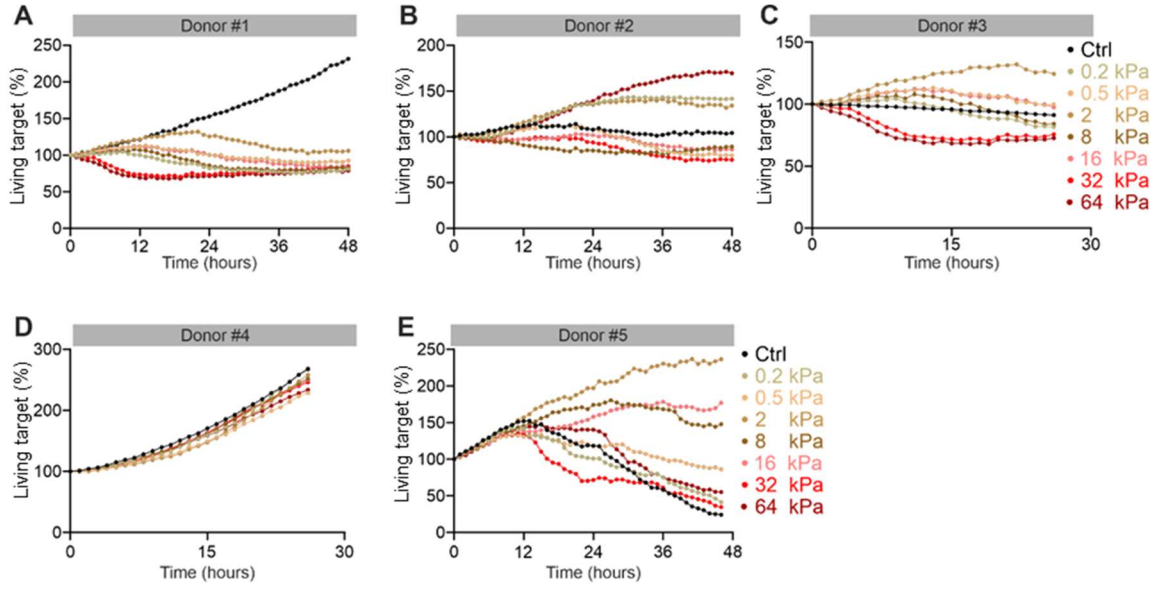

Figure 16: Culturing NK cells on substrate with different stiffness alters their killing efficiency. *(A-E) Freshly isolated PBMCs (not stimulated by IL-2) were cultured on the plates of varied quantified stiffness for 4 days. K562-pCasper were embedded in a 2 mg/ mL collagen and PBMCs were settled on top of the matrix. Time lapse imaging was performed for at least 30 hours on ImageXpress. Effect of substrate stiffness on killing efficiency of PBMCs was highly variable and donor dependent (A-E). Data from five independent experiments is shown here.*

3.1.5. Mechanosensing in NK cells is mediated via PIEZO1

Data till now has shown NK cells to be mechanosensitive and perturbation of mechanosensitive channels with widely used unspecific antagonists such as gadolinium and nifedipine to impair NK cytolytic activity. Hence, the effect of specific mechanosensitive channel widely expressed in human NK cells was investigated. PIEZO1 was shown to be a professional mechanotransducer in many cell types including many immune cells such as T cells, macrophages etc. Microarray data from our lab has shown a very high expression of PIEZO1 but not PIEZO2 in primary human NK cells. To understand the influence of PIEZO1 in NK cells GsMTx4, an antagonist specific for PIEZO1 channel was used. Mechanosensing also includes sensing the stiffness of substrate. Hence, to investigate the functional role of PIEZO1 in mediating NK response to stiffness, NK cells treated with GsMTx4, and corresponding controls were settled on PAAm-co-AA hydrogels with Young's Modulus of 2, 12, and 50 kPa. The response of NK cells to substrates of varied stiffness has been detailed in the earlier section. Application of GsMTx4 completely abrogated the response of NK cells to 50 kPa substrate (Figure 17A, B), no change in one donor on NK cells which responded to 12 kPa (Figure 17C, D), in donors whose NK cells responded to all stiffness, blockade of PIEZO1 completely brought it down (Figure 17E, F) and there was no change in the ones who responded to none (Figure 17G, H). It was however interesting to note that NK cells treated with GsMTx4 responded almost always to 2 KPa stiffness even when the controls did not (Figure 17A-D).

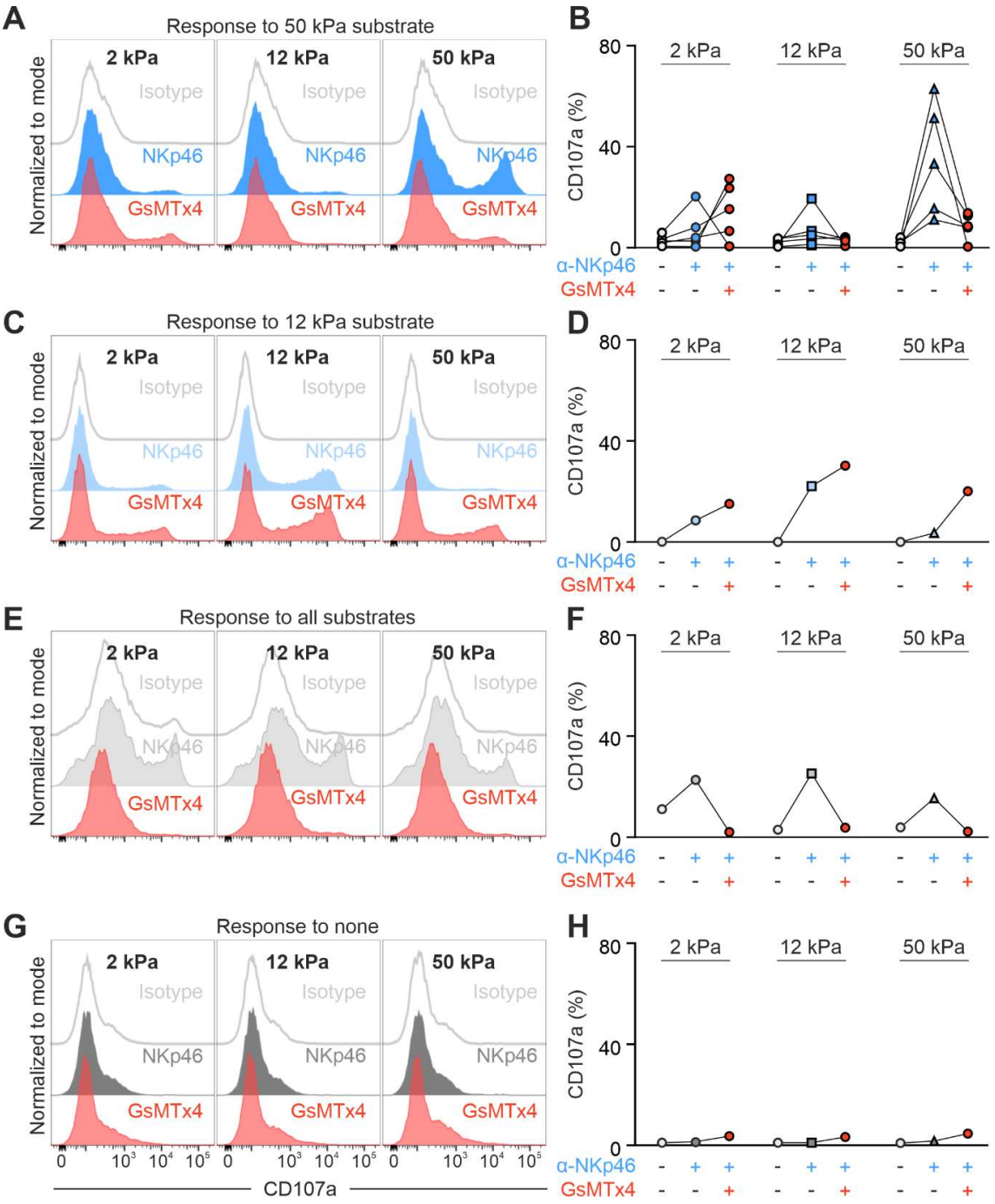

Figure 17: Response of NK cells to substrates of varied quantified stiffness. *Primary human NK cells were stimulated with IL-2 for three days. (A-G) Blockade of PIEZO1 totally eliminates the stiffness induced NK response. The NK cells along with anti-CD107a antibodies and Golgi stop were incubated on functionalized hydrogel substrates at 37°C with 5% CO2 for 4 hours. Later the degranulation data were acquired using flow Blocking of PIEZO1 brought down considerably the*

response of NK cells to 50 kPa (A-B, n=6), not much change in response to 12 kPa (C-D, n=1), completely abrogated the NK response all stiffness levels (E-F, n=1), no change where they did not respond to any stiffness (G-H, n=1). The flow cytometry data of one representative donor is shown here along with the quantification of all donors.

PIEZO1 regulates target cell lysis

The data till now clearly show PIEZO1 to be involved in sensing the stiffness of substrate blockade of which completely brought down NK mediated response. Next step was to investigate the role of PIEZO1 in regulating NK effector functions. For this GsMTx4, an antagonist specific for PIEZO1 channel was used. A 3D killing assay was performed to analyse the killing kinetics of NK cells treated with GsMTx4. The effect of GsMTx4 on the target cell viability was negligible as the proliferation of the target cells in presence of the inhibitor was similar to that of the control (Figure 18A, B). Blockade of PIEZO1 lead to an impaired target cell lysis which can be clearly seen in Figure 18C, D.

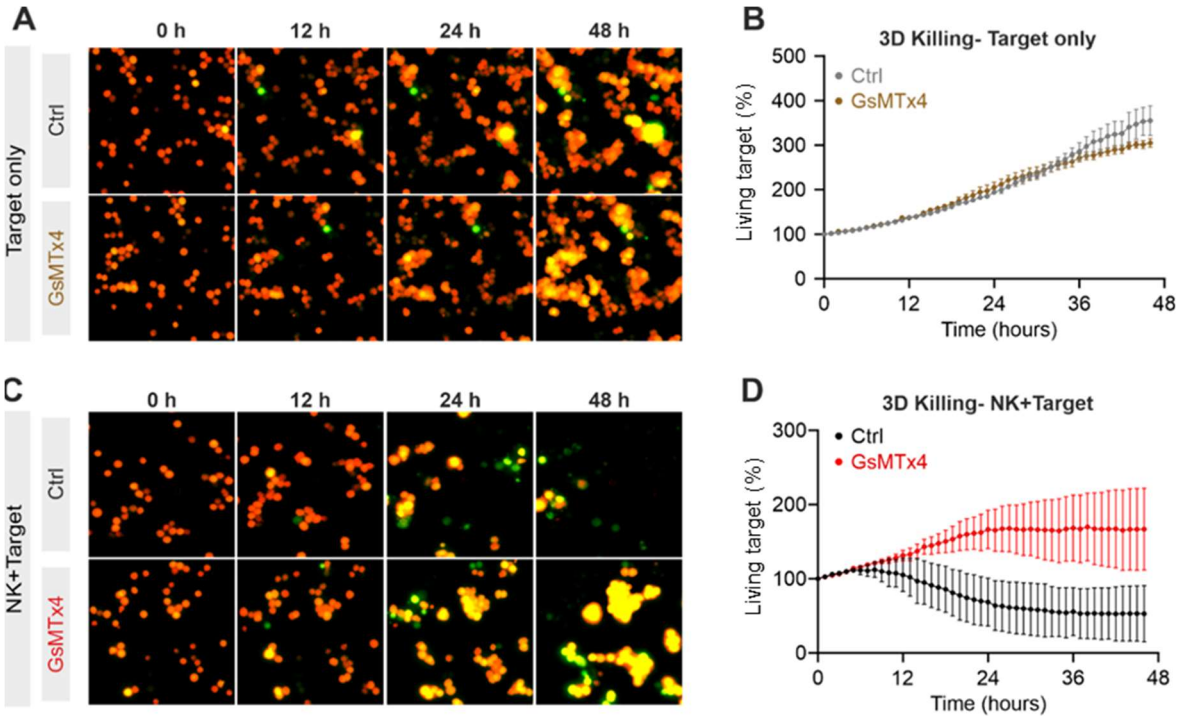

Figure 18: PIEZO1 plays a crucial role in NK cytolytic activity. *Primary human NK cells from healthy donors were stimulated with 100 U/ mL of IL-2. K562 pCasper target cells were co-polymerized in collagen matrices and NK cells were settled on top. K562-pCasper cells in orange-yellow were live cells and in green were apoptotic. (A-B) Blocking PIEZO1 using GsMTx4 (50 µM)*

does not affect target viability where target cells were in GsMTx4 containing medium for 48 hours. Time lapse imaging (A) and corresponding quantification (B) are shown. (C-D) NK cells treated with GsMTx4 showed a diminished killing. E:T ratio of 1:1 was used with the killing being imaged for 48 hours with a 20-minute interval. Time lapse images (C) and corresponding quantification is shown here (D). Scale bars are 40 µm. Data is shown from three independent experiments. The figure has been adapted from [109].

Given the NK cells used here were primary NK cells, proliferation within 48 hours is unlikely. Nevertheless, to rule out the effect on GsMTx4 on the NK cells proliferation they were stained with CFSE and cultured in GsMTx4 containing medium for 48 hours to replicate the conditions of 3D killing. The proliferation of NK cells was determined using a flow cytometer. No significant difference was observed between GsMTx4 treated and untreated NK cells (Figure 17B,C). To further confirm that GsMTx4 did not influence the viability of NK cells, propidium iodide (PI) which is permeates only dead cells was used. NK cells cultured in inhibitor containing medium did not differ in their viability compared to the untreated cells (Figure 17A,B).

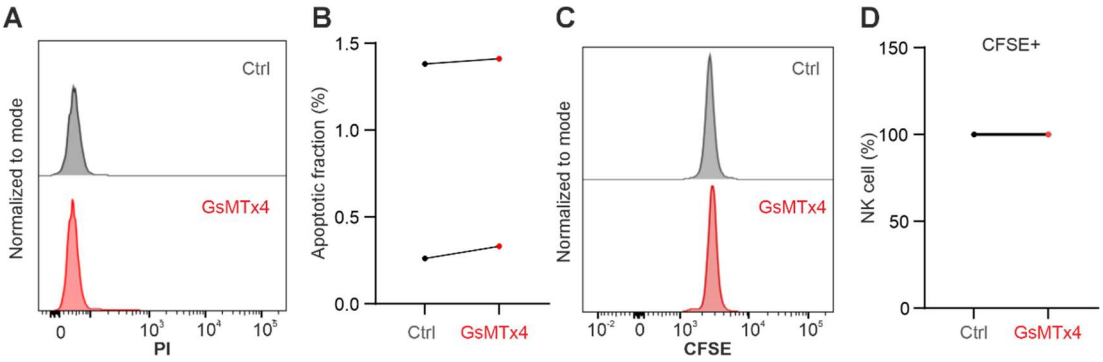

Figure 19: GsMTx4 does not affect the viability of NK cells. *Primary human NK cells were incubated in GsMTx4 containing medium for 48 hours. A PI staining was performed to detect the apoptotic cells. Quantification (B) and one corresponding donor (A) are shown here. A CFSE staining was done to check for the cell proliferation. Quantification (B) and one corresponding donor (A) are shown here. Data is from two independent experiments.*

To discover the underlying mechanism for a drastic decline in the cytotoxicity of NK cells whose PIEZO1 was antagonized lytic granule pathway was studied. Degranulation of NK cells upon contact with the target cells was assessed using CD107a as a marker. There was a slight increase in release of lytic granules by NK cells treated with GsMTx4 but it was not statistically significant (Figure 20A,

B). Perforin and granzymes are the major cytotoxic proteins of the lytic machinery. Hence, the expression of perforin and granzyme B was evaluated using flow cytometry. Perforin and granzyme B was unaltered in NK cells with perturbed PIEZO1 channels (Figure 20C-F).

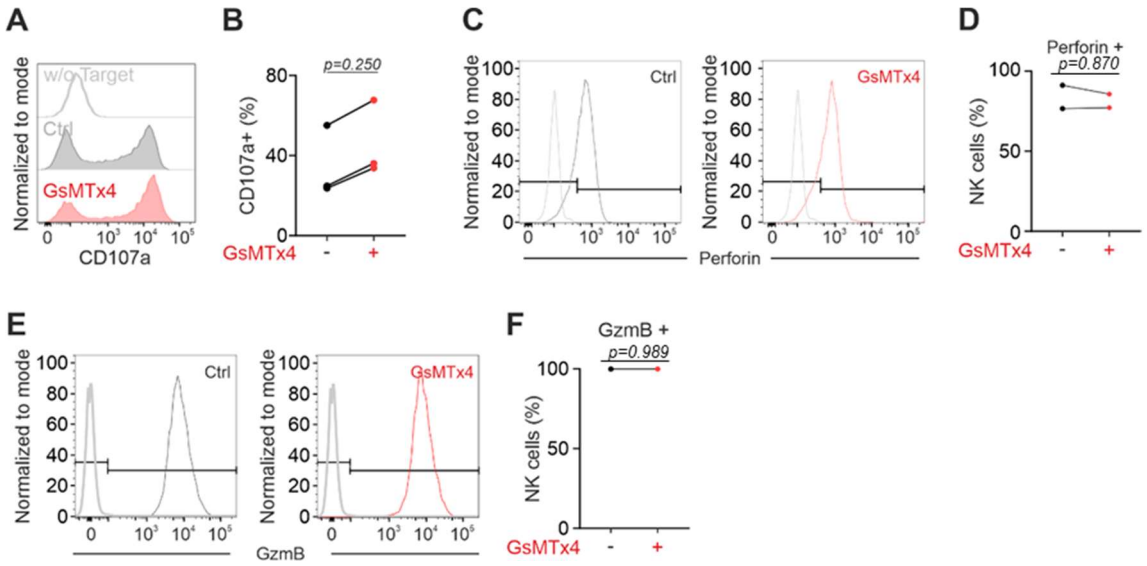

Figure 20: Lytic granule pathway remains unaffected when PIEZO1 mediated mechano-sensing is inhibited. *Degranulation assay was performed for 4 hours with CD107a as a marker for lytic granule release in presence of GsMTx4 containing medium. Inhibition of PIEZO1 did not affect secretion of lytic granules. (A-B) Flow cytometry data from one representative donor (A) and corresponding quantification from three donors (B) is shown here. (C-D) Expression of Perforin is unaltered in NK cells treated with GsMTx4. Flow cytometry data from one representative donor (C) and quantification from two donors (D) is shown here. (E-F) Expression of GzmB is unaltered in NK cells treated with GsMTx4. Flow cytometry data from one representative donor (E) and quantification from three donors (F) is shown here. For statistical analysis, Wilcoxon matched-pairs signed rank test was used.*

PIEZO1 knockdown was performed on freshly isolated primary NK cells using nucleofector technology, an improved electroporation technology by using 150nM (Figure 20) PIEZO1 targeting siRNA. It was not possible to downregulate PIEZO1 expression. PIEZO1 knockdown was also performed NK cells stimulated with 100 U/ mL of IL-2. Protein expression was checked after 24 hours and 36 hours. Unfortunately, knocking down PIEZO1 in primary NK cells ended up with zero success.

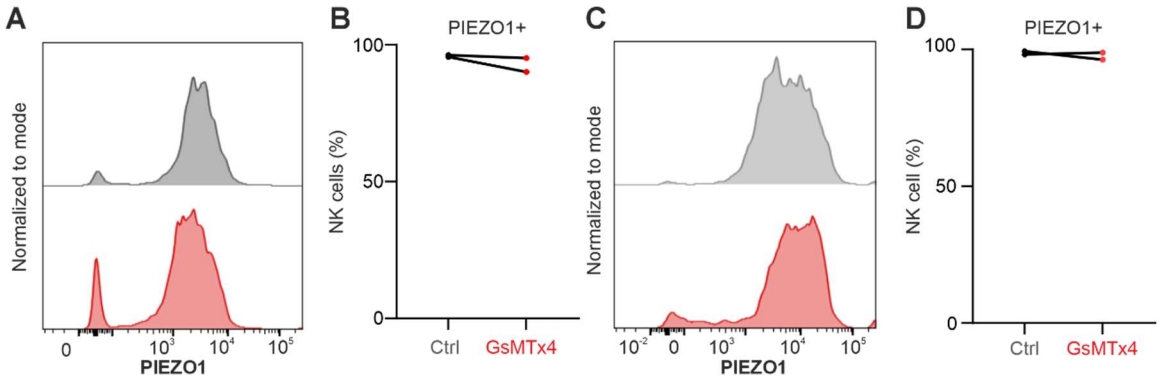

Figure 21: siRNA knockdown of PIEZO1 expression in NK cells. *Primary human NK cells stimulated with 100 U/ mL of IL-2 were used. 24 hours after the transfection PIEZO1 expression was checked using flowcytometry (A,B) of which one representative donor of two and the corresponding quantification are shown. 36 hours after the transfection PIEZO1 expression was checked using flowcytometry (C,D) of which one representative donor of two and the corresponding quantification are shown.*

The data clearly show that PIEZO1 inhibition disarms NK cells of its cytotoxicity. To investigate if activation of this channel would lead to an enhanced target cell lysis Yoda-1, a potent and specific agonist for PIEZO1 was used to activate PIEZO1 of primary NK cells. Different concentrations of Yoda-1 were tested. Very high concentration of Yoda-1 was cytotoxic to the target cells (Figure 22A) and so was 8 µM (Figure 22B).

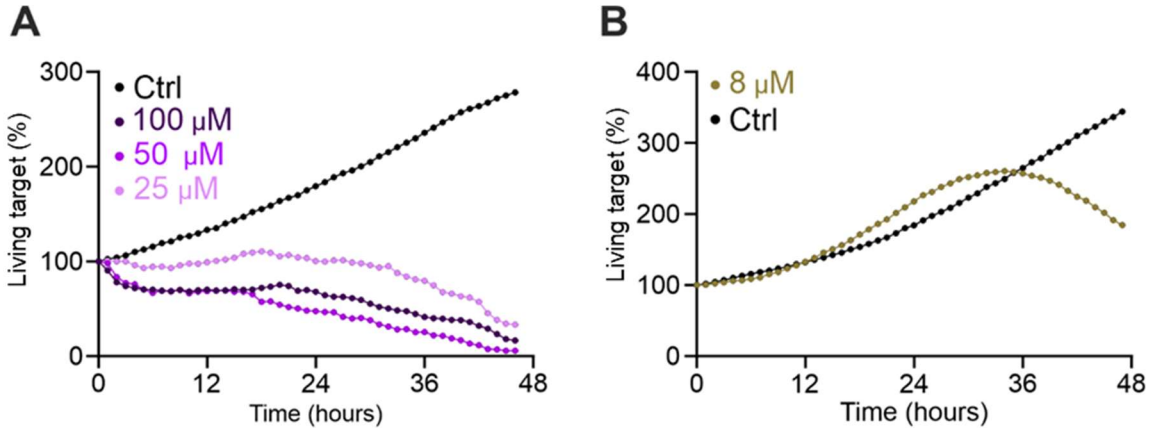

Figure 22: High concentrations of Yoda-1 is cytotoxic to target cells. *K562-pCasper cells were embedded in a 2 mg/ mL collagen matrix. Yoda-1 containing medium for 48 hours was used to*

perform a 3D killing assay for 48 hours. Target cells exposed to a very concentration of Yoda-1 were apoptotic (A-B). NK cells were not added to the target cells here.

To unravel the role of PIEZO1 in NK cytotoxicity, NK cells were treated with Yoda-1. A killing assay was performed in 3D for 48 hours. There was no adverse effect of Yoda-1 on target cell viability and proliferation (Figure 23A). Activation of PIEZO1 channel led to an enhanced target cell lysis when compared to the control (Figure 23B).

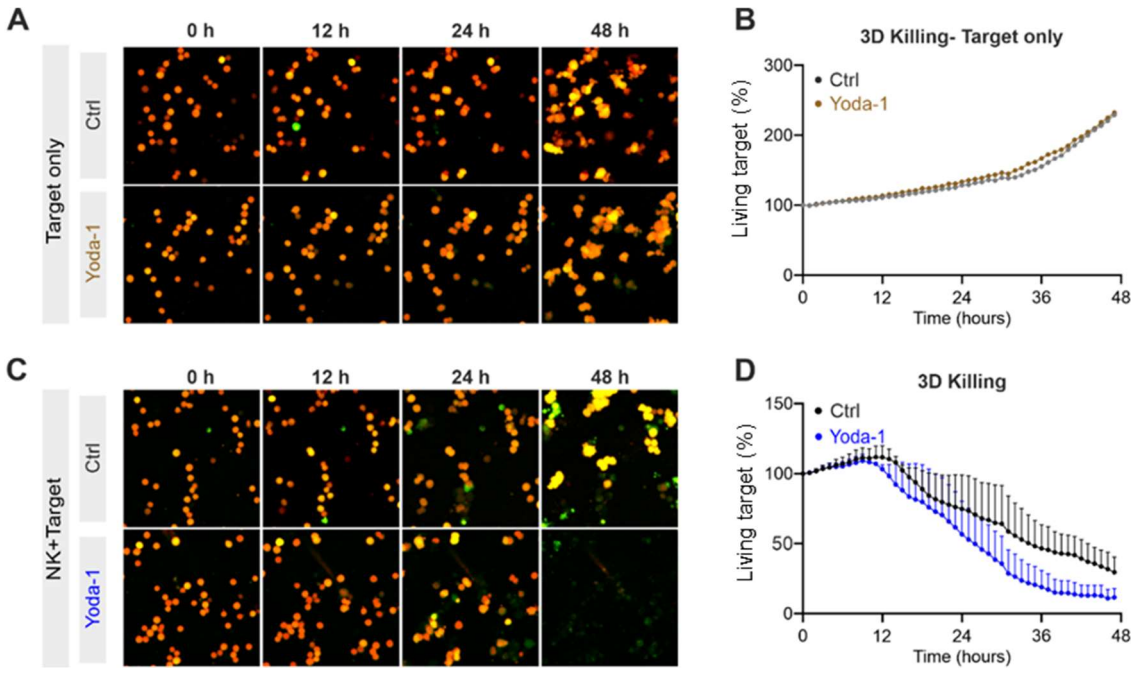

Figure 23: Yoda-1 boosts PIEZO1 mediated killing of the target cells. *Primary human NK cells from healthy donors were stimulated with 100 U/ mL of IL-2. K562 pCasper target cells were co-polymerized in collagen matrices and NK cells were added on top. K562-pCasper cells in orange-yellow were live cells and in green were apoptotic. (A-B) Activation of PIEZO1 using Yoda-1 (1 µM) does not affect target viability where target cells were in Yoda-1 containing medium for 48 hours. Time lapse imaging (A) and corresponding quantification (B) are shown. (C-D) NK cells treated with Yoda-1 showed an enhanced killing efficiency. E:T ratio of 1:1 was used with the killing being imaged for 48 hours with a 20-minute interval. Time lapse images (C) and corresponding quantification (n=3) is shown here (D). Scale bars are 40 µm. Data is shown from three independent experiments. The figure has been adapted from* [109].

In order to investigate the reason for potentiated target cell lysis when PIEZO1 of NK cells was activated, lytic granule pathway was checked. One way to indirectly measure NK cytotoxicity is to check for degranulation induced upon contact with the target. Here, CD107a was used as a marker for NK degranulation which was measured using flow cytometer. There was no difference in release of lytic granules between untreated and Yoda-1 treated NK cells (Figure 24A,B). NK cells without any target in AIMV medium and Yoda-1 containing medium were used as controls to check for spontaneous release of lytic granules. These results imply that the lytic granule pathway is not involved in PIEZO1 pathway of NK cells.

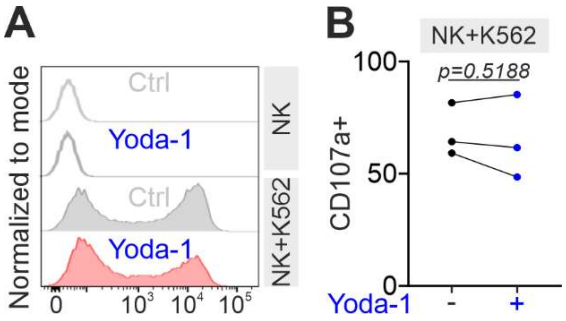

Figure 24: Lytic granule pathway remains unaffected when PIEZO1 was activated. *Degranulation assay was performed for 4 hours with CD107a as a marker for lytic granule release in presence of Yoda-1 containing medium. Activation of PIEZO1 did not affect secretion of lytic granules. Flow cytometry data from one representative donor (A) and corresponding quantification from three donors (B) is shown here. The figure has been adapted from* [109].

Activation of NK cells is a tightly regulated process for which to happen recognition of target cell and formation of a stable contact is essential. Then the cytoskeleton is rearranged, and lytic granules are polarized towards the IS. If there is an increase in the number NK-target conjugates formation this would be reflected in the killing of targets. To elucidate the mechanism mediating the increased NK cytotoxicity, NK-target conjugate formation was evaluated. NK cells were stained with CD56 and target cells with calcein-AM. NK cells were gently mixed with target cells and formation of stable conjugates was evaluated on a flow cytometer. There was no significant difference in formation of NK-target conjugates between untreated and Yoda-1 treated NK cells (Figure 25A,B).

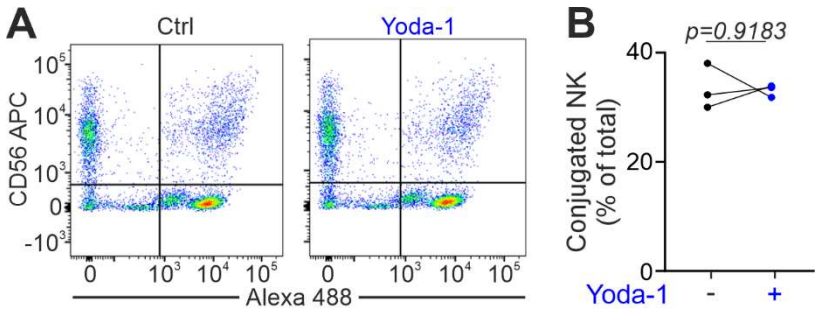

Figure 26: NK-target conjugation is not affected by activation of PIEZO1. *NK cells were stained with CD56 and target cells with calcein-AM. Doublets were counted as NK-target stable conjugates. (A-B) Flow cytometry data from one representative donor (A) and corresponding quantification from three donors (B) is shown here. Data is shown from three independent experiments. The figure has been adapted from* [109].

PIEZO1 plays a crucial role in NK infiltration into 3D matrix

The infiltration of killer cells through the collagen matrix plays a central role in determining the fate of target cells where more killer infiltration leads to faster searching and elimination of target while the opposite leads to a diminished target clearance. Infiltration of immune cells to the site of tumor has been shown to be correlated to the clinical outcome and sensitivity to immune therapy. To uncover if PIEZO1 influences the infiltration of NK cells into a 3D collagen matrix, NK cells stained with CFSE were visualized for 48 hours with a 20-minutes interval on a Imagexpress. NK cells whose PIEZO1 was blocked infiltrated the 3D matrix in substantially low numbers at almost every time point and time taken for the first few NK cells to infiltrate the matrix was more when compared to the untreated NK cells.

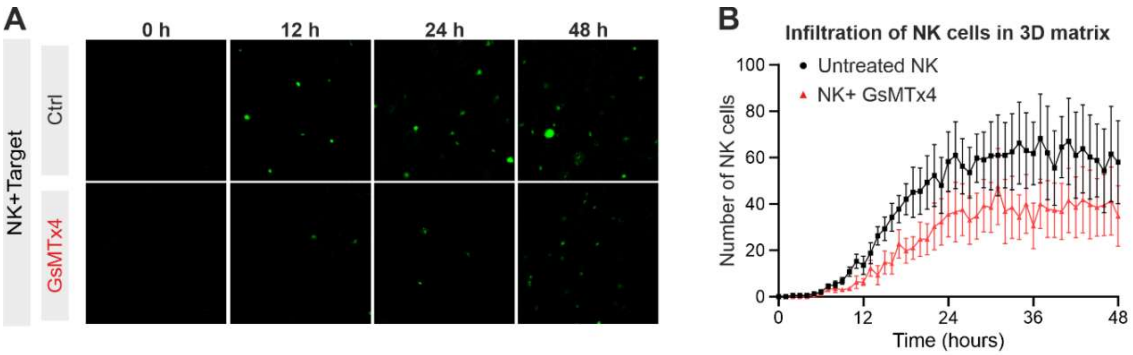

Figure 27: Infiltration of NK cells into a 3D matrix is impacted by PIEZO1 perturbation. *Primary human NK cells from healthy donors were stimulated with 100 U/ mL of IL-2. NK cells stained with CFSE were settled on top of 2 mg/ mL collagen matrix. The infiltration of NK cells into the matrix was imaged for 48 hours with a 20-minute interval. Time lapse images from one representative donor (A) and corresponding quantification from at least three donors (B) is shown here. Scale bars are 40 µm. The figure has been adapted from* [109].

In order to decipher the mechanism which potentiated the killing by NK cells whose PIEZO1 was activated, an infiltration assay in 3D was performed where NK cells were stained with CFSE and settled on top of a collagen matrix. The infiltration of NK cells was imaged for 48 hours on a high through put screening microscope. Infiltration of NK cells into 3D matrix was significantly enhanced when treated with Yoda-1 (Figure 28A). The time taken for the first few cells to infiltrate and appear on focal plane was also much faster for NK cells treated with Yoda-1. Untreated NK cells appeared first on the focal plane at 6.6±1.6 hours, whereas Yoda-1 treated cells were visualized at 4.8±1.7 hours (Figure 28B).

The data till now establish the NK cells to be mechanosensitive and mechanosensitivity mediated by "professional mechanotransducer" PIEZO1 to play a pivotal role in modulating the cytotoxicity of NK cells.

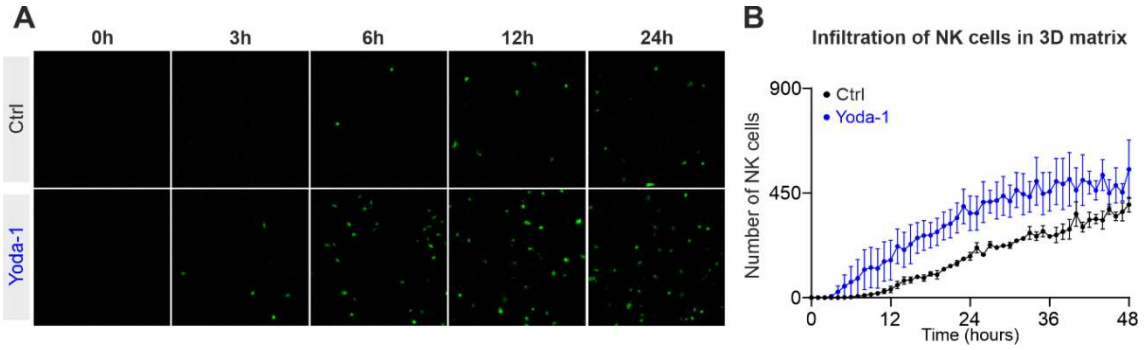

Figure 28: Infiltration of NK cells into a 3D matrix is boosted by PIEZO1 activation. *Primary human NK cells from healthy donors were stimulated with 100 U/ mL of IL-2. NK cells stained with CFSE were settled on top of 2 mg/ mL collagen matrix. The infiltration of NK cells into the matrix was imaged for 48 hours with a 20-minute interval. Time lapse images from one representative donor*

(A) and corresponding quantification from three donors (B) is shown here. Scale bar is 40 µm. The figure has been adapted from [109].

3.2 Part 2 – Characterization of immune response to *ClearColi*-encapsulated PluDA hydrogels

Living therapeutic materials (LTMs) is a recently emerging approach providing promising possibilities in the field of biomedicine as drugs delivering agents against diseases, biosensors, wound healing patches etc. [93]–[95]. The final outcome of the LTMs is to be able to use them in the clinics where a drug / protein producing bacteria is able to ameliorate the disease condition in patients. For potential therapeutical application, immune responses elicited against LTMs could be a major limiting factor. In an ideal case the material and the living component (bacteria in this case) of LTMs should not elicit an immune response. However, given that a foreign material is being introduced into the human body an immune response might be elicited but a hyperactive immune system would be detrimental to the host. In an ideal situation both the material (PluDa) and the engineered bacteria (*ClearColi* in this thesis) should not elicit any immune response. Even though there are many *in vivo* studies carried out to test their therapeutic effects, what immune responses would be triggered by the hydrogel and bacterial components has not been characterized. In this part, I have addressed this point using PBMCs from healthy donors and bacterial encapsulated PluDA hydrogels.

This project was done in collaboration with the group of Bioprogramable Materials, INM- Leibniz Institute for New Materials, Saarbrucken. Preparation of the PluDA gels, encapsulation of *ClearColi* and *E.coli* in hydrogels and the corresponding quality check was done by Shardul Bhusari supervised by Dr. Shrikrishnan Sankaran. I performed PBMC-related experiments and the corresponding analysis.

3.3.1. Immune response elicited by *ClearColi*

To test the immunogenicity of *ClearColi in vitro*, *E.coli* was used as a positive control. PBMCs isolated from healthy donors were cultured for 3 days with *E.coli* or *ClearColi* strains in direct contact or with bacteria separated from the PBMCs using a nanoporous membrane which allows an exchange of soluble factors. PBMCs alone without any bacteria were used as a control. The schematic is depicted in Figure 29A. Cytokine and cytotoxic proteins released by PBMCs in response to the bacteria were assessed using a bead based multiplex cytokine assay. When the PBMCs were in direct

contact with the bacteria, both *E.coli* and *ClearColi* elicited an immune response where high release of IL-6, meagre release of TNFα and IFNγ was observed. The level of factors secreted, especially IL-6 was much higher in *E.coli* when compared to *ClearColi*. In the transwell condition where the bacteria are separated from the PBMCs on day 1 there was negligible release of cytokines or cytotoxic proteins but on day 2 IL-6 was the major cytokine that was released with *E.coli* inducing the release more when compared to *ClearColi* (Figure 29B). A PI staining was performed on day 3 to detect if PBMCs were apoptotic when in direct contact and separated by transwell insert. It was seen that at least half of the PBMCs which were in contact with bacteria or separated by a nanoporous membrane were apoptotic. Hence, cytokine profiles from day 3 are not here (Figure 29C, D). For the remaining PBMCs were harvested on day 3 and a FACS staining was performed to differentiate T and NK cell subtypes. Immune cells polarize to subtypes with diverse functional capabilities. Presence of *E.coli* lead to polarization of NK cells to a more cytotoxic $CD16^{dim}$ subset whereas *ClearColi* did not trigger any such polarization compared to PBMCs without bacteria (Figure 29E,F). $CD4^{+}$ (Figure 29G, H) and $CD8^{+}$ (Figure 29 I, J) subtypes were also examined where no change was observed between Naïve, central memory, effector memory and effector T cells. However, it has to be noted that most of the PBMCs were apoptotic due to exposure to bacteria, so the number population of the cells has become smaller. These results clearly show that *ClearColi* is less immunogenic compared to *E.coli.*

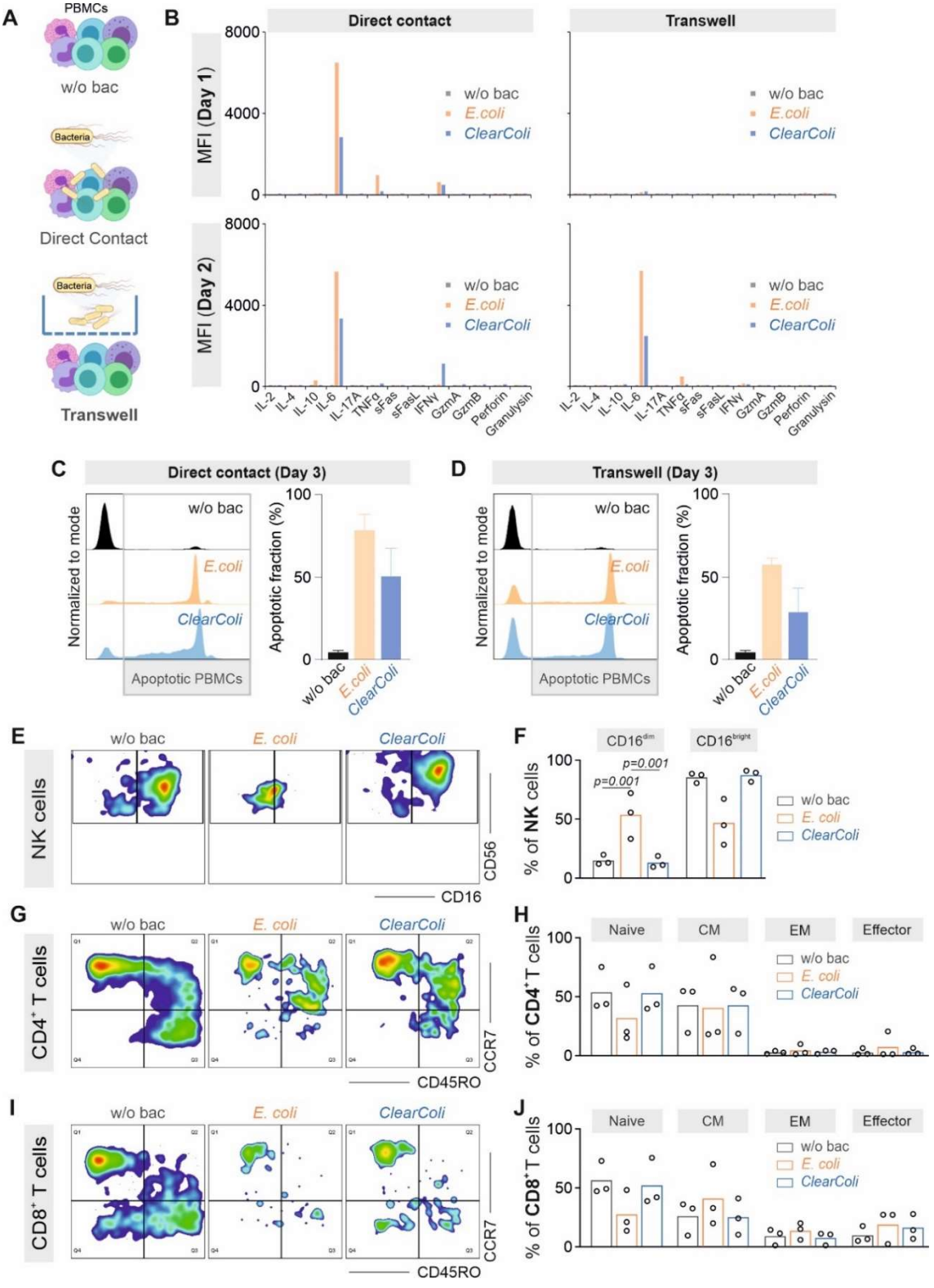
A
PBMCs
w/o bac
Bacteria
Direct Contact
Bacteria
Transwell
B
Direct contact
Transwell
MFI (Day 1)
MFI (Day 2)
8000
4000
0
w/o bac
E.coli
ClearColi
IL-2
IL-4
IL-10
IL-6
IL-17A
TNFα
sFas
sFasL
IFNγ
GzmA
GzmB
Perforin
Granulysin
C
Direct contact (Day 3)
Normalized to mode
w/o bac
E.coli
ClearColi
Apoptotic PBMCs
Apoptotic fraction (%)
100
50
0
D
Transwell (Day 3)
E
NK cells
w/o bac
E. coli
ClearColi
CD56
CD16
F
CD16dim
CD16bright
p=0.001
p=0.001
% of NK cells
G
CD4+ T cells
CCR7
CD45RO
H
Naive
CM
EM
Effector
% of CD4+ T cells
I
CD8+ T cells
J
% of CD8+ T cells

Figure 29: Immune response of PBMCs when in contact or separated by a nanoporous membrane with bacteria. A sketch of different conditions assessed in this work (A). PBMCs cultured in three conditions where they were cultured alone (w/o bac), co-cultured with bacteria (Direct Contact), or with bacteria in a transwell insert (Transwell). B) Cytokine and cytotoxic proteins released by PBMCs. The cell culture media was collected on days 1, 2 and 3. C-D) Viability of PBMCs after 3 days of direct contact with bacteria (C) or separated by a transwell insert (D) was determined using PI staining. E-J) Subtypes of NK cells ($CD3^-/CD16^+/CD56^+$) , $CD4^+$ T cells ($CD3^+CD8^-$) and $CD8^+$ T ($CD3^+CD8^-$) were acquired on flow cytometer upon surface staining. CM: central memory cells. EM: effector memory cells. MFI: mean fluorescence intensity. One representative donor is shown from total of three. The figure has been adapted from [119].

3.3.2. Blank PluDA gels are immune inert

To rule out the possibility of the PluDA hydrogel itself evoking an immune response, PBMCs were co-incubated with PluDA gels without bacteria (blank gel) for 3 days. Cytokine profiling showed that for donors 1 and 2 there was no release of any cytokines or cytotoxic proteins but for donor 3 there was slight IL-6 secretion which was negligible (Figure 30A). PBMCs in direct contact with *E.coli* was treated as a positive control. Blank gels did not alter NK (Figure 30 B,C) and T cell differentiation (Figure 30 D-G).

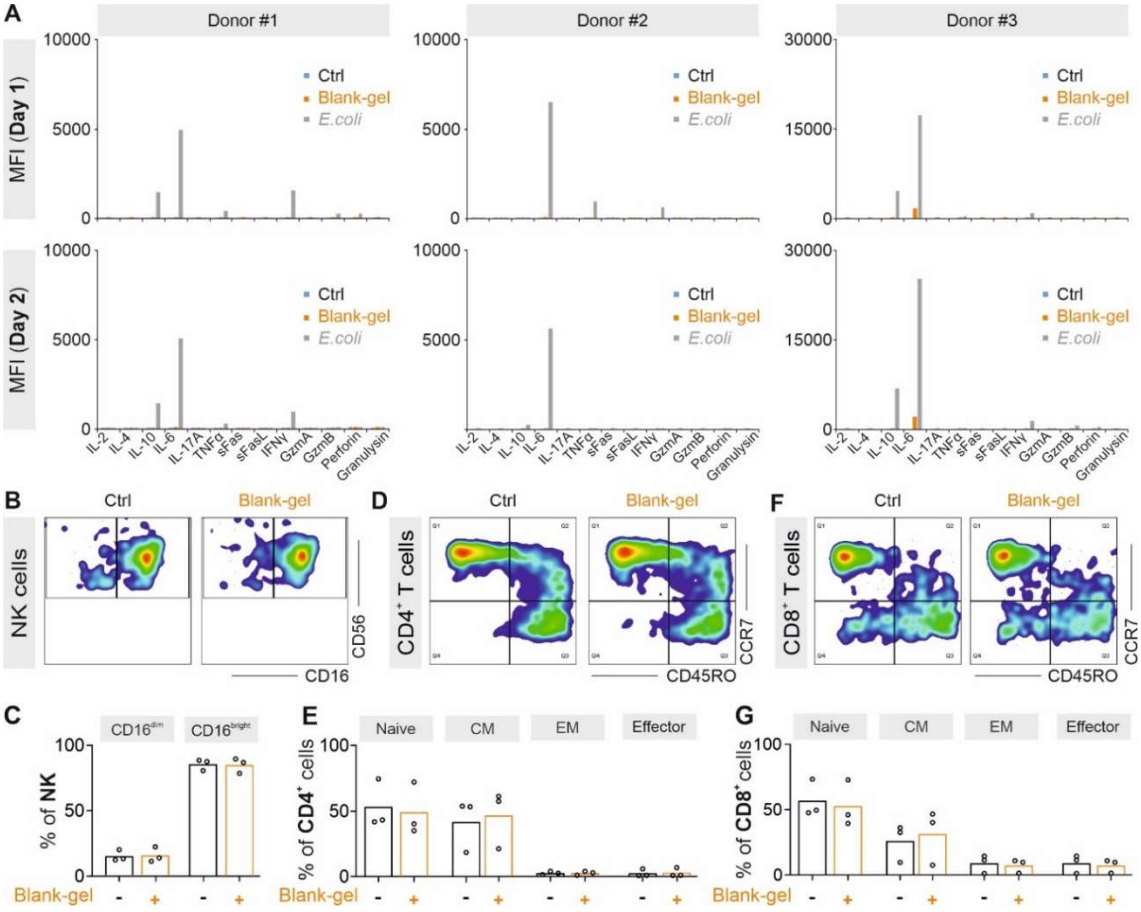

Figure 30: Response of PBMCs to blank PluDA gels. *PBMCs were cultured alone (Ctrl), co-incubated with PluDA hydrogels without any bacteria (Blank-gel), or in direct contact with E.coli (E.coli). A) Immune response of PBMCs when co-incubated with blank gels. The cell culture media collected on days 1 and 2 was used to analyse the cytokine profiles using multiplex cytokine assay. Subtypes of NK cells ($CD3^-/CD16^+/CD56^+$) , $CD4^+$ T cells ($CD3^+CD8^-$) and $CD8^+$ T ($CD3^+CD8^-$) were acquired on flow cytometer upon surface staining. CM: central memory cells. EM: effector memory cells. MFI: mean fluorescence intensity. One representative donor is shown from total of three. Results were from three donors. The figure has been adapted from* [119] [113].

3.3.3. Immune response to *ClearColi*-encapsulated gels

The bacteria were encapsulated in a PluDA hydrogel which has been shown to be non-immunogenic. PBMCs were co-cultured with either *ClearColi* or *E.coli*-encapsulated PluDA hydrogels. Cells were harvested on day 3 and a PI staining was performed to look for apoptotic cells. Close to 50 % of

PBMCs were found to be apoptotic when cultured with *E.coli*-encapsulated gels where as for the *ClearColi*-encapsulated gels the apoptotic fraction was negligible (Figure 31A). Cytokine profiling of the analytes on day 1 showed a release of IL-6 (Donors 1,2), TNFα, IFNγ (Donor 3) in both *E.coli* and *ClearColi*-encapsulated gels with *E.coli* triggering a higher release of the factors (Donors 2,3). Day 2 also followed the same trend with an addition of GzmB which was negligible in donor 1 and moderate in donors 2 and 3. Blank gels did not elicit release of cytokines and cytotoxic proteins during days 1 and 2 apart from a slight IL-6 release in donor 3. But on day 3 there was an IL-2 shoot up arising due to blank gels, *E.coli* and *ClearColi*-encapsulated gels in donor 1. IL-6, IFNγ, GzmB and a slight release of GzmA was also noticed in all the three donors (Figure 31B). It has to be considered here that for *E.coli*-encapsulated gels 50% of the PBMCs were dead on day 3 so the magnitude of cytokines released here would have been much higher had all the cells been alive. Hence, when comparing *E.coli* and *ClearColi*-encapsulated gels the release of cytokines and cytotoxic proteins is notably lower in *ClearColi*-encapsulated gels.

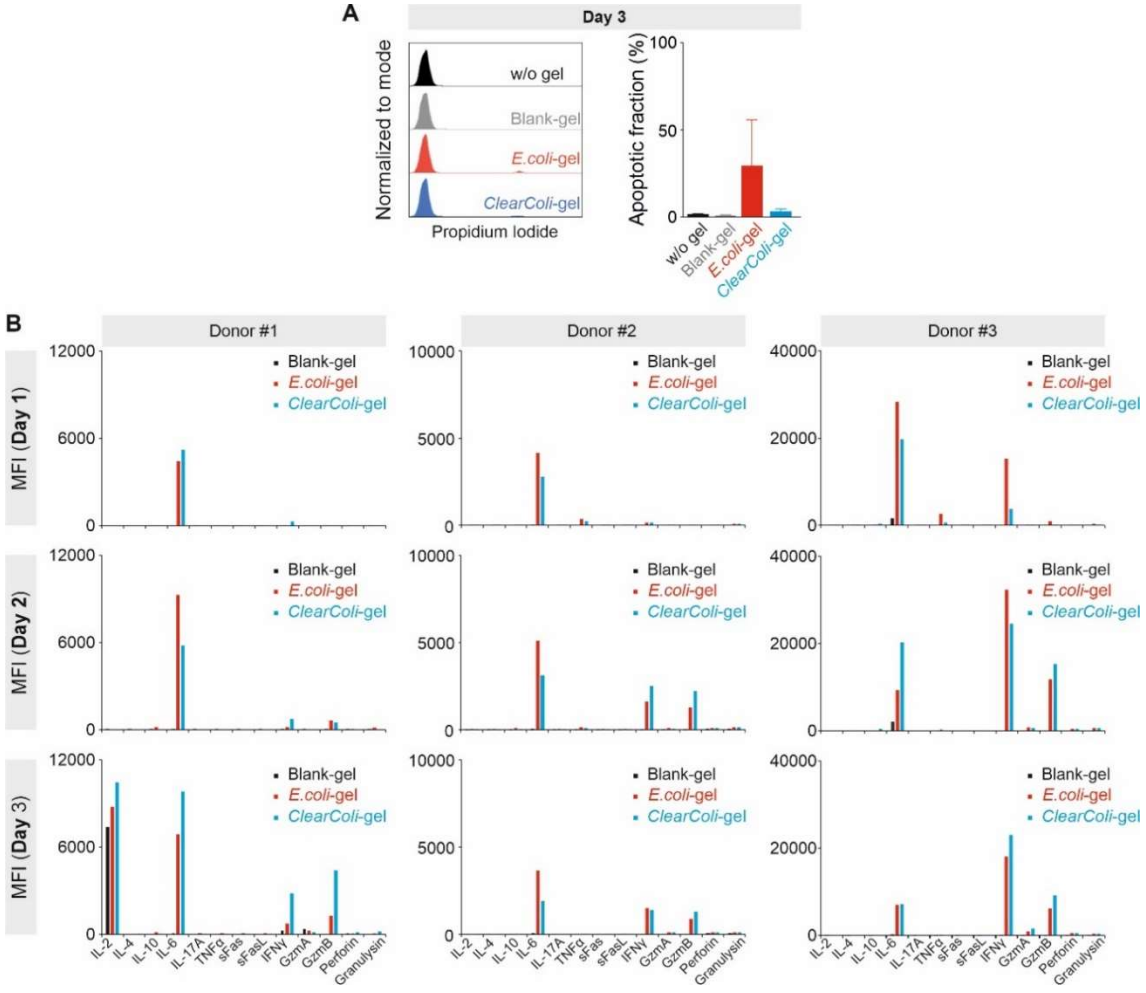

Figure 31: Immune response to PluDA gels with bacteria encapsulated in them. *PBMCs were co-incubated with blank-gel, E.coli*-encapsulated *(E.coli-gel) or ClearColi-encapsulated gels (ClearColi-gel). A) Viability of PBMCs was determined using PI. B) The cell culture media collected on days 1 and 2 was used to analyse the cytokine profiles using multiplex cytokine assay. The results presented are from three donors1. MFI: mean fluoresce intensity. The figure has been adapted from* [119].

3.3.4. *ClearColi*-encapsulated gels do not alter NK and T cell subtype differentiation

To explore if bacteria encapsulated gels would modify the subtype differentiation of NK and T cells, PBMCs co-cultured with *E.coli* and *ClearColi*-encapsulated gels were harvested on day 3. Antigen

specific staining was performed which was measured on a flow cytometer. There was no alteration in differentiation of NK cells and T cells when the bacteria were encapsulated. It was clear from Figure 29E that culturing of *E.coli* strain in direct contact with PBMCs polarized NK cell subtype towards a more cytotoxic $CD16^{dim}$ subtype but with encapsulation this effect was totally abrogated which implies this method of bacterial encapsulation to be an impeccable approach.

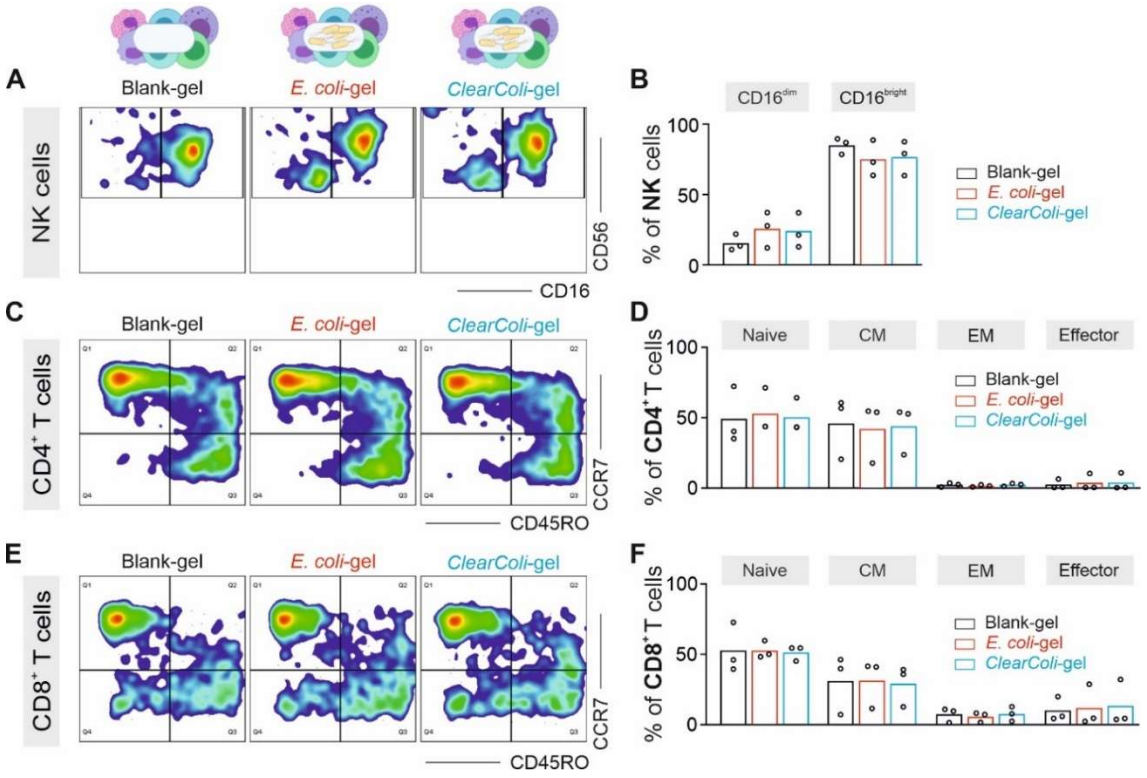

Figure 32:The impact of bacteria encapsulated hydrogels on subtypes of NK and T cells . *PBMCs were co-incubated with blank-gel, E.coli*-encapsulated *(E.coli-gel) or ClearColi*-encapsulated *gels (ClearColi-gel). A,C,E- Subtypes of NK cells ($CD3^-/CD16^+/CD56^+$) , $CD4^+$ T cells ($CD3^+CD8^-$) and $CD8^+$ T ($CD3^+CD8^-$) were acquired on flow cytometer upon surface staining and the corresponding quantification is shown here (B,D,F). CM: central memory cells. One representative donor is shown from a total of three. Results were from three donors. EM: effector memory cells. MFI: mean fluorescence intensity. The figure has been adapted from* [119]

3.3.5. Variable spontaneous IL-2 release among different donors

A total of six donors were used to characterize the immune response to *ClearColi*-encapsulated gels. Interestingly, based on the spontaneous IL-2 release on day 1 (without any external stimulation)

donors could be grouped into two- low spontaneous IL-2 group (donors 1,2 and 3) and a high spontaneous IL-2 releasing group (donors 4,5 and 6) (Figure 33). These two groups responded differently to the encapsulated bacterial gels. The results shown till now belonged to the group of low spontaneous IL-2 releasing group.

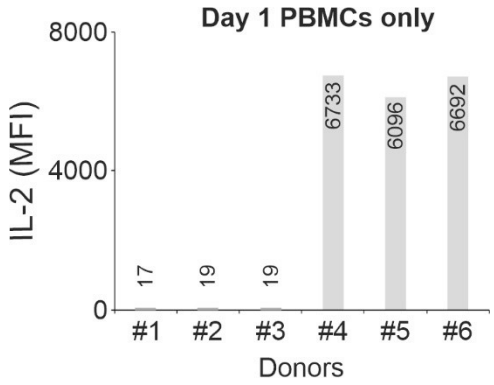

Figure 33: A comparison of IL-2 among different donors. *Cell culture media from PBMCs cultured without any bacteria or hydrogels was collected on day 1 for a multiplex cytokine assay to determine IL-2 levels. MFI: mean fluorescence intensity. The figure has been adapted from* [119]

3.3.6. Cytokine profile of donors with high spontaneous IL-2 release

In the donors with high spontaneous IL- 2 release on day 1 apart from IL-2, negligible IFNγ, GzmA, GzmB (donors 4, 5, 6), perforin and granulysin (donor 4) were observed in PBMCs alone with no bacterial exposure. For days 2 and 3, predominant IFNγ, GzmA and meagre release of GzmB, perforin and granulysin were observed in all donors for PBMCs without bacteria. There was a higher peak for *ClearColi* than *E.coli* for IL-6, IFNγ, GzmB, perforin on day 1(donors 4,5), almost comparable range of analytes (donors 4, 5) and *ClearColi* leading to a higher release of cytokines than *E.coli* (donor 6) on day 2. Day 3 also followed a similar trend apart from donor 5 where *E.coli* triggered release of cytokines was more than that of *ClearColi* (Figure 34A). A comparison between low and high spontaneous IL-2 release donors shows the IFNγ levels to be elevated (Figure 34B), a comparable level of IL-6 (Figure 34C) and an enhanced GzmA (Figure 34D) in the high spontaneous IL-2 group.

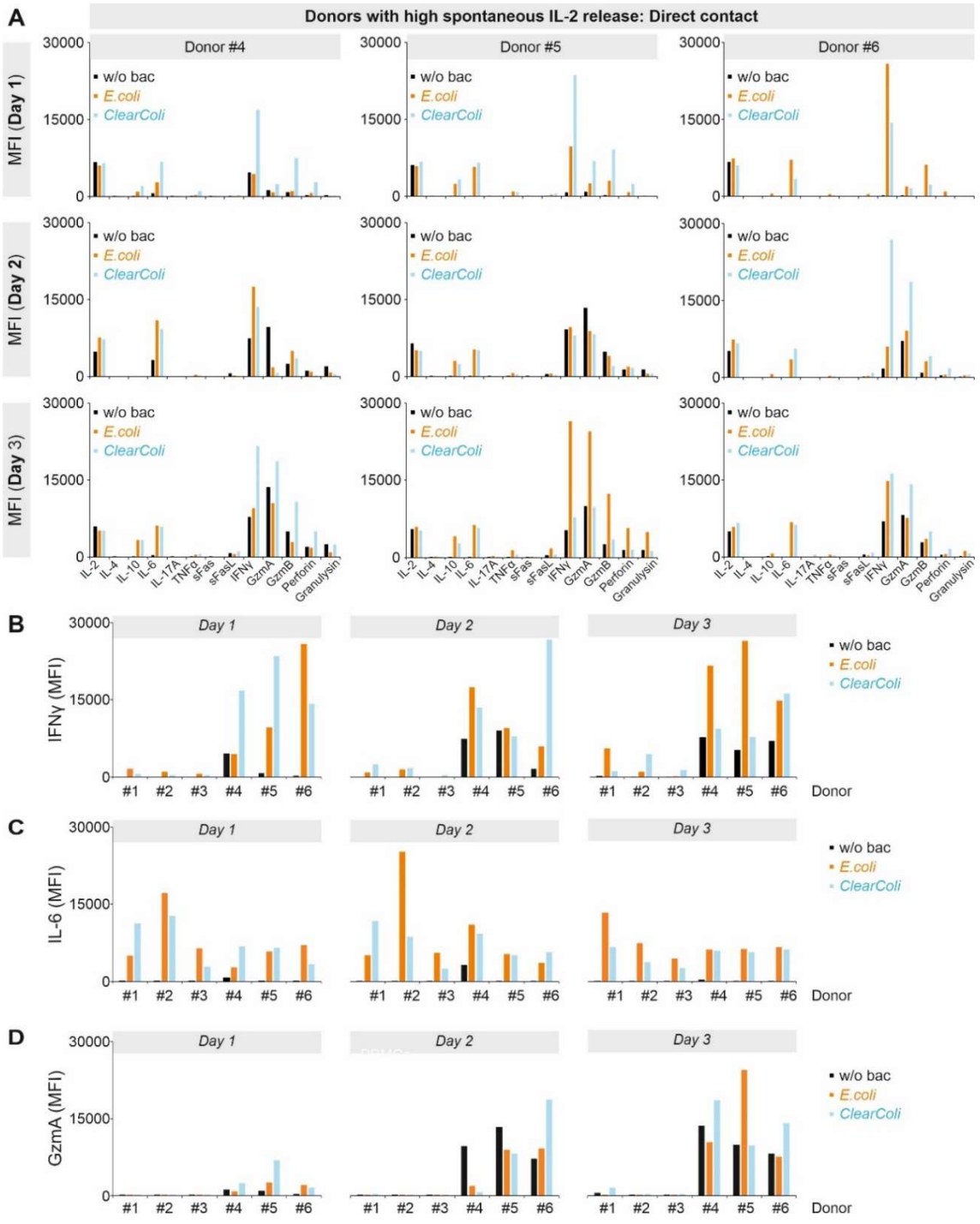

Figure 34: Immune response of PBMCs from donors with high spontaneous IL-2 release when in contact with bacteria. *A) Cytokine and cytotoxic proteins released by PBMCs. PBMCs were cultured with bacteria in direct contact. The cell culture media was collected on days 1, 2 and 3. A*

comparison of cytokine profiles of donors with high and low spontaneous IL-2 release for IFNγ (B), IL-6 (C) and GzmA (D) MFI: mean fluorescence intensity. The figure has been adapted from [119].

E.coli and *ClearColi* were separated from PBMCs by a nanoporous transwell insert allowing an exchange of factors which triggered the immune response. Major contributor for the immune response in this case was IFNγ, to some extent IL-6, GzmA, GzmB, perforin and granulysin. There was also a strong release of cytokines and cytotoxic proteins by PBMCs alone too (Figure 35A). Upon comparing the donors from low and high spontaneous IL-2 release, IFNγ levels were similar (Figure 35B), elevated IL-6 (Figure 35C) and GzmA levels (Figure 35D) in donors with high spontaneous IL-2 release.

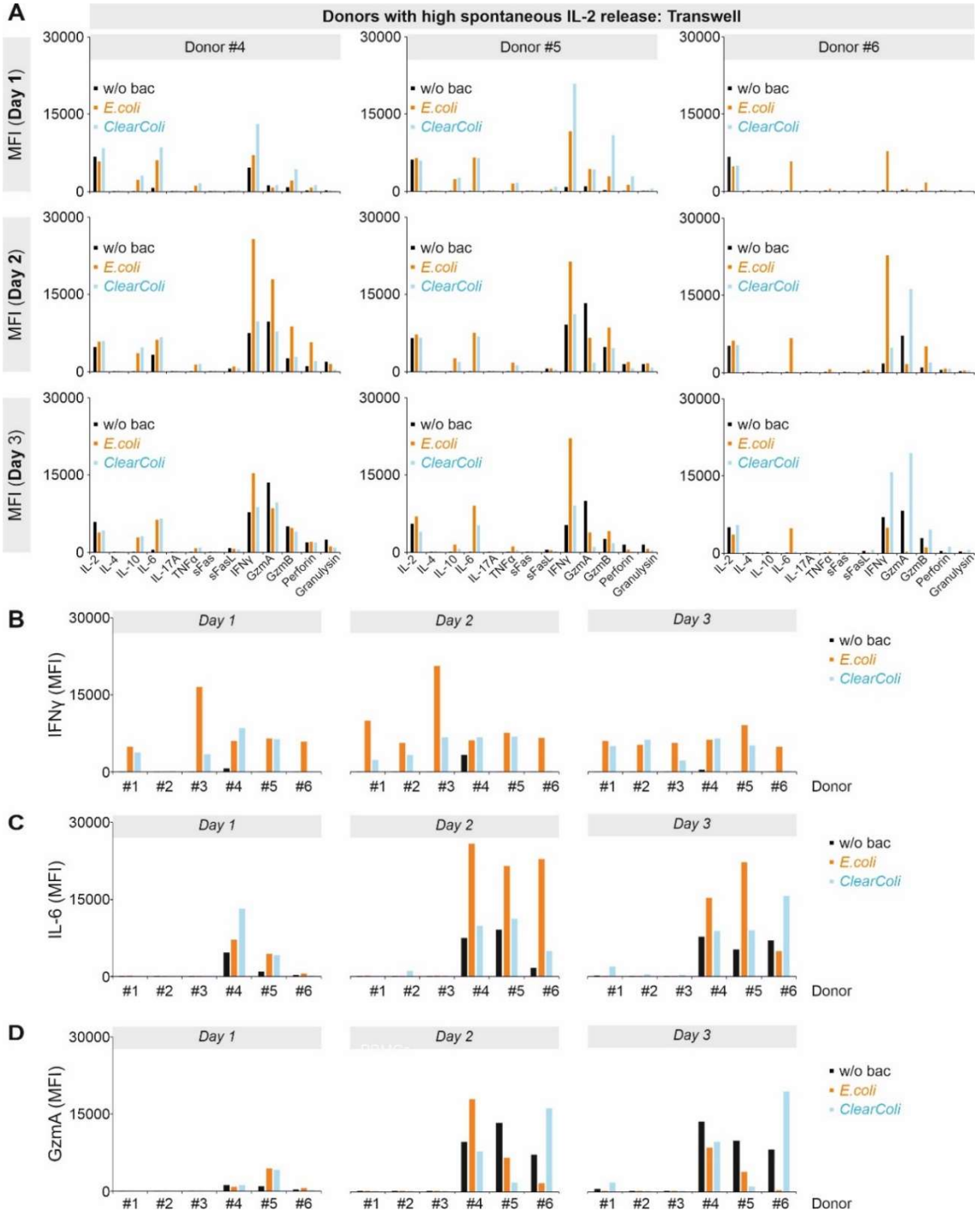

Figure 35: Immune response of PBMCs from donors with high spontaneous IL-2 release when in separated by a nanoporous membrane from the bacteria. *A) Cytokine and cytotoxic proteins released by PBMCs. PBMCs were cultured with bacteria separated by nanoporous membrane. The cell culture media was collected on days 1, 2 and 3 to assess their cytokine profiles. A comparison*

of cytokine profiles PBMCs cultured with bacteria separated by a nanoporous membrane between donors with high and low spontaneous IL-2 release for IFNγ (B), IL-6 (C) and GzmA (D) MFI: mean fluorescence intensity. The figure has been adapted from [119].

Bacteria encapsulated PluDA gels trigger a release of cytokines and cytotoxic proteins

E.coli and *ClearColi*-encapsulated PluDA gels were co-cultured with PBMCs. The cytokine and cytotoxic protein profiles show a clear surge in the release of IL-6, IFNγ, GzmA, GzmB, a moderate IL-10 release (day 3- donor 4) and a negligible release of perforin and granulysin (Figure 36A). A comparison of factors released in response to encapsulated gels between low and high spontaneous IL-2 release donors shows a high IFNγ (Figure 36B), comparable levels of IL-6 (Figure 36C) and enhanced GzmA levels (Figure 36D) in donors with high spontaneous IL-2 release.

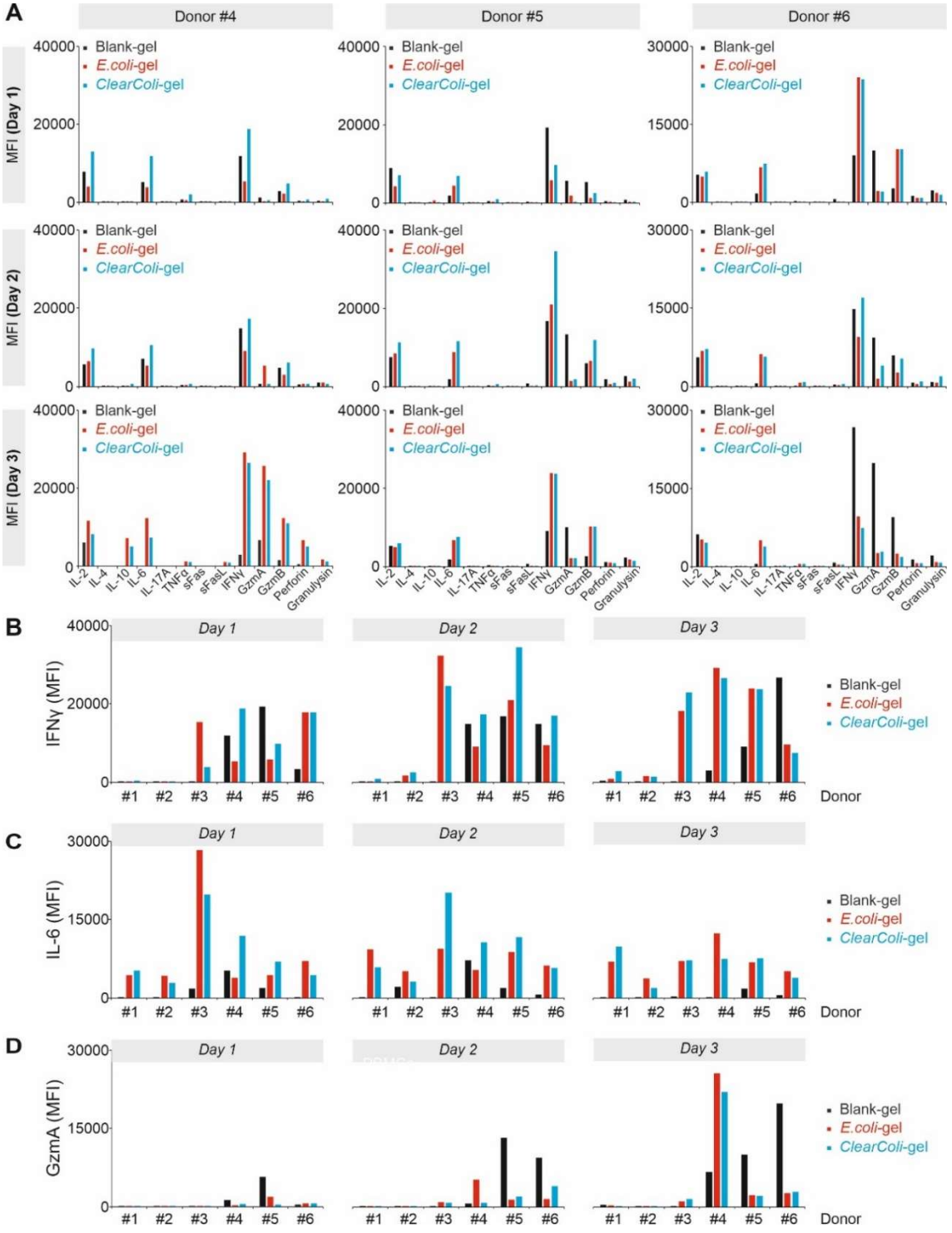

Figure 36: Immune response of PBMCs from donors with high spontaneous IL-2 release when in co-cultured with bacteria encapsulated gels. *A) Cytokine and cytotoxic proteins released by PBMCs. PBMCs were cultured with bacteria encapsulated gels and the cell culture media was*

collected on days 1, 2 and 3 to assess their cytokine profiles. A comparison of cytokine profiles of PBMCs co-cultured with bacteria encapsulated gels between donors with high and low spontaneous IL-2 release for IFNγ (B), IL-6 (C) and GzmA (D) MFI: mean fluorescence intensity. The figure has been adapted from [119].

Response to blank gels

In donors with high spontaneous IL-2 release blank PluDA gels are not immune inert. A comparison with low spontaneous IL-2 release donors paints a clear picture where IL-6, IFNγ, GzmA, GzmB and perforin were elevated (Figure 37). Taken together these results suggest that for donors with high spontaneous IL-2 release even the immune inert blank gels trigger an immune response.

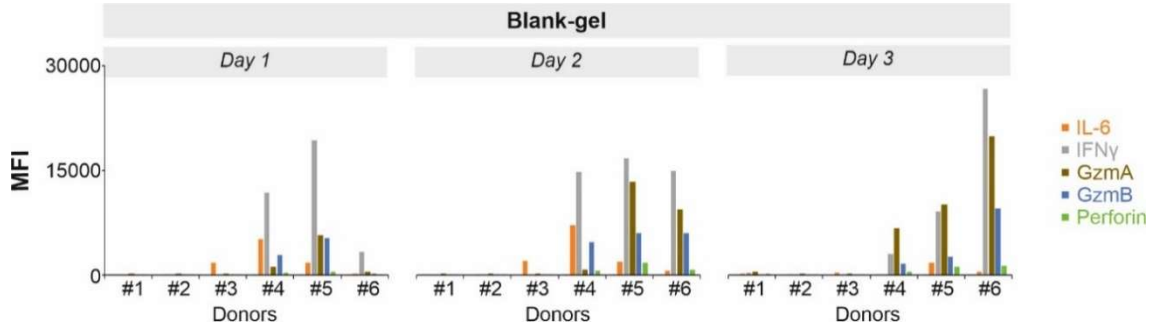

Figure 37: Immune response of PBMCs from donors with high spontaneous IL-2 release when in co-cultured with blank-gels. *PBMCs were cultured with blank-gels and the cell culture media was collected on days 1, 2 and 3 to assess their cytokine profiles. A comparison of IL-6, IFNγ, GzmA, GzmB and perforin of PBMCs co-cultured with blank-gels between donors with high and low spontaneous IL-2 release. The figure has been adapted from* [119].

4. Discussion

4.1 Role of mechanosensing in regulating NK mediated cytotoxicity

To explore the role of substrate stiffness on NK response, NK cells were settled on PAAm-co-AA hydrogels of 2, 12 and 50 kPa stiffness. The degranulation of NK cells was used as a marker to check their activation. NK cells from 12 donors could be grouped into four- activated on 50 kPa in 5 out of 12 donors, on 12 kPa in 3 out of 12 donors, on all substrates in 2 out of 12 donors and 2 out of 12 donors did not respond to any stiffness. These data clearly show NKp46 functionalized stiffer substrates (12, 50 kPa) to activate NK cells whereas soft substrate (2 kPa) did not elicit much response from NK cells. The role of substrate stiffness in modulating the functions of immune cells especially of NK cells has gathered interest only recently. There are recent studies where stiff substrate (142 kPa) elicited a higher release of granzymes A and B, FasL, granulysin and IFN γ compared to soft substrate (1 kPa) [64]. In the same study [64]to mimic tumor cells with various defined stiffness, sodium alginate beads coated with α-NKp30 and anti-LFA-1 were used where soft substrates were 9 kPa, medium were 34 kPa and stiff were 254 kPa. Stiff substrates induced an enhanced degranulation of NK cells whereas MTOC polarization was inhibited on soft substrates[117] . Nanowires coated with the NK activating receptor NKG2D induced NK degranulation when compared to the uncoated nanowires and flat substrates coated with activating ligands [64]. PDMS substrates with Young's moduli of 30 kPa, 150 kPa, and 3 MPa were functionalized with MHC class I chain-related polypeptide A (MICA) ligands which can activate NKG2D activating receptors of NK cells. NK cells were activated the most on 150 kPa substrate and a bell-shaped curve was the output where a stiffness range higher or lower than 150 kPa could not elicit maximum response from NK cells [120]. One major drawback for all these studies has been the range of stiffness. Physiologically the stiffness of cancerous tissue is in the range of 1.08–68 kPa [121]whereas the stiffness of 'stiff' substrates used in the above studies is at least twice or thrice more than the physiological range. MICA antibody was used in the above-mentioned studies to functionalize the substrates which eventually would activate NKG2D receptor. There is a huge amount of data which shows the tumor cells to shed MICA in order to escape immune surveillance. The shed MICA has been shown to bind to NKG2D of NK cells and deactivate the cell [122], [123]. Lack of MICA on the surface of tumor cells would then activate NK cells independent of NKG2D pathway. Hence, using substrates functionalized with MICA as ligand for NKG2D receptor is also not physiologically relevant scenario. Even though these studies are extremely important in deciphering NK response to stiffness they do not depict the actual physiological scenario. The substrates used in this thesis were functionalized with anti-NKp46

antibody which activates NKp46 receptor. NKp46 is a major natural cytotoxicity receptor which has been shown to play a major role in exhibiting tumoricidal activity. It has been shown to cluster around immunological synapses (or the immunological synapse) and has been shown to play a major role in polarization of lytic granules [124]–[126]. In this work the stiffness of the substrates (2, 12, 50 kPa) and their functionalization with NK activating antibody mimics the physiological scenario closely thus making it more relevant in unravelling stiffness related responses of NK cells.

To unravel the stiffness-based activation of NK cells, the stiffness of tumor cells was altered. In this thesis work, tumors cells stiffened with blebbistatin were efficiently killed by NK but their cytotoxic activity against softened tumor cells was impaired. Stiffness of the tumor cells has been shown to reflect the malignant and metastatic potential of cancer. A tumor cell whose fate is to metastasize to a distant tissue has to migrate through narrow and confined spaces in extracellular matrix and between cells. It has been shown that the tumor cell changes its stiffness and becomes soft as it migrates from unconfined space to confined and restricted space [127]; using atomic force microscopy (AFM) stiffness of metastatic cancer cells was shown to be 70% softer than their normal counterparts [128], prostate cancer and breast cancer cells were 85% and 65% less stiffer than normal cells[129]; from the patients with lung, breast, and pancreatic cancer the stiffness of metastatic cells was assessed using AFM showed the metastatic cells to be softer than the normal cells [129]; AFM measurements have shown the ovarian cancer cells to be softer (0.5-1 kPa) than normal cells (2 kPa) [130]; a lower Young's modulus was associated with high motility and metastatic potential (1.44 ± 0.06-1.66 ± 0.08 kPa) of a group of cells in non-small cell lung cancer cell when compared another group which was low in motility as well as metastatic potential (2.71 ± 0.14-3.18 ± 0.38 kPa) [131]; ovarian cancer cells derived from the same tumor have an altered stiffness with the soft cells (HEY A8, ~0.5 kPa) having a higher invasive potential than the stiffer cells (HEY, ~0.9 kPa) [130] ; in 3D organoid models of breast cancer the cells in the centre of the organoid were stiffer with the cells at the periphery were softer and exhibited invasive fronts [132]; using microfluidics cancer stem cells of mouse breast cancer (4T1), human breast cancer (MCF-7) cells were sorted based on their stiffness into soft and stiff cells of which 100 cells from each group were inoculated into NOD/SCID IL-2Rγ-null (NSG) mice where only the soft cells could form a tumor which could also metastasize to lung but not the stiff ones and as low as 10 soft cells could form a tumor but even 100 stiff cells could not form a tumor [133]. The findings of this thesis align with the already available data about the mechanical properties of tumor cells. This thesis further corroborates and establishing that apart from many other factors stiffness based immune evasion by tumor cells to also contribute immensely for tumor progression and metastasis.

To understand the mechanism for impaired killing of soft tumor cells and enhance killing of stiff tumor cells lytic granule pathway was checked. There was no difference in release of lytic granules by NK cells between soft and stiff cells. In order to eliminate a target cell NK cell adheres to target cell, forms a stable IS, polarizes the lytic granules towards the IS, releases contents of lytic granules and ultimately perforin disrupts the membrane integrity and rest of the granules lead to apoptosis. Since, the degranulation of NK cells upon contact with either soft or stiff target cells was unaltered which implies the pathways upstream the cascade of releasing the lytic granules to function optimally in NK cells. It has been shown that the killing efficiency of CTLs for soft tumor repopulating cells was impaired mainly due to inefficiency of the killer cells to form perforin mediated holes in soft target cells which was due to inadequate contractile force [134]. In this thesis there for two donors, no difference was observed in the ability of perforin to drill into soft target cells when compared with stiff cells, but this experiment needs further optimization in terms of the co-incubation time between killer cells and target cell. So, nothing concrete can be derived from this result. It could also be that the pore forming ability by NK cells could be impaired in soft target cell when compared to stiff cells, but this is only speculative. After killing a target cell NK cell detaches from the dead or dying cell and starts searching for a new target. If the time taken for the NK cell to initiate the apoptosis and detaching once the cell undergoes apoptosis is considerably longer, then it would alter the killing kinetics which would be reflected in inefficient target cell clearance. In this thesis this trend was clear where upon conjugate formation the time taken for NK cell to initiate apoptosis of stiffened tumor cell and to detach after the killing event was significantly shorter when compared to softened tumor cells. Lytic granules are a potent machinery that can kill the targets efficiently hence, the release of these secretory lysosomes is tightly regulated. Unfortunately, the mechanism underlying the detachment of NK cell from its target cell and the regulation of lytic machinery is still unclear. But, based on some research done in the field of T cell biology a few parallels can be drawn. It was observed in CTLs that upon formation of a stable conjugate and fusion of lytic granules a diminished cortical actin density at the IS was noticed but once the actin recovered the secretion of lytic granules was halted. Cortical actin density was found to be dependent on Phosphatidylinositol 4,5-bisphosphate (PIP_2). Phospholipase C Gamma 1 signalling pathway was shown to control PIP_2 which in turn regulated the cortical actin density [135]. PKCθ was shown to be not an important player in IS formation but was essential to break the formed IS in naïve T cells [136]. It can only be speculated that these pathways might also play a similar role in regulating the lytic granule release and detachment of NK from the target cell upon killing the latter.

A cell perceives mechanical cues via mechanosensitive channels. To elucidate the effect of these channels on NK cell effector functions, widely used unspecific mechanosensitive channel

antagonizers gadolinium and nifedipine were used. The killing efficiency of NK cells was impaired in presence of gadolinium and nifedipine. Degranulation of NK cells upon contact with the target cells and the expression of cytotoxic proteins was unaltered in presence of these inhibitors. Calcium has been shown to play a major role in NK cells in exert their effector functions. Ca^{2+} has been shown to play an undeniable role in length of IS, downstream signalling cascades initiated after conjugate formation, optimal exocytosis of lytic granules [137]. Apart from antagonizing many mechanosensitive channels, both gadolinium (CRAC channels) and nifedipine (L-type calcium channels) are also potent inhibitors of calcium ions [138]. Thus, the impaired killing of the target cells would also be dependent on the blockade of the Ca^{2+} ions. PIEZO1 has been shown to be a major mechanosensing channel in many immune cells such as macrophages [139], dendritic cells [89] and T cells [88]. In T cells PIEZO1 has been shown to a mechanosensor at IS and essential for optimal T cell activation [87] . Microarray data from our lab has shown a high expression of PIEZO1 in primary human NK cells. GsMTx4, a toxin isolated from spider venom is a specific inhibitor of PIEZO1 channel [90]. Blockade of PIEZO1 in NK cell using GsMTx4 lead to an impaired the target cell lysis. PIEZO1 inhibition did not affect the lytic granule pathway but influenced the infiltration of NK cell into 3D matrix. Antagonizing PIEZO1 channel led to a diminished infiltration of NK cells into 3D matrix. Activation of PIEZO1 using Yoda-1, a chemical agonist for PIEZO1 [140] boosted NK mediated cytolytic activity which was due to an increase in the number of NK cells infiltrating into the 3D matrix. This works unravels a new stiffness mediated mechanism by which tumor cells evade immune surveillance by NK cells. This work could pave way for incorporating mechanics modulated immunotherapy where stiffening of cancer cells would sensitize them to killing by NK cells. It also highlights the role played by PIEZO1 as one of the potential mechanosensors which could influence the infiltration of NK cells into 3D collagen matrices which could be exploited in immunotherapy against solid tumors.

4.2 *In vitro* characterization of immune responses to hydrogels encapsulated with drug-producible bacteria

LTMs are being extensively research for their biomedical applications. However, when LTMs are implanted in the host or in contact with the bodily fluids of the host one major concern that would arise would be of an immune response, which could lead to critical situations if out of control. For potential therapeutical application, bacteria producing desired biologically functional substances are often encapsulated in hydrogels to limit their contact with the immune system and to also protect the bacteria from harsh surrounding environment [141]. In this work, bacteria were encapsulated in the central core of Plu/PluDA hydrogel, and the outer shell had a heavy crosslinking of PluDA to prevent

any leakage of bacteria. To characterize the immune response elicited by the bacteria encapsulated PluDA gels, cytokine profiles and cytotoxic proteins released from PBMCs and the differentiation of NK and T cells into different subtypes which have diverse functions were evaluated. Our results show that co-incubation of PluDA blank gels with PBMCs did not alter their profiles of cytokines and cytotoxic proteins, and had no impact on differentiation of NK cells, CD4+ and CD8+ T cells in donors with low spontaneous release of IL-2. These data indicate that blank PA-gels are immune inert, at least *in vitro*, supporting the application of PluDA as immune-compatible encapsulation materials for therapeutical purposes *in vivo*. *ClearColi* elicited release of IL-6 and IFNγ from PBMCs. Interestingly, the predominantly released cytokine was IL-6 for low spontaneous IL-2 release donors, but IFNγ for high spontaneous IL-2 release donors. Both the transwell condition and the encapsulated gel condition showed the same tendency. IL-6 is a cytokine which has both protective functions and at the same time plays a huge role in inflammatory reactions to the extent that it is being used as a marker for autoimmune diseases and cancer. It is mainly produced by macrophages. It induces production of acute phase proteins, promotes differentiation of $CD4^+$ and $CD8^+$ cells into effector phenotype and B cells into antibody producing plasma cells. Apart from PRR, danger associated molecular patterns (DAMPs) from dying cells also activates IL-6 production. In a cytokine storm predominant production of IL-6 has been observed. A hallmark of activated immune cells especially NK cells, $CD4^+$ and $CD8^+$ cells is production of interferon-γ (IFNγ). It regulates both innate and adaptive immune responses [34], [46]. IFNγ activates NFκB pathway, induces production of other pro-inflammatory cytokines such as IL-12, IL-15, TNFα and has been linked with autoimmune diseases and hyper-inflammation [49]. The levels of IL-6 and IFNγ released by PBMCs from low spontaneous IL-2 donors for *ClearColi-encapsulated* gels are in a comparable range with the factors (IL-6, IFNγ) released by blank gels in donors with high spontaneous IL-2. It has been already shown that blank PluDA gels to be non-immunogenic so this can be treated as response of immune cells upon encountering a foreign body. *E.coli* when co-incubated with PBMCs lead to polarization of NK cells to a more cytotoxic $CD16^{dim}$ subset whereas *ClearColi* did not trigger any such polarization. When the bacteria were in direct contact with the PBMCs they triggered the apoptosis of PBMCs on day 3 but encapsulation of the bacteria in PluDA gels completely abolished this effect. Pre-activated donors are featured with high levels of spontaneous IL-2 release, suggesting an activated status of the immune system, in particular T cells. This speculation is further supported by our observation that NK cells from these donors were polarized to the cytotoxic CD^{16dim} subset. At the time of thrombocyte donation, the healthy status of the donors was ensured by the clinicians on-site and virological test for HIV and hepatitis B. These experiments were carried out in between October and December 2020 when there was a second wave of COVID-19 in Germany along with seasonal flu. It cannot be discounted that

some donors could be asymptomatic or recovered from an infection so their immune system could have been in a pre-activated status needing time to come back to normalcy. This could be one reason for having some donors with high spontaneous IL-2 release. The findings from this work highlight the need for an evaluation of immune status of patient where IL-2 could be used as a marker for pre-activated immune system. These results suggest that an inflammatory reaction could be triggered in such donors at the site of delivery of LTMs. IL-2 could be used as a marker to screen for such donors to administer anti-inflammatory drugs orally or topically. It further calls for development of LTMs clubbed with the feature of sustained released of anti-inflammatory molecules in donors with high spontaneous IL-2.

5. References

[1] J. S. Marshall, R. Warrington, W. Watson, and H. L. Kim, "An introduction to immunology and immunopathology," *Allergy, Asthma & Clinical Immunology*, vol. 14, no. 2, p. 49, 2018, doi: 10.1186/s13223-018-0278-1.

[2] L. B. Nicholson, "The immune system," *Essays Biochem*, vol. 60, no. 3, pp. 275–301, 2016.

[3] M. Roederer *et al.*, "The Genetic Architecture of the Human Immune System: A Bioresource for Autoimmunity and Disease Pathogenesis," *Cell*, vol. 161, no. 2, pp. 387–403, 2015, doi: https://doi.org/10.1016/j.cell.2015.02.046.

[4] J. S. Marshall, R. Warrington, W. Watson, and H. L. Kim, "An introduction to immunology and immunopathology," *Allergy, Asthma & Clinical Immunology*, vol. 14, no. 2, pp. 1–10, 2018.

[5] D. D. Chaplin, "1. Overview of the human immune response," *Journal of Allergy and Clinical Immunology*, vol. 117, no. 2, Supplement 2, pp. S430–S435, 2006, doi: https://doi.org/10.1016/j.jaci.2005.09.034.

[6] S. E. Turvey and D. H. Broide, "Innate immunity," *Journal of Allergy and Clinical Immunology*, vol. 125, no. 2, Supplement 2, pp. S24–S32, 2010, doi: https://doi.org/10.1016/j.jaci.2009.07.016.

[7] S. J. Galli, N. Borregaard, and T. A. Wynn, "Phenotypic and functional plasticity of cells of innate immunity: macrophages, mast cells and neutrophils," *Nat Immunol*, vol. 12, no. 11, pp. 1035–1044, 2011, doi: 10.1038/ni.2109.

[8] F. A. Bonilla and H. C. Oettgen, "Adaptive immunity," *Journal of Allergy and Clinical Immunology*, vol. 125, no. 2, Supplement 2, pp. S33–S40, 2010, doi: https://doi.org/10.1016/j.jaci.2009.09.017.

[9] F. A. Bonilla and H. C. Oettgen, "Adaptive immunity," *Journal of Allergy and Clinical Immunology*, vol. 125, no. 2, pp. S33–S40, 2010.

[10] J. A. Hamerman, K. Ogasawara, and L. L. Lanier, "NK cells in innate immunity," *Curr Opin Immunol*, vol. 17, no. 1, pp. 29–35, 2005, doi: https://doi.org/10.1016/j.coi.2004.11.001.

[11] S. Paul and G. Lal, “The Molecular Mechanism of Natural Killer Cells Function and Its Importance in Cancer Immunotherapy,” *Front Immunol*, vol. 8, 2017, [Online]. Available: https://www.frontiersin.org/articles/10.3389/fimmu.2017.01124

[12] S. Paul and G. Lal, “The Molecular Mechanism of Natural Killer Cells Function and Its Importance in Cancer Immunotherapy,” *Front Immunol*, vol. 8, 2017, [Online]. Available: https://www.frontiersin.org/articles/10.3389/fimmu.2017.01124

[13] A. Poli, T. Michel, M. Thérésine, E. Andrès, F. Hentges, and J. Zimmer, “CD56bright natural killer (NK) cells: an important NK cell subset.,” *Immunology*, vol. 126, no. 4, pp. 458–465, Apr. 2009, doi: 10.1111/j.1365-2567.2008.03027.x.

[14] R. Jacobs *et al.*, “CD56bright cells differ in their KIR repertoire and cytotoxic features from CD56dim NK cells.,” *Eur J Immunol*, vol. 31, no. 10, pp. 3121–3127, Oct. 2001, doi: 10.1002/1521-4141(2001010)31:10<3121::aid-immu3121>3.0.co;2-4.

[15] K. A. Whalen *et al.*, “Engaging natural killer cells for cancer therapy via NKG2D, CD16A and other receptors,” no. 1942–0870 (Electronic).

[16] L. A. Gwalani and J. S. Orange, “Single Degranulations in NK Cells Can Mediate Target Cell Killing,” *The Journal of Immunology*, vol. 200, no. 9, pp. 3231–3243, May 2018, doi: 10.4049/jimmunol.1701500.

[17] E. M. Mace *et al.*, “Cell biological steps and checkpoints in accessing NK cell cytotoxicity,” *Immunol Cell Biol*, vol. 92, no. 3, pp. 245–255, Mar. 2014, doi: https://doi.org/10.1038/icb.2013.96.

[18] N. D. Pennock, J. T. White, E. W. Cross, E. E. Cheney, B. A. Tamburini, and R. M. Kedl, “T cell responses: naive to memory and everything in between.,” *Adv Physiol Educ*, vol. 37, no. 4, pp. 273–283, Dec. 2013, doi: 10.1152/advan.00066.2013.

[19] T. van den Broek, J. A. M. Borghans, and F. van Wijk, “The full spectrum of human naive T cells.,” *Nat Rev Immunol*, vol. 18, no. 6, pp. 363–373, Jun. 2018, doi: 10.1038/s41577-018-0001-y.

[20] M. D. Martin and V. P. Badovinac, “Defining Memory CD8 T Cell,” *Front Immunol*, vol. 9, 2018, [Online]. Available: https://www.frontiersin.org/articles/10.3389/fimmu.2018.02692

[21] R. V. Luckheeram, R. Zhou, A. D. Verma, and B. Xia, "CD4+ T cells: differentiation and functions," *Clin Dev Immunol*, vol. 2012, 2012.

[22] N. Zhang and M. J. Bevan, "CD8+ T cells: foot soldiers of the immune system," *Immunity*, vol. 35, no. 2, pp. 161–168, 2011.

[23] S. Isaaz, K. Baetz, K. Olsen, E. Podack, and G. M. Griffiths, "Serial killing by cytotoxic T lymphocytes: T cell receptor triggers degranulation, re-filling of the lytic granules and secretion of lytic proteins via a non-granule pathway," *Eur J Immunol*, vol. 25, no. 4, pp. 1071–1079, Apr. 1995, doi: https://doi.org/10.1002/eji.1830250432.

[24] M. D. Martin and V. P. Badovinac, "Defining Memory CD8 T Cell," *Front Immunol*, vol. 9, 2018, [Online]. Available: https://www.frontiersin.org/articles/10.3389/fimmu.2018.02692

[25] D. L. Farber, N. A. Yudanin, and N. P. Restifo, "Human memory T cells: generation, compartmentalization and homeostasis," *Nat Rev Immunol*, vol. 14, no. 1, pp. 24–35, 2014.

[26] H. Ham, M. Medlyn, and D. D. Billadeau, "Locked and loaded: mechanisms regulating natural killer cell lytic granule biogenesis and release," *Front Immunol*, vol. 13, p. 871106, 2022.

[27] I. Prager and C. Watzl, "Mechanisms of natural killer cell-mediated cellular cytotoxicity," *J Leukoc Biol*, vol. 105, no. 6, pp. 1319–1329, Jun. 2019, doi: 10.1002/JLB.MR0718-269R.

[28] I. Osińska, K. Popko, U. Demkow, and J. I. Cent Eur, "Perforin: an important player in immune response," no. 1426-3912 (Print).

[29] J. A. Trapani, "Granzymes: a family of lymphocyte granule serine proteases," *Genome Biol*, vol. 2, no. 12, pp. reviews3014-1, 2001.

[30] S. P. Cullen and S. J. Martin, "Caspase activation pathways: some recent progress," *Cell Death Differ*, vol. 16, no. 7, pp. 935–938, 2009, doi: 10.1038/cdd.2009.59.

[31] D. Chowdhury, J. Lieberman, and I. Annu Rev, "Death by a thousand cuts: granzyme pathways of programmed cell death," no. 0732–0582 (Print).

[32] F. Dotiwala, J. Lieberman, and I. Curr Opin, "Granulysin: killer lymphocyte safeguard against microbes," no. 1879–0372 (Electronic).

[33] A. M. Krensky, C. Clayberger, and A. Tissue, “Biology and clinical relevance of granulysin,” no. 1399–0039 (Electronic).

[34] D. Ragab, H. Salah Eldin, M. Taeimah, R. Khattab, and R. Salem, “The COVID-19 Cytokine Storm; What We Know So Far,” *Front Immunol*, vol. 11, 2020, [Online]. Available: https://www.frontiersin.org/articles/10.3389/fimmu.2020.01446

[35] S. A.-O. X. Kany, J. T. Vollrath, B. Relja, and J. M. S. Int, “Cytokines in Inflammatory Disease. LID - 10.3390/ijms20236008 [doi] LID - 6008,” no. 1422–0067 (Electronic).

[36] Z. Şahbudak Bal *et al.*, “Diagnostic Accuracy of Interleukin-6, Interleukin-8, and Interleukin-10 for Predicting Bacteremia in Children with Febrile Neutropenia,” no. 1308-5263 (Electronic).

[37] Q. Zhu *et al.*, “IL-6 and IL-10 Are Associated With Gram-Negative and Gram-Positive Bacteria Infection in Lymphoma,” no. 1664-3224 (Electronic).

[38] E. M. Rincón-López *et al.*, “Interleukin 6 as a marker of severe bacterial infection in children with sickle cell disease and fever: a case-control study,” no. 1471-2334 (Electronic).

[39] Y. V Cavalcanti, J. K. de A. L. Brelaz Mc Fau - Neves, J. C. Neves Jk Fau - Ferraz, V. R. A. Ferraz Jc Fau - Pereira, V. R. Pereira, and M. Pulm, “Role of TNF-Alpha, IFN-Gamma, and IL-10 in the Development of Pulmonary Tuberculosis,” no. 2090–1844 (Electronic).

[40] G. M. Boxx, G. Cheng, and M. Cell Host, “The Roles of Type I Interferon in Bacterial Infection,” no. 1934-6069 (Electronic).

[41] A. Zganiacz *et al.*, “TNF-alpha is a critical negative regulator of type 1 immune activation during intracellular bacterial infection,” no. 0021-9738 (Print).

[42] M. M. Curtis, S. S. Way, and Immunology, “Interleukin-17 in host defence against bacterial, mycobacterial and fungal pathogens,” no. 1365-2567 (Electronic).

[43] M. Walch *et al.*, “Cytotoxic cells kill intracellular bacteria through granulysin-mediated delivery of granzymes,” no. 1097-4172 (Electronic).

[44] D. L. León, I. Fellay, P. Y. Mantel, M. Walch, and B. Methods Mol, "Killing Bacteria with Cytotoxic Effector Proteins of Human Killer Immune Cells: Granzymes, Granulysin, and Perforin," no. 1940-6029 (Electronic).

[45] M. M. Curtis and S. S. Way, "Interleukin-17 in host defence against bacterial, mycobacterial and fungal pathogens," *Immunology*, vol. 126, no. 2, pp. 177–185, 2009.

[46] C. A. Hunter and S. A. Jones, "IL-6 as a keystone cytokine in health and disease," *Nat Immunol*, vol. 16, no. 5, pp. 448–457, 2015, doi: 10.1038/ni.3153.

[47] N. Parameswaran, S. Patial, and E. Crit Rev Eukaryot Gene, "Tumor necrosis factor-α signaling in macrophages," no. 1045-4403 (Print).

[48] A. K. Mehta, D. T. Gracias, M. Croft, and Cytokine, "TNF activity and T cells," no. 1096–0023 (Electronic).

[49] S. H. Lee, J. ye Kwon, S.-Y. Kim, K. Jung, and M.-L. Cho, "Interferon-gamma regulates inflammatory cell death by targeting necroptosis in experimental autoimmune arthritis," *Sci Rep*, vol. 7, no. 1, p. 10133, 2017, doi: 10.1038/s41598-017-09767-0.

[50] K. A. Smith, "Interleukin-2," in *Encyclopedia of Hormones*, H. L. Henry and A. W. Norman, Eds., New York: Academic Press, 2003, pp. 412–416. doi: https://doi.org/10.1016/B0-12-341103-3/00152-2.

[51] S. H. Ross, D. A. Cantrell, and I. Annu Rev, "Signaling and Function of Interleukin-2 in T Lymphocytes," no. 1545-3278 (Electronic).

[52] D. Klatzmann and A. K. Abbas, "The promise of low-dose interleukin-2 therapy for autoimmune and inflammatory diseases," *Nat Rev Immunol*, vol. 15, no. 5, pp. 283–294, 2015, doi: 10.1038/nri3823.

[53] F. Sparber and S. LeibundGut-Landmann, "Interleukin-17 in Antifungal Immunity," *Pathogens*, vol. 8, no. 2, 2019, doi: 10.3390/pathogens8020054.

[54] G. Zenobia C Fau - Hajishengallis, G. Hajishengallis, and Periodontol, "Basic biology and role of interleukin-17 in immunity and inflammation," no. 1600–0757 (Electronic).

[55] P. Chatterjee, V. L. Chiasson, K. R. Bounds, and B. M. Mitchell, "Regulation of the Anti-Inflammatory Cytokines Interleukin-4 and Interleukin-10 during Pregnancy," *Front*

Immunol, vol. 5, 2014, [Online]. Available: https://www.frontiersin.org/articles/10.3389/fimmu.2014.00253

[56] G. Santoni, C. Amantini, M. Santoni, F. Maggi, M. B. Morelli, and A. Santoni, "Mechanosensation and Mechanotransduction in Natural Killer Cells.," *Front Immunol*, vol. 12, p. 688918, 2021, doi: 10.3389/fimmu.2021.688918.

[57] H. Du *et al.*, "Tuning immunity through tissue mechanotransduction," *Nat Rev Immunol*, vol. 23, no. 3, pp. 174–188, 2023, doi: 10.1038/s41577-022-00761-w.

[58] J.-Y. Yang and B.-S. Qiu, "The Advance of Magnetic Resonance Elastography in Tumor Diagnosis," *Front Oncol*, vol. 11, 2021, [Online]. Available: https://www.frontiersin.org/articles/10.3389/fonc.2021.722703

[59] S. K. Venkatesh *et al.*, "MR elastography of liver tumors: preliminary results," no. 1546-3141 (Electronic).

[60] J. Y. Yang, B. S. Qiu, and O. Front, "The Advance of Magnetic Resonance Elastography in Tumor Diagnosis," no. 2234–943X (Print).

[61] R. Reiter *et al.*, "Prostate cancer assessment using MR elastography of fresh prostatectomy specimens at 9.4 T," *Magn Reson Med*, vol. 84, no. 1, pp. 396–404, Jul. 2020, doi: https://doi.org/10.1002/mrm.28127.

[62] W. Xu, R. Mezencev, B. Kim, L. Wang, J. McDonald, and T. Sulchek, "Cell stiffness is a biomarker of the metastatic potential of ovarian cancer cells," 2012.

[63] P. Simmonds, D. Friedman, A. Hale, N. W. Hodson, M. R. H. White, and D. M. Davis, "Natural Killer cell immune synapse formation and cytotoxicity is controlled by mechanical tension of the target." Am Assoc Immnol, 2020.

[64] L. Mordechay, G. Le Saux, A. Edri, U. Hadad, A. Porgador, and M. Schvartzman, "Mechanical regulation of the cytotoxic activity of natural killer cells," *ACS Biomater Sci Eng*, vol. 7, no. 1, pp. 122–132, 2020.

[65] B. Emon, J. Bauer, Y. Jain, B. Jung, and T. Saif, "Biophysics of Tumor Microenvironment and Cancer Metastasis - A Mini Review," *Comput Struct Biotechnol J*, vol. 16, pp. 279–287, 2018, doi: https://doi.org/10.1016/j.csbj.2018.07.003.

[66] Y. Chen, L. Ju, M. Rushdi, C. Ge, C. Zhu, and C. Mol Biol, “Receptor-mediated cell mechanosensing,” no. 1939-4586 (Electronic).

[67] P. Agarwal, R. Zaidel-Bar, and B. Curr Opin Cell, “Mechanosensing in embryogenesis,” no. 1879–0410 (Electronic).

[68] B. A.-O. Kuehlmann, C. A. Bonham, I. A.-O. Zucal, L. A.-O. Prantl, G. C. Gurtner, and J. C. Med, “Mechanotransduction in Wound Healing and Fibrosis. LID - 10.3390/jcm9051423 [doi] LID - 1423,” no. 2077–0383 (Print).

[69] A. S. Yap, K. Duszyc, V. Viasnoff, and B. Cold Spring Harb Perspect, “Mechanosensing and Mechanotransduction at Cell-Cell Junctions. LID - 10.1101/cshperspect.a028761 [doi] LID - a028761,” no. 1943–0264 (Electronic).

[70] D. E. Jaalouk and J. Lammerding, “Mechanotransduction gone awry,” *Nat Rev Mol Cell Biol*, vol. 10, no. 1, pp. 63–73, 2009, doi: 10.1038/nrm2597.

[71] E. Judokusumo, E. Tabdanov, S. Kumari, M. L. Dustin, and L. C. Kam, “Mechanosensing in T lymphocyte activation,” *Biophys J*, vol. 102, no. 2, pp. L5–L7, 2012.

[72] M. Rushdi, K. Li, Z. Yuan, S. Travaglino, A. Grakoui, and C. Zhu, “Mechanotransduction in T cell development, differentiation and function,” *Cells*, vol. 9, no. 2, p. 364, 2020.

[73] K. Haneef, A. G. Memon, R. Saleem, F. Batool, and M. Sadeeq, “B cell receptor (BCR) guided mechanotransduction: Critical hypothesis to instruct SARS-CoV-2 specific B cells to trigger proximal signalling and antibody reshaping,” *Med Hypotheses*, vol. 153, p. 110640, 2021.

[74] F. Martino, A. R. Perestrelo, V. Vinarský, S. Pagliari, and G. Forte, “Cellular Mechanotransduction: From Tension to Function,” *Front Physiol*, vol. 9, 2018, [Online]. Available: https://www.frontiersin.org/articles/10.3389/fphys.2018.00824

[75] B. Canales Coutiño, R. Mayor, and D. Cells, “Mechanosensitive ion channels in cell migration,” no. 2667-2901 (Electronic).

[76] H. Zhang, G. P. Walcott, and J. M. Rogers, “Effects of gadolinium on cardiac mechanosensitivity in whole isolated swine hearts,” *Sci Rep*, vol. 8, no. 1, p. 10506, 2018.

[77] H. Cho, J. Shin, C. Y. Shin, S.-Y. Lee, and U. Oh, “Mechanosensitive ion channels in cultured sensory neurons of neonatal rats,” *Journal of Neuroscience*, vol. 22, no. 4, pp. 1238–1247, 2002.

[78] S. Dobner, O. C. Amadi, and R. T. Lee, “Cardiovascular mechanotransduction,” in *Muscle*, Elsevier, 2012, pp. 173–186.

[79] R. A. Caldwell, H. F. Clemo, and C. M. Baumgarten, “Using gadolinium to identify stretch-activated channels: technical considerations,” *American Journal of Physiology-Cell Physiology*, vol. 275, no. 2, pp. C619–C621, 1998.

[80] P. J. M. E. et al Snutch TP, *Molecular Properties of Voltage-Gated Calcium Channels.* 2000.

[81] M. R. Zocchi, P. Rubartelli A Fau - Morgavi, A. Morgavi P Fau - Poggi, A. Poggi, and J. Immunol, “HIV-1 Tat inhibits human natural killer cell function by blocking L-type calcium channels,” no. 0022-1767 (Print).

[82] X. Li, J. Hu, X. Zhao, J. Li, and Y. Chen, “Piezo channels in the urinary system,” *Exp Mol Med*, vol. 54, no. 6, pp. 697–710, 2022, doi: 10.1038/s12276-022-00777-1.

[83] B. Coste *et al.*, “Piezo1 and Piezo2 are essential components of distinct mechanically activated cation channels,” no. 1095-9203 (Electronic).

[84] W. Yuan, X. Zhang, and X. Fan, “The Role of the Piezo1 Mechanosensitive Channel in Heart Failure,” *Curr Issues Mol Biol*, vol. 45, no. 7, pp. 5830–5848, 2023, doi: 10.3390/cimb45070369.

[85] A. Jairaman *et al.*, “Piezo1 channels restrain regulatory T cells but are dispensable for effector CD4+ T cell responses,” *Sci Adv*, vol. 7, no. 28, pp. eabg5859–eabg5859, 2021.

[86] J. M. Hope *et al.*, “Fluid shear stress enhances T cell activation through Piezo1,” *BMC Biol*, vol. 20, no. 1, p. 61, 2022, doi: 10.1186/s12915-022-01266-7.

[87] C. S. C. Liu *et al.*, “Cutting Edge: Piezo1 Mechanosensors Optimize Human T Cell Activation,” *The Journal of Immunology*, vol. 200, no. 4, pp. 1255–1260, Feb. 2018, doi: 10.4049/jimmunol.1701118.

[88] C. S. C. Liu and D. Ganguly, “Mechanical Cues for T Cell Activation: Role of Piezo1 Mechanosensors.,” *Crit Rev Immunol*, vol. 39, no. 1, pp. 15–38, 2019, doi: 10.1615/CritRevImmunol.2019029595.

[89] Y. Wang *et al.*, “Dendritic cell Piezo1 directs the differentiation of T(H)1 and T(reg) cells in cancer. LID - 10.7554/eLife.79957 [doi] LID - e79957,” no. 2050–084X (Electronic).

[90] R. Gnanasambandam *et al.*, “GsMTx4: Mechanism of Inhibiting Mechanosensitive Ion Channels,” no. 1542–0086 (Electronic).

[91] A. Rodrigo-Navarro, S. Sankaran, M. J. Dalby, A. del Campo, and M. Salmeron-Sanchez, “Engineered living biomaterials,” *Nat Rev Mater*, vol. 6, no. 12, pp. 1175–1190, 2021, doi: 10.1038/s41578-021-00350-8.

[92] P. Lavrador, V. M. Gaspar, J. F. Mano, and EbioMedicine, “Engineering mammalian living materials towards clinically relevant therapeutics,” no. 2352-3964 (Electronic).

[93] Y. Yu, Q. Wang, C. Wang, and L. Shang, “Living Materials for Regenerative Medicine,” *Engineered Regeneration*, vol. 2, pp. 96–104, 2021, doi: https://doi.org/10.1016/j.engreg.2021.08.003.

[94] A. M. Duraj-Thatte *et al.*, “Genetically Programmable Self-Regenerating Bacterial Hydrogels,” *Advanced Materials*, vol. 31, no. 40, p. 1901826, 2019, doi: https://doi.org/10.1002/adma.201901826.

[95] S. Yu, H. Sun, Y. Li, S. Wei, J. Xu, and J. Liu, “Hydrogels as promising platforms for engineered living bacteria-mediated therapeutic systems,” *Mater Today Bio*, vol. 16, p. 100435, 2022, doi: https://doi.org/10.1016/j.mtbio.2022.100435.

[96] Y.-C. Lu, W.-C. Yeh, and P. S. Ohashi, “LPS/TLR4 signal transduction pathway,” *Cytokine*, vol. 42, no. 2, pp. 145–151, 2008.

[97] M. Lufton *et al.*, “Living Bacteria in Thermoresponsive Gel for Treating Fungal Infections,” *Adv Funct Mater*, vol. 28, no. 40, p. 1801581, 2018, doi: https://doi.org/10.1002/adfm.201801581.

[98] X. Liu *et al.*, “3D Printing of Living Responsive Materials and Devices,” *Advanced Materials*, vol. 30, no. 4, p. 1704821, 2018, doi: https://doi.org/10.1002/adma.201704821.

[99] T. G. Johnston *et al.*, "Compartmentalized microbes and co-cultures in hydrogels for on-demand bioproduction and preservation," *Nat Commun*, vol. 11, no. 1, p. 563, 2020, doi: 10.1038/s41467-020-14371-4.

[100] C. Kummerow, E. C. Schwarz, B. Bufe, F. Zufall, M. Hoth, and B. Qu, "A simple, economic, time-resolved killing assay," *Eur J Immunol*, vol. 44, no. 6, pp. 1870–1872, Jun. 2014, doi: https://doi.org/10.1002/eji.201444518.

[101] R. Zhao, A. K. Yanamandra, and B. Qu, "A high-throughput 3D kinetic killing assay," *Eur J Immunol*, vol. n/a, no. n/a, p. 2350505, Jul. 2023, doi: https://doi.org/10.1002/eji.202350505.

[102] J. Zhang *et al.*, "Micropatterned soft hydrogels to study the interplay of receptors and forces in T cell activation," *Acta Biomater*, vol. 119, pp. 234–246, 2021, doi: https://doi.org/10.1016/j.actbio.2020.10.028.

[103] P. Rosendahl *et al.*, "Real-time fluorescence and deformability cytometry — flow cytometry goes mechanics," *bioRxiv*, p. 187435, Jan. 2017, doi: 10.1101/187435.

[104] B. Deng, Z. Zhao, W. Kong, C. Han, X. Shen, and C. Zhou, "Biological role of matrix stiffness in tumor growth and treatment," *J Transl Med*, vol. 20, no. 1, p. 540, 2022, doi: 10.1186/s12967-022-03768-y.

[105] K. E. C. Blokland *et al.*, "Substrate stiffness engineered to replicate disease conditions influence senescence and fibrotic responses in primary lung fibroblasts," *Front Pharmacol*, vol. 13, 2022, doi: 10.3389/fphar.2022.989169.

[106] D. Friedman *et al.*, "Natural killer cell immune synapse formation and cytotoxicity are controlled by tension of the target interface.," *J Cell Sci*, vol. 134, no. 7, Apr. 2021, doi: 10.1242/jcs.258570.

[107] L. Zamai *et al.*, "Understanding the synergy of NKp46 and co-activating signals in various NK cell subpopulations: paving the way for more successful NK-cell-based immunotherapy," *Cells*, vol. 9, no. 3, p. 753, 2020.

[108] B. Lipinski *et al.*, "NKp46-specific single domain antibodies enable facile engineering of various potent NK cell engager formats," *Protein Science*, vol. 32, no. 3, p. e4593, 2023.

[109] A. K. Yanamandra *et al.*, “PIEZO1-mediated mechanosensing governs NK cell killing efficiency in 3D,” *bioRxiv*, p. 2023.03.27.534435, Jan. 2023, doi: 10.1101/2023.03.27.534435.

[110] A. L. Blajeski, T. J. Phan Va Fau - Kottke, S. H. Kottke Tj Fau - Kaufmann, S. H. Kaufmann, and J. C. Invest, “G(1) and G(2) cell-cycle arrest following microtubule depolymerization in human breast cancer cells,” no. 0021-9738 (Print).

[111] R. J. Vasquez, A. M. Howell B Fau - Yvon, P. Yvon Am Fau - Wadsworth, L. Wadsworth P Fau - Cassimeris, L. Cassimeris, and C. Mol Biol, “Nanomolar concentrations of nocodazole alter microtubule dynamic instability *in vivo* and *in vitro*,” no. 1059-1524 (Print).

[112] S. L. Coué M Fau - Brenner, I. Brenner Sl Fau - Spector, E. D. Spector I Fau - Korn, E. D. Korn, and F. Lett, “Inhibition of actin polymerization by latrunculin A,” no. 0014-5793 (Print).

[113] A. Holzinger and B. Methods Mol, “Jasplakinolide: an actin-specific reagent that promotes actin polymerization,” no. 1940-6029 (Electronic).

[114] M. Kovács, C. Tóth J Fau - Hetényi, A. Hetényi C Fau - Málnási-Csizmadia, J. R. Málnási-Csizmadia A Fau - Sellers, J. R. Sellers, and J. B. Chem, “Mechanism of blebbistatin inhibition of myosin II,” no. 0021-9258 (Print).

[115] G. Le Saux and M. Schvartzman, “Advanced Materials and Devices for the Regulation and Study of NK Cells.,” *Int J Mol Sci*, vol. 20, no. 3, Feb. 2019, doi: 10.3390/ijms20030646.

[116] L. Mordechay, G. Le Saux, A. Edri, U. Hadad, A. Porgador, and M. Schvartzman, “Mechanical regulation of the cytotoxic activity of natural killer cells,” *ACS Biomater Sci Eng*, vol. 7, no. 1, pp. 122–132, 2020.

[117] D. Friedman *et al.*, “Natural killer cell immune synapse formation and cytotoxicity are controlled by tension of the target interface,” *J Cell Sci*, vol. 134, no. 7, p. jcs258570, 2021.

[118] Y. Liu *et al.*, “DNA-based nanoparticle tension sensors reveal that T-cell receptors transmit defined pN forces to their antigens for enhanced fidelity,” *Proceedings of the National Academy of Sciences*, vol. 113, no. 20, pp. 5610–5615, May 2016, doi: 10.1073/pnas.1600163113.

[119] A. K. Yanamandra, S. Bhusari, A. del Campo, S. Sankaran, and B. Qu, "*In vitro* evaluation of immune responses to bacterial hydrogels for the development of living therapeutic materials," *Biomaterials Advances*, vol. 153, p. 213554, 2023, doi: https://doi.org/10.1016/j.bioadv.2023.213554.

[120] L. Mordechay *et al.*, "Mechanical Regulation of the Cytotoxic Activity of Natural Killer Cells," no. 2373-9878 (Electronic).

[121] B. Emon, J. Bauer, Y. Jain, B. Jung, and T. Saif, "Biophysics of Tumor Microenvironment and Cancer Metastasis - A Mini Review," *Comput Struct Biotechnol J*, vol. 16, pp. 279–287, 2018, doi: https://doi.org/10.1016/j.csbj.2018.07.003.

[122] S. Xing and L. de Andrade, "NKG2D and MICA/B shedding: a 'tag game' between NK cells and malignant cells," *Clin Transl Immunology*, vol. 9, no. 12, p. e1230, 2020, doi: https://doi.org/10.1002/cti2.1230.

[123] L. Ferrari de Andrade *et al.*, "Inhibition of MICA and MICB Shedding Elicits NK-Cell-Mediated Immunity against Tumors Resistant to Cytotoxic T Cells," no. 2326-6074 (Electronic).

[124] A. D. Barrow, C. J. Martin, and M. Colonna, "The Natural Cytotoxicity Receptors in Health and Disease," *Front Immunol*, vol. 10, 2019, doi: 10.3389/fimmu.2019.00909.

[125] S. Sivori *et al.*, "NKp46 is the major triggering receptor involved in the natural cytotoxicity of fresh or cultured human NK cells. Correlation between surface density of NKp46 and natural cytotoxicity against autologous, allogeneic or xenogeneic target cells," no. 0014-2980 (Print).

[126] U. Hadad *et al.*, "NKp46 Clusters at the Immune Synapse and Regulates NK Cell Polarization," no. 1664-3224 (Print).

[127] C. Rianna, M. Radmacher, and S. Kumar, "Direct evidence that tumor cells soften when navigating confined spaces," *Mol Biol Cell*, vol. 31, no. 16, pp. 1726–1734, 2020.

[128] S. E. Cross *et al.*, "AFM-based analysis of human metastatic cancer cells," no. 0957-4484 (Print).

[129] Q. S. Li, G. Y. H. Lee, C. N. Ong, and C. T. Lim, “AFM indentation study of breast cancer cells,” *Biochem Biophys Res Commun*, vol. 374, no. 4, pp. 609–613, 2008, doi: https://doi.org/10.1016/j.bbrc.2008.07.078.

[130] W. Xu, R. Mezencev, B. Kim, L. Wang, J. McDonald, and T. Sulchek, “Cell stiffness is a biomarker of the metastatic potential of ovarian cancer cells,” 2012.

[131] K. Iida *et al.*, “Cell softening in malignant progression of human lung cancer cells by activation of receptor tyrosine kinase AXL,” no. 2045-2322 (Electronic).

[132] Y. L. Han *et al.*, “Cell swelling, softening and invasion in a three-dimensional breast cancer model,” no. 1745-2473 (Print).

[133] J. Lv *et al.*, “Cell softness regulates tumorigenicity and stemness of cancer cells,” *EMBO J*, vol. 40, no. 2, p. e106123, 2021, doi: https://doi.org/10.15252/embj.2020106123.

[134] Y. Liu *et al.*, “Cell Softness Prevents Cytolytic T-cell Killing of Tumor-Repopulating Cells,” *Cancer Res*, vol. 81, no. 2, pp. 476–488, Jan. 2021, doi: 10.1158/0008-5472.CAN-20-2569.

[135] A. T. Ritter, S. M. Kapnick, S. Murugesan, P. L. Schwartzberg, G. M. Griffiths, and J. Lippincott-Schwartz, “Cortical actin recovery at the immunological synapse leads to termination of lytic granule secretion in cytotoxic T lymphocytes,” *Proceedings of the National Academy of Sciences*, vol. 114, no. 32, pp. E6585–E6594, 2017, doi: 10.1073/pnas.1710751114.

[136] T. N. Sims *et al.*, “Opposing Effects of PKCθ and WASp on Symmetry Breaking and Relocation of the Immunological Synapse,” *Cell*, vol. 129, no. 4, pp. 773–785, 2007, doi: https://doi.org/10.1016/j.cell.2007.03.037.

[137] E. C. Schwarz, B. Qu, and M. Hoth, “Calcium, cancer and killing: The role of calcium in killing cancer cells by cytotoxic T lymphocytes and natural killer cells,” *Biochimica et Biophysica Acta (BBA) - Molecular Cell Research*, vol. 1833, no. 7, pp. 1603–1611, 2013, doi: https://doi.org/10.1016/j.bbamcr.2012.11.016.

[138] H. N. Rubaiy and Pharmaceuticals, “ORAI Calcium Channels: Regulation, Function, Pharmacology, and Therapeutic Targets. LID - 10.3390/ph16020162 [doi] LID - 162,” no. 1424-8247 (Print).

[139] G. Cai *et al.*, “Piezo1-mediated M2 macrophage mechanotransduction enhances bone formation through secretion and activation of transforming growth factor-β1,” no. 1365-2184 (Electronic).

[140] W. M. Botello-Smith *et al.*, “A mechanism for the activation of the mechanosensitive Piezo1 channel by the small molecule Yoda1,” *Nat Commun*, vol. 10, no. 1, p. 4503, 2019, doi: 10.1038/s41467-019-12501-1.

[141] V. H. Pérez-Luna, O. González-Reynoso, and Gels, “Encapsulation of Biological Agents in Hydrogels for Therapeutic Applications. LID - 10.3390/gels4030061 [doi] LID - 61,” no. 2310-2861 (Electronic), 2018.

6. Publications

1. **Archana K. Yanamandra**, Jingnan Zhang, Galia Montalvo, Doreen Biedenweg, Markus Hoth, Franziska Lautenschläger, Oliver Otto, Aránzazu del Campo, Bin Qu, PIEZO1-mediated mechanosensing governs NK cell killing efficiency in 3D, Preprint doi: https://doi.org/10.1101/2023.03.27.534435 (Manuscript in revision)
2. **Yanamandra AK***, Bhusari S*, Del Campo A, Sankaran S, Qu B. *In vitro* evaluation of immune responses to bacterial hydrogels for the development of living therapeutic materials. Biomater Adv. 2023;153:213554. doi:10.1016/j.bioadv.2023.213554
3. Zhao R, **Yanamandra AK**, Qu B. A high-throughput 3D kinetic killing assay [published online ahead of print, 2023 Jul 27]. Eur J Immunol. 2023; e2350505. doi:10.1002/eji.202350505,
4. Xiangdong Dai, Xiangda Zhou, Rui Shao, Renping Zhao, **Archana K Yanamandra**, Zhimei Xing, Mingyu Ding, Junhong Wang, Tao Liu, Qi Zheng, Peng Zhang, Han Zhang, Yi Wang, Bin Qu, Yu Wang, Bioactive Constituents of Verbena officinalis Alleviate Inflammation and Enhance Killing Efficiency of Natural Killer Cells. Int J Mol Sci. 2023;24(8):7144. 2023 Apr12. doi:10.3390/ijms24087144
5. Zhou X, Zhao R, **Yanamandra AK**, Hoth M, Qu B. Light-Sheet Scattering Microscopy to Visualize Long-Term Interactions Between Cells and Extracellular Matrix. Front Immunol. 2022;13:828634. Published 2022 Jan 28. doi:10.3389/fimmu.2022.828634
6. Wenjuan Yang, Andreas Denger, Caroline Diener, Frederic Küppers, Leticia Soriano-Baguet, Gertrud Schäfer, **Archana K Yanamandra**, Renping Zhao, Arne Knörck, Eva C Schwarz, Martin Hart, Frank Lammert, Leticia Prates Roma, Dirk Brenner, Grigorios Christidis, Volkhard Helms, Eckart Meese, Markus Hoth, Bin Qu. Unspecific CTL Killing Is Enhanced by High Glucose via TNF-Related Apoptosis-Inducing Ligand. Front Immunol. 2022;13:831680. Published 2022 Feb 21. doi:10.3389/fimmu.2022.831680
7. Gutschalk CM, **Yanamandra AK**, Linde N, Meides A, Depner S, Mueller MM. GM-CSF enhances tumor invasion by elevated MMP-2, -9, and -26 expression. Cancer Med. 2013;2(2):117-129. doi:10.1002/cam4.20

Acknowledgements

I would like to express my heartfelt gratitude to Prof. del Campo, Prof. Markus Hoth and PD Dr. Bin Qu for giving me an opportunity to work on this topic. I am eternally grateful to Dr. Bin Qu for her expert guidance and unwavering support both professionally and personally. I can't thank her enough for boosting my morale when things were not going as expected. I would not have been able to finish my thesis without her support. I am indebted to Prof. Markus Hoth for his guidance and valuable inputs throughout my thesis tenure. I sincerely express my gratitude for the support I got from him while working on my grant. I learnt from him how a person should lead a research group. He has been a wonderful mentor. I profusely thank Prof. del Campo for providing valuable inputs during my PhD work and for the collaboration. She played a major role in motivating me towards the field of biomaterials and gave me an opportunity to work on interdisciplinary projects. I would like to thank her from core of my heart for her constant support, guidance and inputs while I was working on my project proposal. I would like to thank Dr. Shrikrishnan Sankaran and Dr. Shardul Bhusari for a fruitful collaboration. I would to thank Prof. Oliver Otto for collaborating on the project and providing us with some key results. I would like to Galia Montalvo for supporting me with some experiments. I would like to thank Renping Zhao, Xiangda Zhou, Shulagna Sharma and all the old and current member of Dr. Qu's group. A special thanks to the excellent technical assistance offered by Carmen Haessig, Gertrud Schwaer, Cora Hoxha and Kathrin Förderer. I specially thank Dr. Dalia Alansary for the wonderful and lively conversations and for her support. A huge thanks to Dr. Eva Schwarz and Dr. Annette Lis for their support and guidance. I would like to extend my thanks to each and every member of Hoth/Niemeyer group for creating a wonderful working ambience. All of this would not have been possible without the support and blessings of my parents especially my father for igniting a passion for research and love for science in me. I would like to thank my parents-in-law for their immense love and support. I take this opportunity to thank my husband who has been my pillar of strength. Finally thanks to all my friends and well-wishers.